2010

Structure and Reactivity of Hexacoordinate Hemoglobins

Smita Kakar
Iowa State University

Structure and reactivity of hexacoordinate hemoglobins

by

Smita Kakar

A dissertation submitted to the graduate faculty

in partial fulfillment of the requirements for the degree of

DOCTOR OF PHILOSOPHY

Major: Biophysics

Program of Study Committee:

Mark Hargrove, Major Professor
Richard Honzatko
Amy Andreotti
Alan Dispirito
Emily Smith

Iowa State University

Ames, Iowa

2010

TABLE OF CONTENTS

LIST OF FIGURES

LIST OF TABLES

CHAPTER 1. INTRODUCTION

STRUCTURE AND REACTIVITY OF HEXACOORDINATE HEMOGLOBINS

In press at Biophysical Chemistry

Smita Kakar[1], Frederico G. Hoffman[2], Jay F. Storz[2], Marian Fabian[3], and Mark S. Hargrove[1]

Abstract:

The heme prosthetic group in hemoglobins is most often attached to the globin through coordination of either one or two histidine side chains. Those proteins with one histidine coordinating the heme iron are called "pentacoordinate" hemoglobins, a group represented by red blood cell hemoglobin and most other oxygen transporters. Those with two histidines are called "hexacoordinate hemoglobins", which have broad representation among eukaryotes. Coordination of the second histidine in hexacoordinate Hbs is reversible, allowing for binding of exogenous ligands like oxygen, carbon monoxide, and nitric oxide.

[1]Department of Biochemistry, Biophysics, and Molecular Biology, Iowa State University, Ames, Iowa 50011

[2]Department of Biological Sciences, University of Nebraska, Lincoln, Nebraska 68588

[3]Department of Biochemistry and Cell Biology, Rice University, Houston, Texas 77251

Research over the past several years has produced a fairly detailed picture of the structure and biochemistry of hexacoordinate hemoglobins from several species including neuroglobin and cytoglobin in animals, and the nonsymbiotic hemoglobins in plants. However, a clear understanding of the physiological functions of these proteins remains an elusive goal.

Introduction:

The term "hemoglobin" has spent decades at the forefront of biochemical research, including the eras of "grind-and-find", protein structure determination, and the relationship between protein structure and function. It has also served as a familiar target in genomic annotation, and as a guidepost to study the evolution of primary structure and protein function. We have learned over the past fifteen years that most organisms contain genes with homology to globins, and that not all globins are oxygen transport proteins [1-4]. In fact, it is presumptuous to assume that all globins use a heme prosthetic group as part of their physiological functions [5]. Most of what has been learned during this period originated from wide spread sequencing of genomes representing all kingdoms of life, followed by biochemical analysis of proteins resulting from select members of these new-found sequences, in most cases using recombinant methods for their production.

The infrastructure for detailed biophysical research with hemoglobins (Hbs) has been in place for decades, established in an effort to understand how the structures of oxygen transport Hbs confer this function. All of the newly discovered Hbs have been naturally welcomed into this framework, which has produced a wealth of structures, spectroscopic characterizations, and

biochemical investigations of recombinant Hbs from the three kingdoms of life. The downside of all the ready physical analysis is that such work, when not guided by knowledge of a clear physiological function, sometimes digresses from biology and can mislead functional hypotheses by asking leading questions. Thus, organizing globins based on function is currently difficult. Nevertheless, irrespective of functional hypotheses, structural and chemical studies of newly discovered Hbs have revealed unusual behavior that has challenged some of the principles distilled from the wealth of research on oxygen transport Hbs.

The familiar oxygen transport Hbs of plants and animals use pentacoordinate heme iron (Figure 1-1A) to reversibly bind oxygen in the Fe^{2+} (ferrous) oxidation state. In all cases, a single histidine side chain coordinates an axial site on the heme iron to help hold the prosthetic group in place, leaving the other axial site open for oxygen binding. Only the ferrous oxidation state will reversibly bind oxygen, and the tissues in which these proteins function have mechanisms to prevent or reverse the spontaneous oxidation to the Fe^{3+} (ferric) oxidation state. In newly-discovered Hbs, absent the knowledge of physiological function, there is no way to know what oxidation state is biologically relevant or how heme coordination relates to function. The heme iron could potentially exist (or cycle through) in the Fe^{2+} (ferrous), Fe^{3+} (ferric), or Fe^{4+} (ferryl) oxidation state, attachment to the protein could potentially result from a number of amino acids capable of donating a pair of electrons to form a coordination bond [6], and attachment to the protein could result from one or two coordinate bonds (two if both axial binding sites are filled by proteinaceous amino acids).

In practice, recombinant Hbs in the laboratory will readily adopt the ferrous and ferric oxidations states, and can be pushed into the ferryl state by exposure to hydrogen peroxide [7-9]. But without knowledge of function *in vivo*, it is difficult to judge the objective importance of these observations. However, the number of bonds coordinating the heme group can be objectively measured spectroscopically and by observation of protein structure, and has provided an important distinguishing classification for Hbs. In fact, the first discoveries of non-oxygen transport Hbs in plants and animals revealed recombinant proteins with coordination states distinct from pentacoordinate oxygen transporters [10, 11] (Figure 1-1B). These Hbs share the features of having their heme groups coordinated by two histidine side chains, one of which is capable of reversible dissociation to allow the stable binding of exogenous ligands like oxygen, carbon monoxide, and nitric oxide. While these proteins do not necessarily share sequence homology, and sequence alone has not yet been used to predict coordination state, the shared structural similarity of six coordinate bonds to the heme iron has resulted in these proteins being collectively referred to as "hexacoordinate" Hbs (hxHbs). The purpose of this review is to describe hexacoordinate Hbs by comparing their structures, ligand reactivities and biochemical activities.

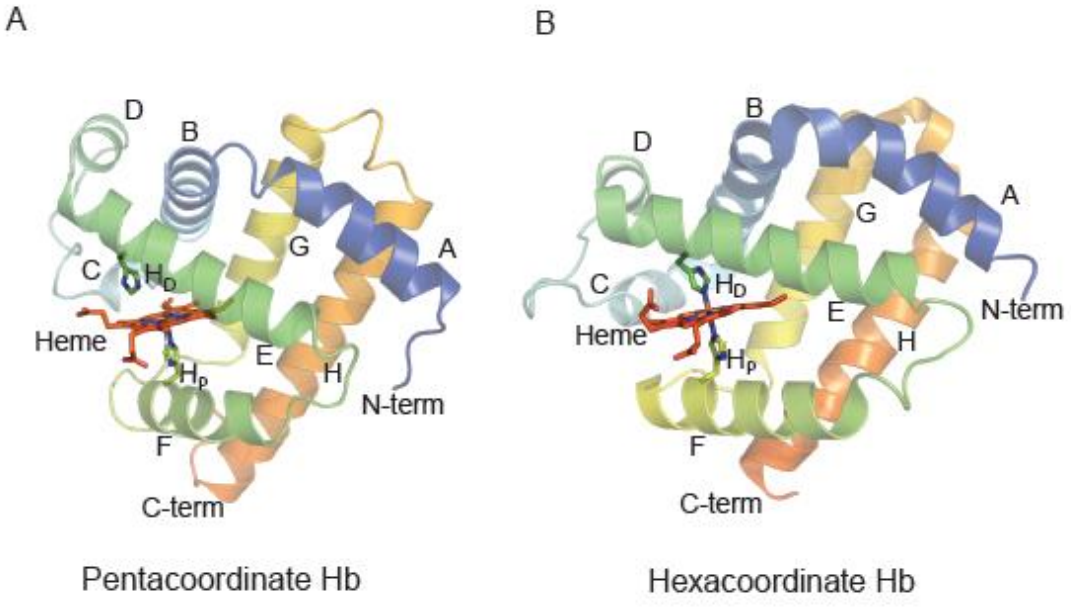

Figure 1-1. Pentacoordinate and hexacoordinate hemoglobins. A) The structure of ferric sperm whale myoglobin (2MBW.pdb) shows a pentacoordinate, low spin heme weakly bound to water. B) The structure of Neuroglobin (1QIF.pdb) demonstrates hexacoordinate hemoglobin with the binding site occupied by the side chain of the distal histidine. In each structure, eight alpha-helices are labeled (A through H) along with showing the N-terminus (N-term), the C-terminus (C-term) and the distal (H_D) and proximal (H_P) histidines.

In what organisms are hexacoordinate hemoglobins found?

Plant hemoglobins- HxHbs have been found in plants, animals, and cyanobacteria [11-13]. They were first noted in the plant "nonsymbiotic" hemoglobins (nsHbs), which were discovered during a search for globins in plants that are unrelated to oxygen transport [11]. Prior to the discovery of nsHbs, it was thought that Hbs in plants were limited to nitrogen fixing legumes, where these "leghemoglobins" (Lbs) scavenge oxygen and deliver it to respiring symbiotic bacteria in the root nodules [14, 15]. The identification of globin genes in many other plants helped to explain the evolutionary origin of the Lbs, and brought about the continuing question of the physiological function of nsHbs [16]. Since the discovery and characterization of

nsHbs in barley [11] and rice [17] nearly 15 years ago, dozens of plant globin genes have been sequenced and can be grouped into three different clades, corresponding to the three different classes of plant Hbs (Figure 1-2) that exhibit distinct physical behavior [4].

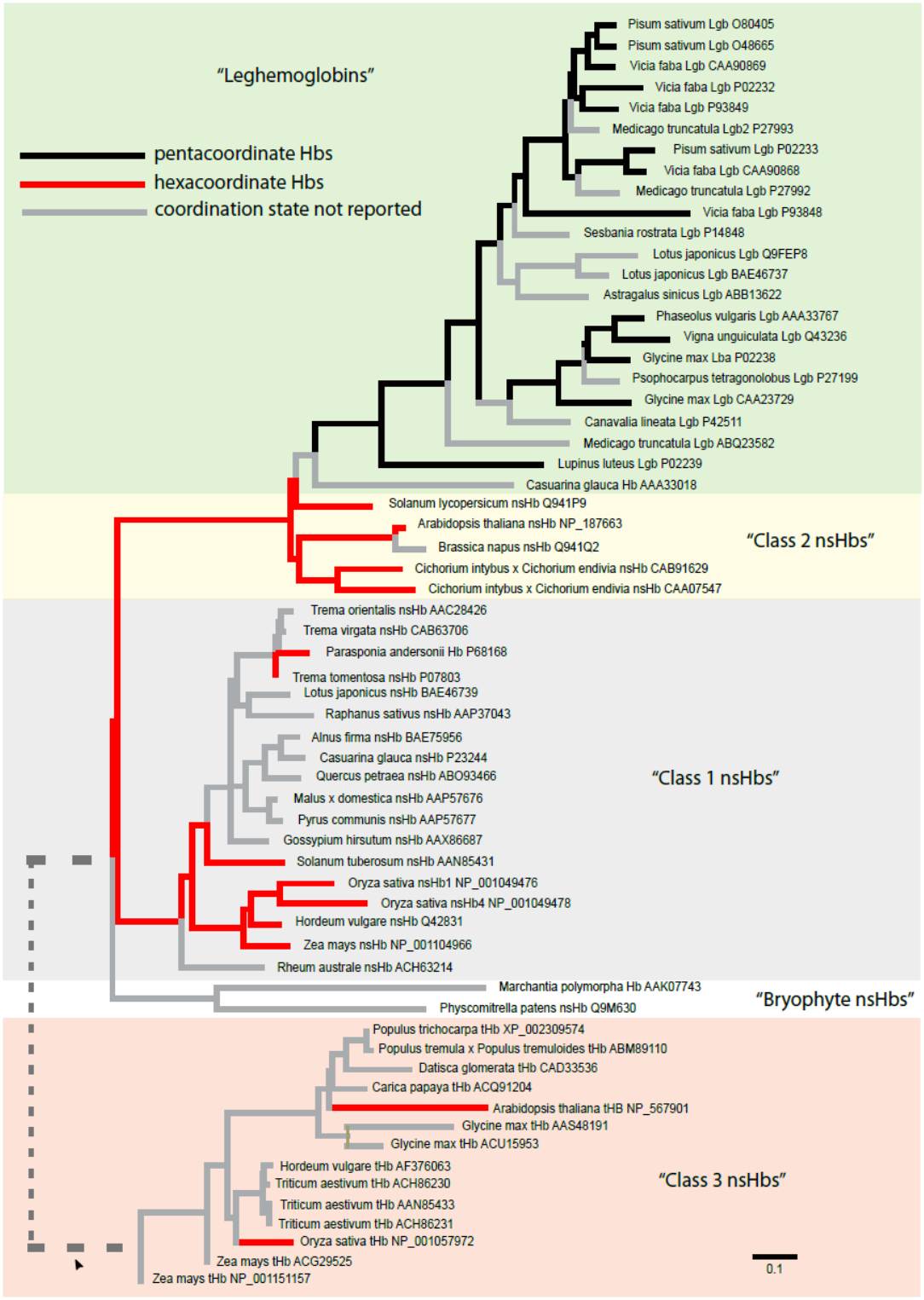

Figure 1-2. Maximum likelihood phylogram of select plant globin sequences. Plant globins can be classified into three "classes", each containing hexacoordinate members (red lines). The term nonsymbiotic hemoglobin" (nsHb) is in deference to the previously discovered symbiotic "leghemoglobins", which are pentacoordinate oxygen transporters.

With the exception of the Lbs, all plant Hbs show some degree of hexacoordinate character. The Class 2 nsHbs have the highest affinities for distal histidine coordination in the ferrous oxidation state (K_H in Table 1-1), whereas the degree of coordination in Class 1 nsHbs is much less [4, 18]. The Class 3 nsHbs share greater sequence similarity (40-45%) with bacterial Hbs of the "2-on-2" structural motif [19-25] than with the other nsHbs (<25%) [26], and likely result from horizontal gene transfer from bacteria [27]. Many of the bacterial "2-on-2" Hbs are also shorter in primary structure, but the Class 3 nsHbs are actually longer than the other nsHbs and typical globins. The only reported bacterial hxHb is found in the cyanobacterium *Synechocystis* [13, 28, 29], which contains a "2-on-2" Hb (SynHb) that is hexacoordinate in both the ferrous and ferric oxidation states [30, 31].

Animal hemoglobins- Concurrent with the discovery of hxHbs in plants was the identification of new globin sequences in the genomes of hundreds of species spanning all kingdoms of life [2, 12, 32-37]. Examination of recombinant proteins resulting from many of these gene sequences has identified the presence of hxHbs within each of the three major groups of animal Hbs (Figure 1-3). Animal Hbs can be grouped into three separate clades in a manner that is consistent with the nature of the circulatory system of the corresponding organism and with how the oxygen transport Hbs are packaged within the circulatory system. In the phylogeny shown in Figure 1-3, for example, the top-most clade corresponds to arthropod and mollusk Hbs, two groups that have open circulatory systems. The middle clade consists of intracellular oxygen-transport Hbs from organisms that have closed circulatory systems. The bottom-most clade consists of extracellular Hbs from organisms that have closed circulatory systems.

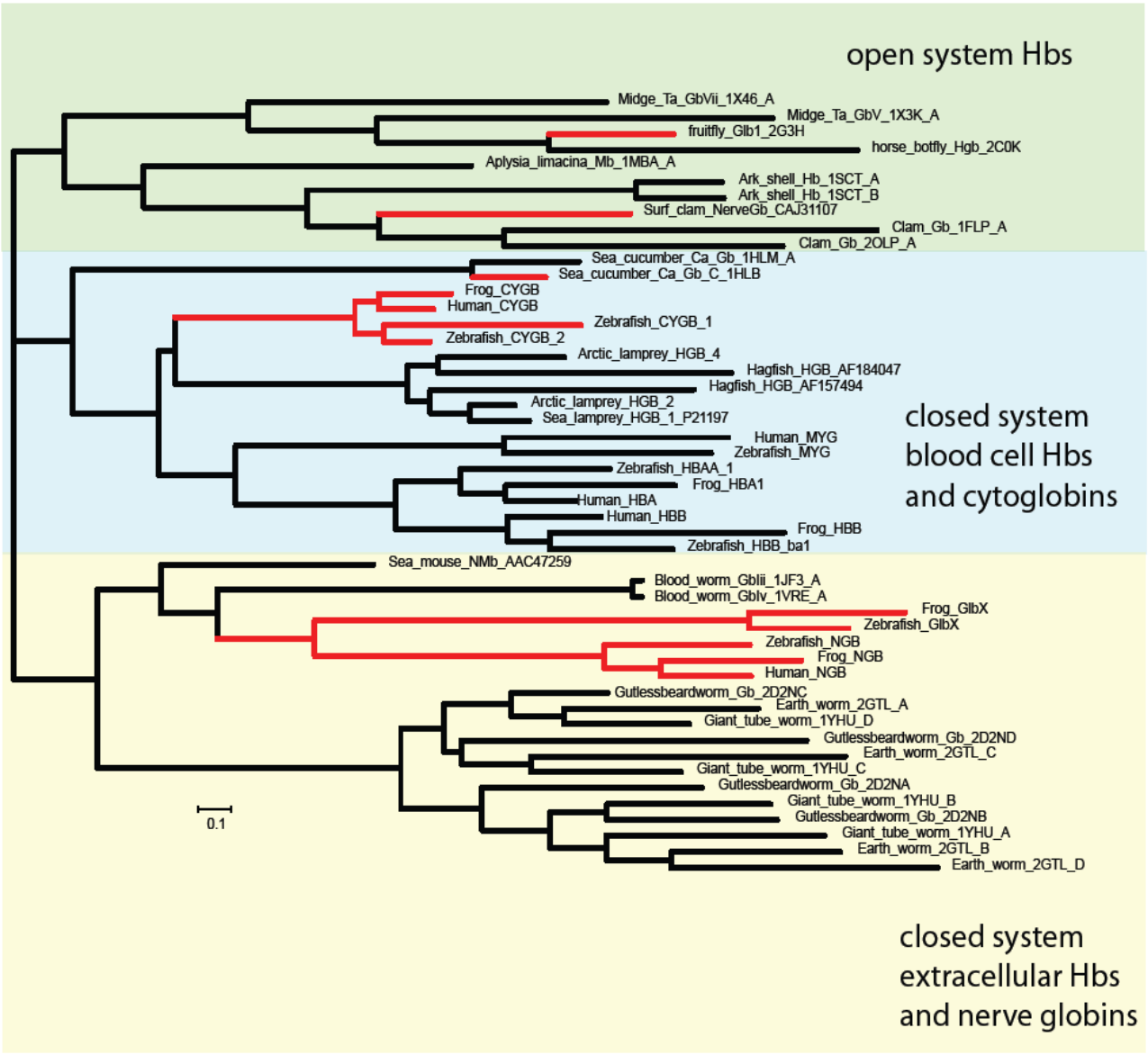

Figure 1-3. Maximum likelihood phylogram of select metazoan globin sequences. Multicellular animal globin sequences segregate into three major clades, and there are hexacoordinate members of each clade (shown in red). In each case, the phylogeny indicates that hxHbs have evolved from pentacoordinate progenitors.

The animal hxHbs that are most closely related to the cell-bound Hbs in closed circulatory systems are the "cytoglobins" (Cgb) found in vertebrates and “Hb Chain C” from the sea cucumber *Caudina arenicola* [2, 33, 38]. The two other vertebrate hxHbs, "neuroglobins" (Ngb) and "globin X" (GlbX), are more closely related to extracellular oxygen transport Hbs

present in animals with closed circulatory systems [12, 36, 37]. In general, the Ngbs are very strongly coordinated by the distal histidine in both the ferrous and ferric oxidation states, Cgbs are intermediate in this regard, and hxHbs from branch 1 of the tree are most weakly hexacoordinate, on par with the nsHbs from plants [33, 34, 39-42] (Table 1-1).

The chemistry of hexacoordinate hemoglobins:

Because our knowledge of hxHbs is based mainly on *in vitro* reactions with recombinant proteins, our knowledge of their chemistry and reactions with ligands is limited to what they *can* do under controlled experimental conditions. And because the experimental questions asked are often influenced by our knowledge of the function and reactivity of oxygen transporters, much of what we know about hxHbs is derived from similar experiments. Thus, the data presented in Tables 1-1 and 1-2 and the following discussion of the chemistry and reactivity of hxHbs is grounded in a comparison to their pentacoordinate oxygen transport counterparts.

Table 1-1 Rates and Equilibrium Constants for Hexacoordination by HisE7

Kinetic and equilibrium constants for reversible distal histidine coordination					
Protein	E_{mid} (mv)	k_{H2} (s^{-1})	k_{-H2} (s^{-1})	K_{H2}	reference
Mb	55	~0		~0	
Mb $_{H64V/V68H}$	-128	>20,000	>200	~100	[46][1]
Ngb_{human}	-115	1900	1.5	2,000	
Ngb_{mouse}	-129	1000	0.5	2,000	
$Ngb_{zebrafish}$		2500	2	1,250	[32], [39, 41][2]
Cgb	-28	315	1.3	~400	[33, 40]
DrosHb		550	30	18	[42]
Mollusk nHb		14,000	1,000	14	[34]
Plant nsHb1 (average)		**130**	**75**	**1.7**	
Rice nsHb1	-143	75	40	1.9	
Plant nsHb2 (average)		**1500**	**25**	**84**	
Tomato nsHb2		1400	30	60	
SynHb	-195	4200	14	300	[41]

[1]Average values for members of each class are in bold. The value of K_{H2} for Mb $_{H64V/V68H}$ is unpublished, and is from a personal communication from John S. Olson; other values are from [46]. [2]For Ngb, K_H is average of values from these references.

Table 1-2 Kinetic and Equilibrium Constants for Ligand Binding to Ferrous Hexacoordinate Hemoglobins

Kinetic and equilibrium constants for ligand binding to ferrous Hexacoordinate hemoglobins									
Proteins	$k'_{CO,pent}$ ($\mu M^{-1}s^{-1}$)	$k_{CO,}$ (s^{-1})	K_{CO} (μM^{-1})	k'_{O2} ($\mu M^{-1}s^{-1}$)	$k_{O2,}$ (s^{-1})	K_{O2} (μM^{-1})	P_{50} (torr) from kinetics	P_{50} (torr) from EQ	k_{autox} (s^{-1})
Mb	0.51	0.02	25.5	17	15	1.1	0.5	0.33	
Mb H64V/V68H	0.1	0.005	15						Fast
Ngb_{human}	39	0.01	2	150	0.6	0.13	5	5	0.18(25) 5.4 (37)
Ngb_{mouse}	72	0.013	2.7	200	0.4	0.25	2.4	2.2	19 (37)
$Ngb_{zebrafish}$	70	na	na	250	0.3	0.7	0.9	0.7	
Cgb	5	0.003	4	30	0.35		3	1	
DrosHb	13	na	na	64	1	3.3	0.2	0.1	
Mollusk nHb	75	na	na	130	30	0.3	1.9	0.6	
nsHb1 (average)	8.4	na	na	67	0.14	410	0.002		
Rice nsHb1	6.8	0.001	2300	60	0.038	540			0.08 (20, pH7)
nsHb2 average	39	0.001	460	76	1.1	2.9	0.2		
Tomato nsHb2	26	na	na	45	0.4	1.8	0.3		
SynHb	90	na	na	240	0.014	57	0.01		

References for these values are as follows: Mb [43, 146], Mb $_{H64V/V68H}$ (average values from human and pig [46]), Ngb_{human} (CO values [10, 32, 39], O_2 (average values from [10, 32, 147]), Ngb_{mouse} (O_2 values [147], CO values [39]), $Ngb_{zebrafish}$ [32, 148], Cgb [33], O_2 values [33, 40], DrosHb [42], Mollusk Hb [34], nsHb1 (average values [17]), nsHb2 [4] (CO off values [149]), SynHb [28].

Absent any bound ligands, myoglobin (Mb) is pentacoordinate in both the ferrous and ferric oxidation states. This is readily evident from electronic absorbance spectra of both oxidation states, and from electron paramagnetic resonance spectroscopy for the ferric protein (Figure 1-4). The characteristic visible-region absorption bands are weak and broad, with peaks near 500 and 635 nm for the ferric proteins, and a single asymmetric absorbance band near 555 nm for the ferrous proteins, indicating that the heme iron is in the high-spin electronic

configuration in both oxidation states (Figure 1-4A) [43]. On the contrary, histidine coordination to the sixth axial position converts the heme iron of hxHbs to the low-spin electronic configuration in both oxidation states giving rise to stronger visible absorbance in the ferric state, and splitting of the ferrous visible absorbance band into two peaks near 560 and 530 nm (Figure 1-4B). EPR is a particularly sensitive measure of the spin state in ferric Hbs, where high spin (usually pentacoordinate) Hbs exhibit a strong axial signal at g= 5.4 and 2 demonstrating a single species in the sample (Figure 1-4C), and low spin Hbs (like the hxHbs) exhibit weaker and more complex spectra dominated by a rhombic signal with features at g values of 3, 2.2 and 2 (Figure 1-4D) [44].

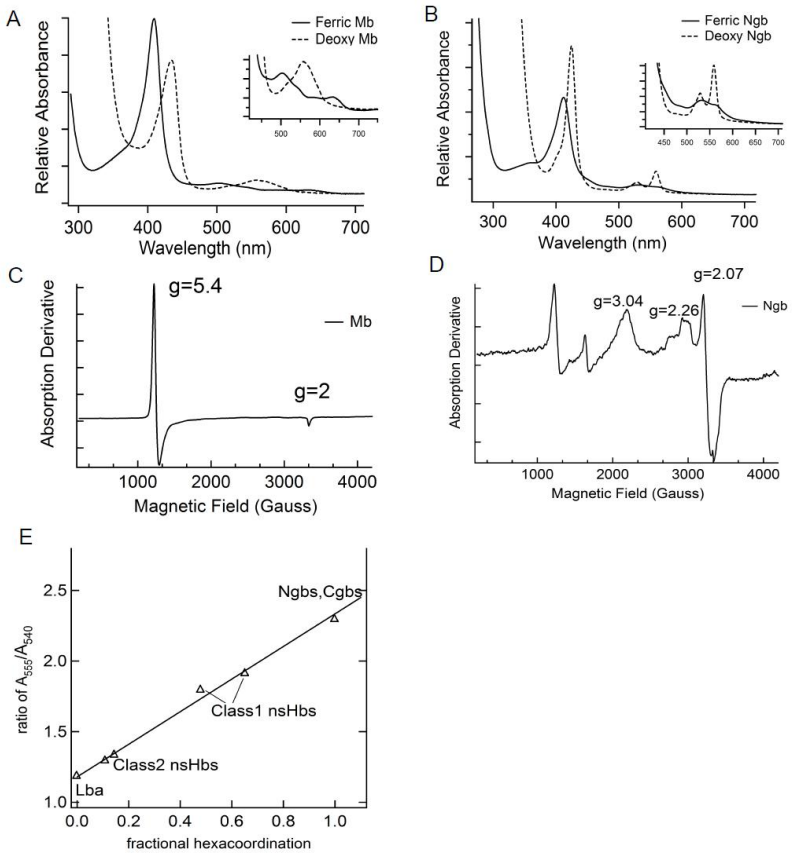

Figure 1-4. Electronic and paramagnetic spectral characteristics of hxHbs. A) Absorbance spectra of ferric and ferrous sperm whale Mb demonstrate characteristics of high spin, pentacoordinate hemoglobins. B) Absorbance spectra of Ngb in the ferric and ferrous oxidation

states demonstrate characteristics typical of low spin hxHbs. C) The EPR spectrum of ferric sperm whale Mb shows the axial high spin signal of iron at g= 5.4 and 2 D) The EPR spectrum of a low spin heme with g values of 3.04, 2.26 and 2.07, characteristic of a low spin iron as depicted by Ngb. EPR spectra were collected at 10° K with amplitude modulation of 10 G and frequency of 9.26 GHz.

While all ferric hxHbs bind the distal histidine with equilibrium constants >> 10 [45], the strength of coordination in the ferrous state is variable (Figure 1-4E, Table 1-2) [41]. Ferrous Ngbs, Cgbs, and SynHb are very tightly coordinated compared to the plant nsHbs, drosophila Hb (DrosHb), and mollusk nerve Hb (Mollusk nHb). The "Class 3" nsHbs are low spin in the ferric form, and transition to the high-spin, pentacoordinate state upon reduction [26]. The differential strength of coordination is observed in the lower midpoint reduction potentials of hxHbs (Table 1-2), which are all well below 0, and typically near -130 mv [39, 45, 46].

Reversible binding of ligands to pentacoordinate Hbs is a bimolecular process often carried out under pseudo first order reaction conditions, with the ligand in excess of the protein [47]. Under these conditions, the observed rate of binding is linearly dependent on ligand concentration, with the slope of the line equal to the bimolecular rate constant. The first observations of ligand binding to hxHbs revealed limiting rates of bimolecular binding resulting from coordination of the distal histidine, which blocks the ligand binding site [17, 33, 39, 47]. This complicates ligand binding reactions by preceding bimolecular interactions with a reversible first order event, as shown in Equation 1 [47-49].

$$Hb_H \underset{k_H}{\overset{k_{-H}}{\rightleftarrows}} Hb_P \xrightarrow{k'_L [L]} Hb_L \quad \text{Equation 1}$$

The degree to which distal histidine coordination affects binding time courses for exogenous ligands is influenced by two factors [41, 50]: 1) the speed with which the coordinating histidine associates and dissociates from the heme iron, and 2) the equilibrium fraction of protein in the hexacoordinate state. If the speed of coordination (k_H) and dissociation (k_{-H}) is very rapid compared to the association of exogenous ligands ($k'_L[L]$), then the hexacoordination reactions are at fast exchange on the time scale of the ligand binding reaction, and the observed time course will described by a single rate ($k_{obs,L}$) influenced by the time-average of all three reactions.

$$k_{obs,L} = \frac{k_{-H} k'_L[L]}{k_H + k_{-H} + k'_L[L]} \quad \text{Equation 2}$$

If the speed of coordination is much slower than exogenous ligand binding, the observed time course will be limited by histidine dissociation and will potentially exhibit two phases, one for the fraction of Hb in the hexacoordinate state, and one for the fraction that is pentacoordinate.

$$\Delta A_{obs} = \Delta A_T (F_P e^{-k'_L[L]*t} + F_H e^{-k'_{obs,L}[L]*t}) \quad \text{Equation 3}$$

Regardless of the kinetics of the reaction, the influence of hexacoordination on equilibrium affinity constants is directly related to the affinity constant for histidine coordination [10, 33].

$$K_{Effective} = \frac{K_{pentacoordinate}}{1 + K_H}$$ Equation 4

Equation 4 demonstrates how hexacoordination could augment the innate equilibrium affinity constant of a pentacoordinate Hb by lowering the effective strength of binding [10, 33, 39].

The reaction central to the function of oxygen transport Hbs such as Mb and red blood cell Hb is the reversible binding of oxygen. The ferrous form of these proteins reacts with oxygen reversibly to form a stable protein usually referred to as the "oxy-ferrous" complex, although the exact electronic state of the oxygen and heme iron are still in question. There is evidence to support the oxygen bound complex existing mainly as Fe^{3+}-O_2^-, but upon reversible dissociation of oxygen, the heme iron is left in the Fe^{2+} state [43]. Occasionally, O^{2-} will dissociate leaving the Fe^{3+} heme iron in one mechanism of oxidation (or "autooxidation") of the Hb [51]. This process is relatively slow in oxygen transport Hbs due to stabilization of bound oxygen by the distal histidine [52], but there are many features of Hb structure that can affect rates of autooxidation by allowing solvent access to the heme pocket, and in ways that are not completely understood [53, 54]. The mechanisms used to establish appropriate oxygen binding kinetics (and thus affinities) in oxygen transport proteins involve the combined efforts of the proximal and distal histidines [15, 52]. In general, to facilitate oxygen diffusion, the oxygen dissociation rate constant must be at least 1 s^{-1}, affinities must be appropriate to maintain fractional saturation between the source and sink, and the Hb concentration must be higher than that of oxygen in solution [4, 55-57].

Due to the augmentation of affinity by hexacoordination (Equation 4), several hxHbs have affinity constants appropriate for oxygen transport [4, 10, 33]. However, rates of oxygen dissociation from hxHbs are generally too slow for oxygen transport, with the exception of the mollusk nHb, DrosHb, and the Class 2 nsHbs [4, 17, 34, 35, 41]. Of the hxHbs for which autooxidation has been measured, rates are generally much faster than the pentacoordinate Hbs [39]. The reasons for the rapid rates of oxidation are not well understood, but could be related to rates of electron transfer, which is generally faster in hxHbs [58]. The rate constants for association and dissociation of oxygen and other diatomic ligands (like CO) are not exceptional in hxHbs, and fall within the range observed for the variety of pentacoordinate Hbs that have been reported [56]. Due to the increased strength of coordination by the distal histidine in the ferric oxidation state, ferric hxHbs are generally less reactive than their ferrous counterparts. This is indicated by generally slow and weak binding to ferric ligands such as cyanide and azide (Table 1-3).

Reaction of Hbs with NO and other nitrogenous compounds of various oxidation states have been reported since the discovery of the role of NO as a biological signaling molecule that acts through binding the heme group of guanylyl cyclase [59, 60]. It has been demonstrated that blood cell Hb and Mb are likely scavengers of NO *in vivo* [61-63], and that bacterial and fungal "flavohemoglobins" (flavoHbs) are scavengers of NO in those organisms [64]. While there is still some discussion of the mechanisms of these reactions [65], the most likely is the reaction of NO with oxy-ferrous Hb, yielding nitrate and ferric Hb (known as the nitric oxide dioxygenase reaction, or NOD) [61, 63, 64, 66]. The possibility of a similar function has been tested in

several hxHbs. In all cases, ferrous hxHbs will bind reversibly to NO [8], the ferric forms will react with NO [67] in some cases showing slow reduction [8, 68-71], and the oxy-ferrous hxHbs will scavenge NO resulting in their oxidation (Table 1-3) [68, 72-76]. In spite of the fact that the efficiency of these reactions is at best on-par with Mb and red blood cell Hb, and is certainly limited *in vivo* by as-of-yet unknown mechanisms for re-reduction of the heme iron [4], observation of the NOD reaction has been proposed as support for an NO scavenging function in nsHbs [73, 77], Ngbs [72], and Cgbs [78]. However, unlike Mb and red blood cell Hb, whose high concentrations allow them to serve as effective NO scavengers *in vivo* in spite of relatively slow reduction mechanisms, hxHbs are present in very low concentrations, and only one specific reductase (for a nsHb [79]) has been identified that might support catalytic NO scavenging. Thus, there is still little direct chemical evidence supporting hxHbs functioning as NO scavengers to a degree greater than Mb and red blood cell Hb.

Table 1-3 Rates and Equilibrium Constants for Ligand Binding to Ferric Hexacoordinate Hemoglobins, and for the NOD reaction

Kinetic and equilibrium constants for ligand binding to ferric hexacoordinate hemoglobins						
Protein	k'_{CN} ($M^{-1}s^{-1}$)	K_{DCN} (mM)	k'_{azide} ($M^{-1}s^{-1}$)	K_{Dazide} (mM)	k'_{NO} ($\mu M^{-1}s^{-1}$)	$k_{NOD,}$ ($\mu M^{-1}s^{-1}$)
Mb	320	0.001	2900	0.034	22	34 s^{-1}
Ngb	1.6					300 s^{-1}
Cgb						500 s^{-1}
DrosHb	180					
nsHb1	1.8			0.625		100 s^{-1}
SynHb	0.7	2		200		~ 100 s^{-1}

References for these values are as follows: Mb [48] (k_{NOD} [61]), Ngb ($K_{D,CN}$ [8], k_{NOD} [72]), Cgb [68], nsHb1 [68], SynHb [30] (k_{NOD} [68], estimated from scavenging), DrosHb [42].

Structures of Hexacoordinate Hemoglobins:

There are ten crystal structures of unbound and ligand-bound hxHbs published to date [30, 35, 80-86] (The PDB entries are listed in Figure 1-6**)**. These include structures of hexacoordinate representatives of each of the three branches of the animal phylogenetic tree, one of the three "classes" of plant hxHbs, and prokaryotic SynHb. In addition, the structure of a hexacoordinate globin domain from the multi-domain sensor GLB-6 of *C. elegans* has been solved [87]. Evaluation of quaternary structure from these crystal structures suggests that mouse Ngb and DrosHb are monomeric [39, 42], and that rice nsHb and Cgb are dimeric [88-90]. Direct measurement of quaternary structure in solution by analytical ultracentrifugation has shown that rice nsHb dimerizes with a dissociation equilibrium constant of 86 µM [91], and that mouse Ngb is in fact monomeric [39]. Attempts to measure cooperativity in ligand binding studies with Ngb and Cgb by Weber and coworkers have shown Hill coefficients of ~1 for Ngb

consistent with it being monomeric, and 0.63-1.63 for Cgb, implying possible heme-heme interactions for a dimer [92].

In general, the monomeric units of each structure of the eukaryotic hxHbs share the characteristic globin fold of eight helices (labeled A through H, Figure 1-1) with a "3-on-3" helix assembly (Figure 1-5A). This is in contrast to SynHb, which has the "2-on-2" □-helical "sandwich" fold common to many bacterial Hbs [93] (Figure 1-5B). Among the eukaryotic hxHbs, the presence of a conspicuous D helix is variable [94], and the folding and stability of this helix has been implicated in the control of reversible distal histidine coordination [84, 95]. Each hxHb crystal structure shows clear coordination by both the distal and proximal histidines. Additionally, there have been NMR, EPR, and vibrational spectroscopic characterizations to test heme iron hexacoordination in solution. Resonance Raman and EPR have confirmed heme iron hexacoordination in the ferric and the ferrous states of mouse Ngb [96], but NMR studies of reveal axial histidine orientations that are not consistent with those seen in crystal structures [7, 81, 97-99]. It is believed that this inconsistency may be due to the higher solvent content in solution, and fewer hydrogen bond acceptors N-H protons of the coordinating histidines [98]. EPR spectroscopic investigations of mouse Ngb by Vinck and coworkers are consistent with the X-ray diffraction data of the ferric protein [100, 101].

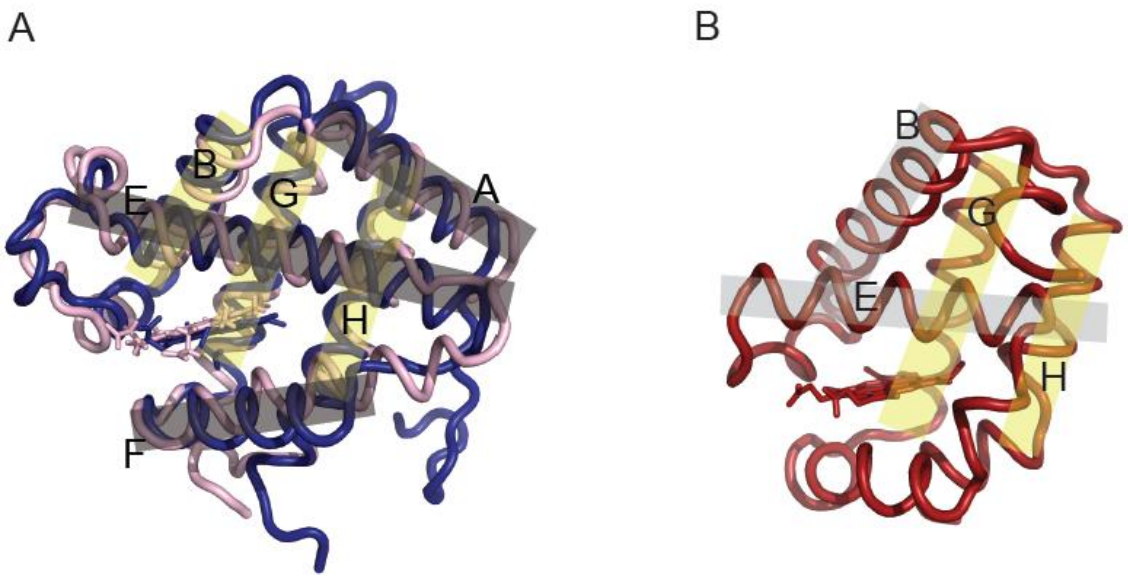

Figure 1-5. Structural features of hxHbs. A) Rice nsHb1 overlayed with DrosHb shows a "3-on-3" globin core composed the A, E, and F helices stacking on top of the B, G, and H helices. B) The structure of SynHb belongs to structural class of globins with a "2-on-2" helical core consisting of the G and H helices stacking against the B and E helices. The N-terminal end of Helix A is largely truncated and CD loop and D-helix region shortened to three residues.

One of the most unusual properties of hxHbs is their ability to bind exogenous ligands. Other heme proteins with bis-histidyl coordination do not bind ligands [102, 103], and a hexacoordinate Mb mutant protein is structurally constrained, and limited in its ability to bind exogenous ligands [46]. Thus, there has been interest in observing the structural changes accompanying ligand binding in the context of naturally occurring hxHbs. Structures of hexacoordinate and ligand-bound hxHbs have been solved for Ngb [81, 82, 104], class 1 plant nsHbs [84, 85], DrosHb [35, 83], and SynHb [30, 86]. The structural rearrangements revealed for each protein are surprisingly distinct. In the case of class 1 plant nsHbs, distal histidine dissociation from the heme iron is accompanied by rotation and translation of the E helix, formation of a D helix through contacts that span several helices, and development of several new trans-helical contacts in the EF turn (Figure 1-6A). Figure 1-6E shows the rms deviation between ligand-bound and hexacoordinate nsHb, indicating that most of the changes are

associated with the E helix and its termini. The structured D helix and the stabilization of the EF turn are believed to support the pentacoordinate E helix position. The structure of ligand-bound rice nsHb is consistent with the structures of Lbs, which evolved from class 2 nsHbs to become fixed in the pentacoordinate configuration [85, 105].

In the case of cyanide-bound SynHb, the heme is tilted by ~6 degrees from the orientation seen in the unliganded structure. The A and B helices swing inward towards the heme, and the A helix lies in close proximity to the E helix (Figure 1-6B). Additionally, the E helix and EF loop shift outward away from the heme cofactor in ligand-bound SynHb [30, 86]. In general, ligand binding in plant nsHbs and bacterial Hbs involves large-scale motions of the E-helix. This is evident from the root mean square deviation between unbound and bound ligand states for Rice Hb1 and SynHb (Figure 1-6E). Structures of DrosHb reveal translation and flattening of the heme inside the heme pocket, and heme rotation accompanying ligand binding. A rearrangement of the CD loop and amino terminal half of the E-helix region is also observed upon ligand binding [35, 83]. However, these conformational changes do not involve large movements of E-helix, as seen in nsHbs (Figure 1-6C).

In contrast to the examples above, the structural transition exhibited by mouse Ngb upon ligand binding is very modest (Figure 1-6D, 1-6E). The heme slides deeper into the heme pocket away from the distal histidine to produce a binding site, but the overall protein structure is not significantly altered [82]. However, the ligand-bound crystal was prepared by reduction and carbon monoxide (CO) exposure to ferric hexacoordinate crystals, and the crystals had to be frozen prior to data collection to avoid cracking [82]. In fact, many hxHb crystal forms shatter

when exogenous ligands are introduced, consistent with a structural change incompatible with the crystal lattice. Thus, it is possible that the CO-bound murine Ngb structure is not at equilibrium and that a larger structural change might be observed in crystals grown in the presence of a bound exogenous ligand.

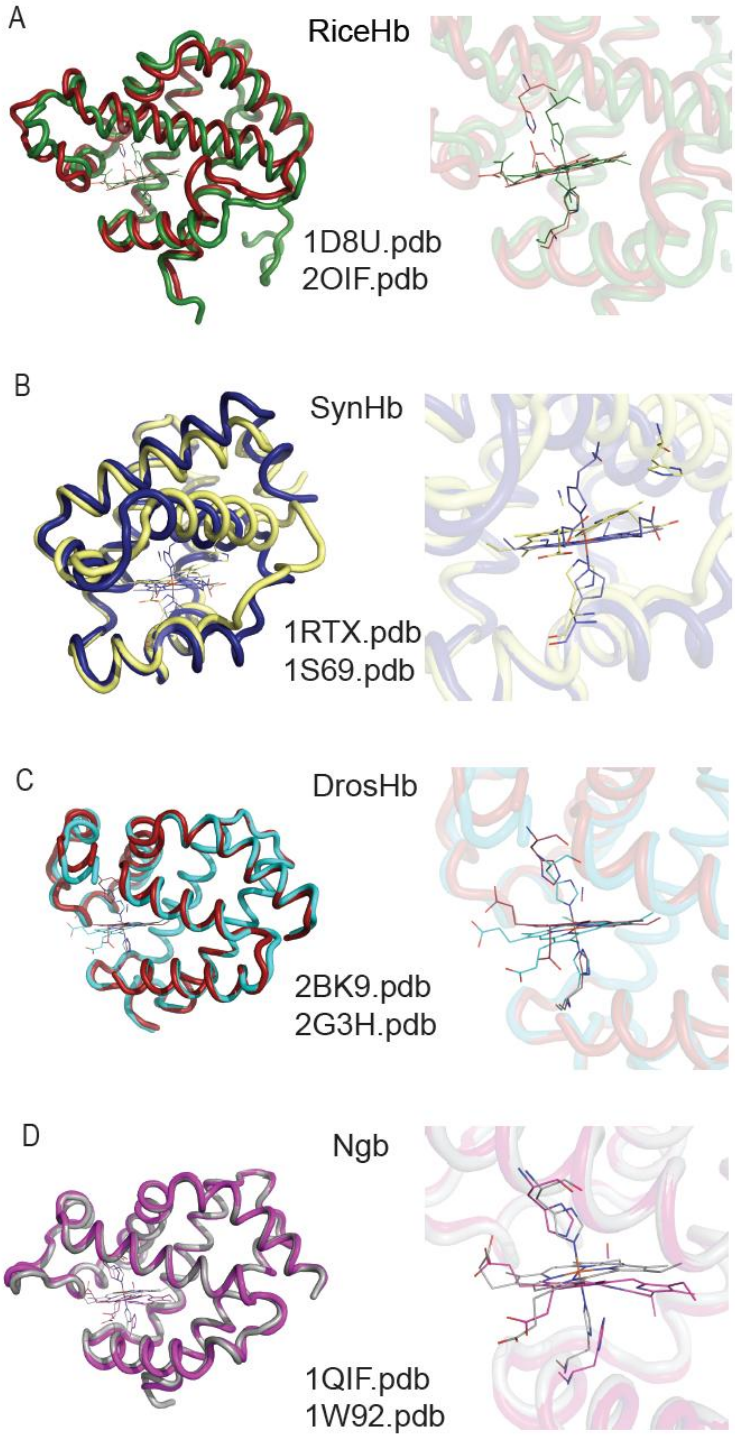
A
RiceHb
1D8U.pdb
2OIF.pdb
B
SynHb
1RTX.pdb
1S69.pdb
C
DrosHb
2BK9.pdb
2G3H.pdb
D
Ngb
1QIF.pdb
1W92.pdb

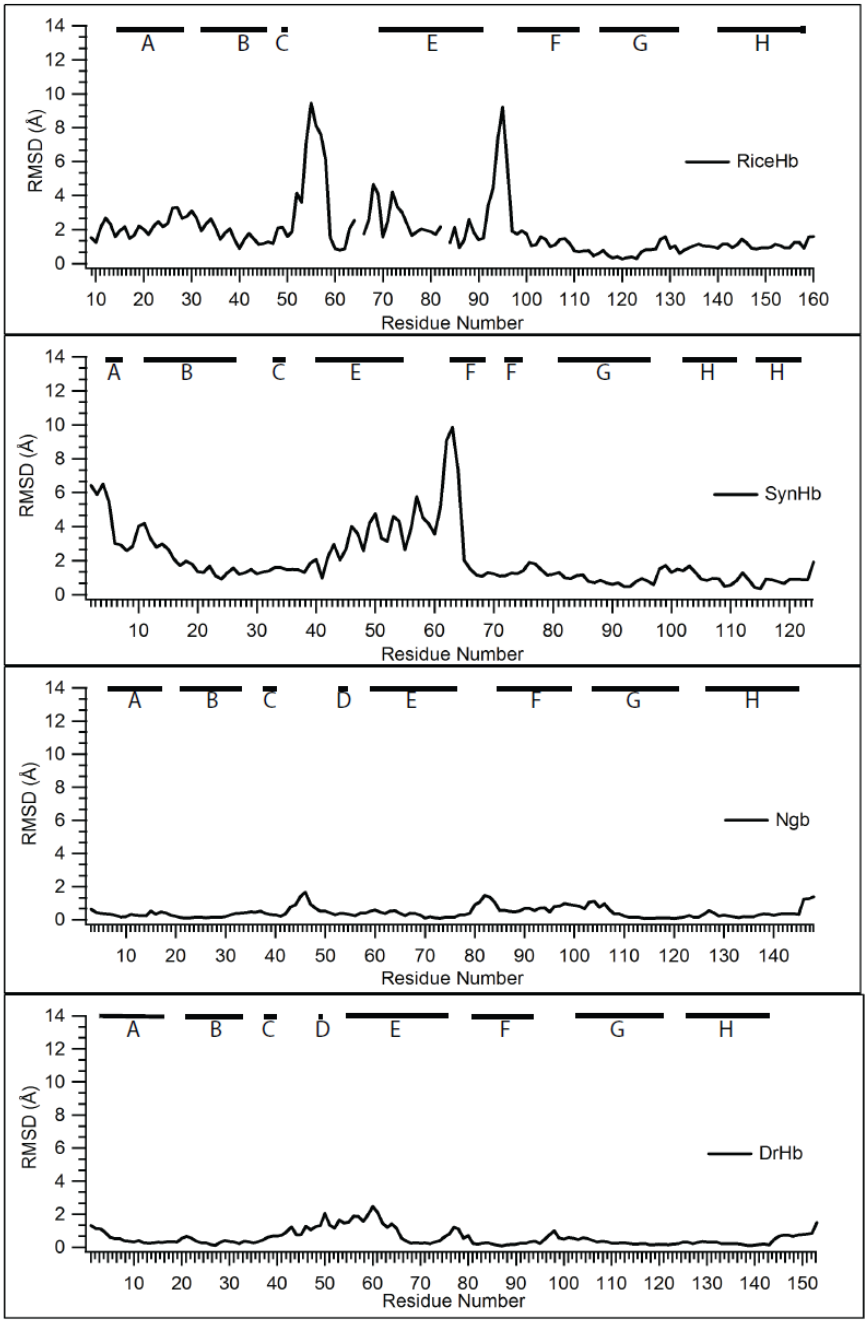

Figure 1-6. Structural changes upon ligand binding in hxHbs. These are structural overlays of A) Rice hxHb, B) Drosophila hxHb, C) SynHb, and D) Mouse Ngb in the hexacoordinate and exogenous ligand-bound states. E) Plot of root mean square deviation between hexacoordinate and ligand-bound crystal structures for each of the proteins above.

Physiological functions of Hexacoordinate Hemoglobins:

Neuroglobin- Because Ngb is found in the human brain, retina, and other nervous system tissues, the discovery of its physiological function has received a disproportionate amount of attention [106]. Figure 1-7 summarizes three hypotheses for the physiological function of Ngb that have received the most attention. 1) Based on sequence similarity between Ngb and G-protein regulators, Wakasugi and coworkers have proposed a role for Ngb in G-protein mediated signaling [7, 107, 108]. Antibody pull-down assays and surface plasmon resonance experiments have demonstrated binding of Ngb to human $G\alpha_{i/o}$, one of the many $G\alpha$ proteins associated with heterotrimeric G protein signaling in animals. Binding occurs only to the GDP-bound (inactive) form of $G\alpha_{i/o}$, which prevents $G\alpha_{i/o}$ from being recycled. As $G\alpha_{i/o}$ inactivation has been linked to protection of neurons during oxidative stress [109], Ngb could serve as a mechanism to limit ischemic damage by mitigating the deleterious effects of $G\alpha_{i/o}$:GDP [110]. Although there is significant sequence conservation among Ngb sequences from various species, this activity is not exhibited by other Ngbs, such as that from zebrafish [108]. Thus, these observations tend to question the importance of this interaction *in vivo*.

2) The first hypothesis proposed for Ngb was that of oxygen transport. This was based on it being a hemoglobin [111], its presence in the retina (which consumes a lot of oxygen) [89, 112, 113], its intercellular location near mitochondria [12], and up-regulation of Ngb mRNA in response to hypoxia [114, 115], although other studies refute this observation [116, 117]. However, this hypothesis is not supported by the low concentrations of Ngb found *in vivo*, slow

oxygen dissociation rate constants, and high oxygen equilibrium affinity constants observed for these proteins [12, 118].

3) Currently, the most popular hypothesis for Ngb function is protection against hypoxia and oxidative stress, probably through a mechanism involving NO scavenging. Reperfusion of tissues following hypoxia is a well-known cause of damage resulting from reactive oxygen species, and Ngb is suggested to have a neuroprotective effect under such conditions [114, 119-122]. Greenberg and coworkers have shown that expression of Ngb increases after ischemic stroke and that Ngb might be a novel target in stroke therapy [123]. A cognate reductase is required for NO scavenging, and there has been a lot research directed toward finding one, but none has been identified yet [39, 68, 124, 125]. Thus, there is currently no biochemical mechanism to explain how Ngb increases cell survival following ischemia.

Fago and coworkers have proposed a different molecular mechanism for the protective effect of Ngb in cell death induced by hypoxia, based on a fast electron-transfer transfer between ferrous Ngb and ferric cytochrome c [118, 126]. In this mechanism, Ngb causes rapid reduction of ferric cytochrome c, thereby maintaining levels of non-apoptotic ferrous cytochrome c and simultaneously generating ferric Ngb. Raychaudhuri *et al.* have reported a similar neuroprotective role of Ngb by way of inhibiting apoptosis [127]. This hypothesis also requires a mechanism for reduction of Ngb, and a candidate reductase, Apoptosis Inducing Factor (AIF), was proposed for this function. However, a direct test of this activity *in vitro* failed to support a role for AIF in Ngb reduction [124].

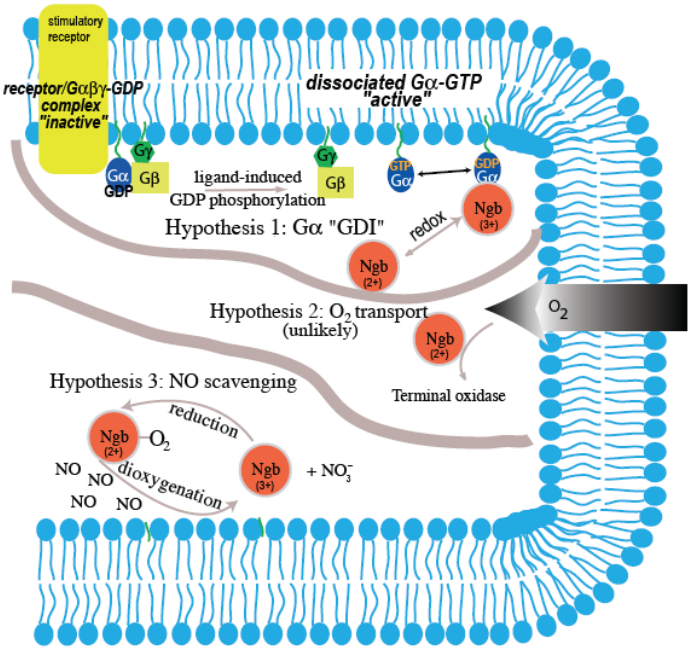

Figure 1-7. Proposed functions of Neuroglobin. Three proposed physiological functions for Ngb include A) a role in G-protein mediated signaling, B) Oxygen transport, and C) protection against Hypoxia and Oxidative stress.

Cytoglobin- Cgb is expressed in almost all types of human tissues [2, 33], but was first identified in a proteomic screen of conditions activating hepatic stellate cells [128]. Although all other hxHbs have very high oxygen affinity, Cgb possesses an oxygen affinity comparable to that of Mb [33, 129], and is up-regulated following hypoxia [88, 130]. Thus, it is possible that Cgb replaces Mb function in tissues where the latter is not expressed [131]. In a role similar to one proposed for Ngb, Cgb is a possible NO scavenger for the purpose of fibroblast proliferation [78], or cytoprotection under oxidizing conditions such as ischemic reperfusion injury [132]. Alternatively, others have proposed roles for Cgb in collagen synthesis [88], and tumor suppression [133], but distinct mechanisms for these roles remain to be established.

Drosophila Hemoglobin: DrosHb is a monomeric globin discovered in the fruit fly, *Drosophila melanogaster* [42, 134]. It is present in low concentrations in the tracheal system and the fat body of both larval and adult fly. Early research speculated a role in facilitated oxygen diffusion across tracheal walls for the protein. However, the Hb expression levels decreased under limiting oxygen conditions making it unlikely to function as an oxygen storage protein [42]. Like Ngb and Cgb, DrosHb is also a candidate for protection against reactive oxygen species produced by oxygen diffused via the trachea**,** but there is no clear evidence or mechanism supporting this role [135].

Mollusk nerve Hb- The nerve Hb from the bivalve mollusk, *S.solidissima* is believed to be an oxygen transport protein [34]. Such glial nerve Hbs are common in species exposed to hypoxia, and enable neuronal function under these conditions [136]. These globins enable mollusk neuronal function and survival under low levels of oxygen, either prevalent in natural habitats or under ischemic conditions [137, 138]. This globin has oxygen binding rate constants very similar to the leghemoglobins, and could seemingly transport oxygen effectively as a pentacoordinate Hb. Thus, the role of hexacoordination in its function could be simply to lower the overall affinity to that needed in this specific environment.

Globin X- GlbX is weakly expressed in amphibia and fish [37]. Its primary sequence is longer than other HxHbs, possessing 25-30 extra amino acids at both the N- and C-termini. However, the proximal and distal histidines along with phenylalanine at CD1 position are conserved [36]. GlbX is distantly related to Ngb, but mRNA expression analysis in goldfish has

shown that it is not a neuronal protein [37]. The function of this globin is still unknown (hence the name Globin X").

Caudina arenicola Chain C- The sea cucumber *Caudina arenicola* has four different globin chains, which together facilitate cooperative oxygen transport. The mechanism of cooperativity is not completely understood, but appears to involve changes in heteromeric quaternary structure linked to ligand binding [38]. In spite of very high sequence similarity among these chains, only the "Chain C" subunit is hexacoordinate. When first discovered in the absence of other known hxHbs, this observation could have been considered an aberrant conformation resulting from experimental conditions, or an alternative conformation rarely occupied *in vivo* (such as the case with low-pH human □ chains). However, it is also possible that hexacoordination plays a role in these systems, as proposed for human □ chains, where it could help to maintain ferrous heme iron by facilitating reduction [139].

Plant nsHbs- Class 1 nsHbs are expressed at low levels in root tissues and have high oxygen affinities with low dissociation rate constants, indicating that they are unlikely to serve as oxygen transport proteins [4, 15]. Robert Hill and coworkers have proposed a function for Class 1 nsHbs in the maintenance of redox and energy status in plant cells under hypoxia [140, 141]. Cells expressing Class 1 nsHb display elevated ATP levels, low accumulation of NO, and decreased cell death under hypoxia [142]. NOD function has also been explored for these Hbs [68, 75, 143], and the rate of NADH-dependent reduction is enhanced by cytosolic monodehydroascorbate reductase, a likely cognate reductase *in vivo* [79]. Much less is known about Class 2 and Class 3 nsHbs. It has been shown that, similar to Class 1 nsHb, over-

expression of Class 2 nsHbs increases cell survival during hypoxia. Class 2 Hbs exhibit tighter hexacoordination than Class 1 nsHbs and thus have lower oxygen affinities, increasing the likelihood of possible roles in sensing sustained low levels of oxygen [18, 144].

Class 3 nsHbs are found in most plant genomes, with expression reported to be in root and shoot tissues, and down-regulated during hypoxia [26, 145]. A Class 3 nsHb from *Arabidopsis* shows transient hexacoordination upon reduction, and has unusual ligand binding kinetics [26]. However, these properties have not yet been examined in much detail, and there has been little discussion of potential physiological roles for this class of proteins. Further characterization is needed to determine if the "2-on-2" structural motif observed in their prokaryotic homologous is present in the plant proteins, even though their primary sequences are longer than the "truncated" versions found in bacteria.

SynHb- SynHb has been shown to have a nitric oxide scavenging function *in vitro* [68]. However, a reductase remains to be characterized in order to sustain the reaction *in vivo*. Large structural motions on ligand binding suggest that SynHb might play a role in signaling mechanisms, as has been proposed for human Ngb [107, 108]. An enzymatic role in oxidation-reduction chemistry has also been proposed based on the hydrogen bond networks in the crystal structure [86].

Which came first, pentacoordinate or hexacoordinate Hbs?

The globins found in prokaryotes, eukaryotes, and archaea are believed to have evolved from a common ancestor with a function unrelated to oxygen transport [136]. Whether this primordial Hb was of the "3-on-3" or the "2-on-2" structural variety, and whether its coordination state was pentacoordinate or hexacoordinate is unknown. In fact, examination of Figures 1-2 and 1-3 suggests a difference in coordination state for the progenitors of plant and animal Hbs, respectively. In plants, pentacoordinate oxygen transporters have evolved from hexacoordinate Hbs in both Class 1 and Class 2 nsHbs [4, 146], and there are no examples of hxHbs evolving from pentacoordinate proteins. By contrast, all animal hxHbs evolved from a pentacoordinate ancestral state. In fact, phylogenetic evidence indicates that evolutionary transitions from an ancestral pentacoordinate state to a derived hexacoordinate state have occurred four times independently (Figure 1-3). As the tree in Fig. 3 illustrates, DrosHb, nHb of mollusks, Cgb of gnathostome vertebrates, and the Ngbs of all animals have each independently evolved hexacoordination from different ancestral starting points. There is no evidence of pentacoordinate Hbs arising from hxHbs in the metazoan phylogeny. However, the predominance of pentacoordinate Hbs in bacteria suggest that this coordination state has existed far longer than it has served as a scaffold for oxygen transport. Therefore, hxHbs could very well have evolved from pentacoordinate Hbs in contrast to earlier suggestions [15, 99].

References

[1] Hankeln T., Ebner B., Fuchs C., Gerlach F., Haberkamp M., Laufs T., Roesner A., Schmidt M., Weich B., Wystub S., Saaler-Reinhardt S., Reuss S., Bolognesi M., De Sanctis D., Marden M., Kiger L., Moens L., Dewilde S., Nevo E., Avivi A., Weber R., Fago A., Burmester T., Neuroglobin and cytoglobin in search of their role in the vertebrate globin family., J Inorg Biochem 99 (2005) 110-119.

[2] Burmester T., Ebner B., Weich B., Hankeln T., Cytoglobin: a novel globin type ubiquitously expressed in vertebrate tissues., Mol Biol Evol 19 (2002) 416-421.

[3] Wittenberg J., Bolognesi M., Wittenberg B., Guertin M., Truncated hemoglobins: a new family of hemoglobins widely distributed in bacteria, unicellular eukaryotes, and plants., J Biol Chem 277 (2002) 871-874.

[4] Smagghe B., Hoy J., Percifield R., Kundu S., Hargrove M., Sarath G., Hilbert J., Watts R., Dennis E., Peacock W., Dewilde S., Moens L., Blouin G., Olson J., Appleby C., Review: correlations between oxygen affinity and sequence classifications of plant hemoglobins., Biopolymers 91 (2009) 1083-1096.

[5] Murray J., Delumeau O., Lewis R., Structure of a nonheme globin in environmental stress signaling., Proc Natl Acad Sci U S A 102 (2005) 17320-17325.

[6] Smith L., Kahraman A., Thornton J., Heme proteins--diversity in structural characteristics, function, and folding., Proteins 78 (2010) 2349-2368.

[7] Hua S., Antao S., Corbett A., Witting P., The significance of neuroglobin in the brain., Curr Med Chem 17 (2010) 160-172.

[8] Herold S., Fago A., Weber R., Dewilde S., Moens L., Reactivity studies of the Fe(III) and Fe(II)NO forms of human neuroglobin reveal a potential role against oxidative stress., J Biol Chem 279 (2004) 22841-22847.

[9] Witting P., Douglas D., Mauk A., Reaction of human myoglobin and H2O2. Involvement of a thiyl radical produced at cysteine 110., J Biol Chem 275 (2000) 20391-20398.

[10] Trent J.r., Watts R., Hargrove M., Human neuroglobin, a hexacoordinate hemoglobin that reversibly binds oxygen., J Biol Chem 276 (2001) 30106-30110.

[11] Duff S., Wittenberg J., Hill R., Expression, purification, and properties of recombinant barley (Hordeum sp.) hemoglobin. Optical spectra and reactions with gaseous ligands., J Biol Chem 272 (1997) 16746-16752.

[12] Burmester T., Weich B., Reinhardt S., Hankeln T., A vertebrate globin expressed in the brain., Nature 407 (2000) 520-523.

[13] Scott N., Lecomte J., Cloning, expression, purification, and preliminary characterization of a putative hemoglobin from the cyanobacterium Synechocystis sp. PCC 6803., Protein Sci 9 (2000) 587-597.

[14] Appleby C., Tjepkema J., Trinick M., Hemoglobin in a Nonleguminous Plant, Parasponia: Possible Genetic Origin and Function in Nitrogen Fixation., Science 220 (1983) 951-953.

[15] Kundu S., Trent J.r., Hargrove M., Plants, humans and hemoglobins., Trends Plant Sci 8 (2003) 387-393.

[16] Bogusz D., Appleby C., Landsmann J., Dennis E., Trinick M., Peacock W., Functioning haemoglobin genes in non-nodulating plants., Nature 331 (1988) 178-180.

[17] Arredondo-Peter R., Hargrove M., Sarath G., Moran J., Lohrman J., Olson J., Klucas R., Rice hemoglobins. Gene cloning, analysis, and O2-binding kinetics of a recombinant protein synthesized in Escherichia coli., Plant Physiol 115 (1997) 1259-1266.
[18] Bruno S., Faggiano S., Spyrakis F., Mozzarelli A., Abbruzzetti S., Grandi E., Viappiani C., Feis A., Mackowiak S., Smulevich G., Cacciatori E., Dominici P., The reactivity with CO of AHb1 and AHb2 from Arabidopsis thaliana is controlled by the distal HisE7 and internal hydrophobic cavities., J Am Chem Soc 129 (2007) 2880-2889.
[19] Yamauchi K., Tada H., Usuki I., Structure and evolution of Paramecium hemoglobin genes., Biochim Biophys Acta 1264 (1995) 53-62.
[20] Iwaasa H., Takagi T., Shikama K., Protozoan myoglobin from Paramecium caudatum. Its unusual amino acid sequence., J Mol Biol 208 (1989) 355-358.
[21] Iwaasa H., Takagi T., Shikama K., Protozoan hemoglobin from Tetrahymena pyriformis. Isolation, characterization, and amino acid sequence., J Biol Chem 265 (1990) 8603-8609.
[22] Takagi T., Iwaasa H., Yuasa H., Shikama K., Takemasa T., Watanabe Y., Primary structure of Tetrahymena hemoglobins., Biochim Biophys Acta 1173 (1993) 75-78.
[23] Potts M., Angeloni S., Ebel R., Bassam D., Myoglobin in a cyanobacterium., Science 256 (1992) 1690-1691.
[24] Couture M., Das T., Lee H., Peisach J., Rousseau D., Wittenberg B., Wittenberg J., Guertin M., Chlamydomonas chloroplast ferrous hemoglobin. Heme pocket structure and reactions with ligands., J Biol Chem 274 (1999) 6898-6910.
[25] Couture M., Yeh S., Wittenberg B., Wittenberg J., Ouellet Y., Rousseau D., Guertin M., A cooperative oxygen-binding hemoglobin from Mycobacterium tuberculosis., Proc Natl Acad Sci U S A 96 (1999) 11223-11228.
[26] Watts R., Hunt P., Hvitved A., Hargrove M., Peacock W., Dennis E., A hemoglobin from plants homologous to truncated hemoglobins of microorganisms., Proc Natl Acad Sci U S A 98 (2001) 10119-10124.
[27] Vinogradov S., Hoogewijs D., Bailly X., Arredondo-Peter R., Guertin M., Gough J., Dewilde S., Moens L., Vanfleteren J., Three globin lineages belonging to two structural classes in genomes from the three kingdoms of life., Proc Natl Acad Sci U S A 102 (2005) 11385-11389.
[28] Hvitved A., Trent J.r., Premer S., Hargrove M., Ligand binding and hexacoordination in synechocystis hemoglobin., J Biol Chem 276 (2001) 34714-34721.
[29] Couture M., Das T., Savard P., Ouellet Y., Wittenberg J., Wittenberg B., Rousseau D., Guertin M., Structural investigations of the hemoglobin of the cyanobacterium Synechocystis PCC6803 reveal a unique distal heme pocket., Eur J Biochem 267 (2000) 4770-4780.
[30] Hoy J., Kundu S., Trent J.r., Ramaswamy S., Hargrove M., The crystal structure of Synechocystis hemoglobin with a covalent heme linkage., J Biol Chem 279 (2004) 16535-16542.
[31] Vu B., Jones A., Lecomte J., Novel histidine-heme covalent linkage in a hemoglobin., J Am Chem Soc 124 (2002) 8544-8545.
[32] Fuchs C., Heib V., Kiger L., Haberkamp M., Roesner A., Schmidt M., Hamdane D., Marden M., Hankeln T., Burmester T., Zebrafish reveals different and conserved features of vertebrate neuroglobin gene structure, expression pattern, and ligand binding., J Biol Chem 279 (2004) 24116-24122.
[33] Trent J.r., Hargrove M., A ubiquitously expressed human hexacoordinate hemoglobin., J Biol Chem 277 (2002) 19538-19545.

[34] Dewilde S., Ebner B., Vinck E., Gilany K., Hankeln T., Burmester T., Kreiling J., Reinisch C., Vanfleteren J., Kiger L., Marden M., Hundahl C., Fago A., Van Doorslaer S., Moens L., The nerve hemoglobin of the bivalve mollusc Spisula solidissima: molecular cloning, ligand binding studies, and phylogenetic analysis., J Biol Chem 281 (2006) 5364-5372.
[35] de Sanctis D., Dewilde S., Vonrhein C., Pesce A., Moens L., Ascenzi P., Hankeln T., Burmester T., Ponassi M., Nardini M., Bolognesi M., Bishistidyl heme hexacoordination, a key structural property in Drosophila melanogaster hemoglobin., J Biol Chem 280 (2005) 27222-27229.
[36] Fuchs C., Burmester T., Hankeln T., The amphibian globin gene repertoire as revealed by the Xenopus genome., Cytogenet Genome Res 112 (2006) 296-306.
[37] Roesner A., Fuchs C., Hankeln T., Burmester T., A globin gene of ancient evolutionary origin in lower vertebrates: evidence for two distinct globin families in animals., Mol Biol Evol 22 (2005) 12-20.
[38] Mitchell D., Kitto G., Hackert M., Structural analysis of monomeric hemichrome and dimeric cyanomet hemoglobins from Caudina arenicola., J Mol Biol 251 (1995) 421-431.
[39] Dewilde S., Kiger L., Burmester T., Hankeln T., Baudin-Creuza V., Aerts T., Marden M., Caubergs R., Moens L., Biochemical characterization and ligand binding properties of neuroglobin, a novel member of the globin family., J Biol Chem 276 (2001) 38949-38955.
[40] Hamdane D., Kiger L., Dewilde S., Green B., Pesce A., Uzan J., Burmester T., Hankeln T., Bolognesi M., Moens L., Marden M., The redox state of the cell regulates the ligand binding affinity of human neuroglobin and cytoglobin., J Biol Chem 278 (2003) 51713-51721.
[41] Smagghe B., Sarath G., Ross E., Hilbert J., Hargrove M., Slow ligand binding kinetics dominate ferrous hexacoordinate hemoglobin reactivities and reveal differences between plants and other species., Biochemistry 45 (2006) 561-570.
[42] Hankeln T., Jaenicke V., Kiger L., Dewilde S., Ungerechts G., Schmidt M., Urban J., Marden M., Moens L., Burmester T., Characterization of Drosophila hemoglobin. Evidence for hemoglobin-mediated respiration in insects., J Biol Chem 277 (2002) 29012-29017.
[43] Antonini E., and Brunori, M., Hemoglobin and Myoglobin in Their Reactions with Ligands, North-Holland Publishing Company, Amsterdam., 1971.
[44] Peisach J., Blumberg W., Wittenberg B., Wittenberg J., Kampa L., Hemoglobin A: an electron paramagnetic resonance study of the effects of interchain contacts on the heme symmetry of high-spin and low-spin derivatives of ferric alpha chains., Proc Natl Acad Sci U S A 63 (1969) 934-939.
[45] Halder P., Trent J.r., Hargrove M., Influence of the protein matrix on intramolecular histidine ligation in ferric and ferrous hexacoordinate hemoglobins., Proteins 66 (2007) 172-182.
[46] Dou Y., Admiraal S., Ikeda-Saito M., Krzywda S., Wilkinson A., Li T., Olson J., Prince R., Pickering I., George G., Alteration of axial coordination by protein engineering in myoglobin. Bisimidazole ligation in the His64-->Val/Val68-->His double mutant., J Biol Chem 270 (1995) 15993-16001.
[47] Hargrove M., A flash photolysis method to characterize hexacoordinate hemoglobin kinetics., Biophys J 79 (2000) 2733-2738.
[48] Brancaccio A., Cutruzzolá F., Allocatelli C., Brunori M., Smerdon S., Wilkinson A., Dou Y., Keenan D., Ikeda-Saito M., Brantley R.J., Structural factors governing azide and cyanide binding to mammalian metmyoglobins., J Biol Chem 269 (1994) 13843-13853.

[49] Coletta M., Angeletti M., De Sanctis G., Cerroni L., Giardina B., Amiconi G., Ascenzi P., Kinetic evidence for the existence of a rate-limiting step in the reaction of ferric hemoproteins with anionic ligands., Eur J Biochem 235 (1996) 49-53.
[50] Smagghe B., Halder P., Hargrove M., Measurement of distal histidine coordination equilibrium and kinetics in hexacoordinate hemoglobins., Methods Enzymol 436 (2008) 359-378.
[51] Brantley R.J., Smerdon S., Wilkinson A., Singleton E., Olson J., The mechanism of autooxidation of myoglobin., J Biol Chem 268 (1993) 6995-7010.
[52] Olson J., Phillips G.J., Kinetic pathways and barriers for ligand binding to myoglobin., J Biol Chem 271 (1996) 17593-17596.
[53] Liong E., Dou Y., Scott E., Olson J., Phillips G.J., Waterproofing the heme pocket. Role of proximal amino acid side chains in preventing hemin loss from myoglobin., J Biol Chem 276 (2001) 9093-9100.
[54] Aranda R.t., Cai H., Worley C., Levin E., Li R., Olson J., Phillips G.J., Richards M., Structural analysis of fish versus mammalian hemoglobins: effect of the heme pocket environment on autooxidation and hemin loss., Proteins 75 (2009) 217-230.
[55] Murray J., Wyman J., Facilitated diffusion. The case of carbon monoxide., J Biol Chem 246 (1971) 5903-5906.
[56] Gibson Q., Wittenberg J., Wittenberg B., Bogusz D., Appleby C., The kinetics of ligand binding to plant hemoglobins. Structural implications., J Biol Chem 264 (1989) 100-107.
[57] Wittenberg J., Appleby C., Wittenberg B., The kinetics of the reactions of leghemoglobin with oxygen and carbon monoxide., J Biol Chem 247 (1972) 527-531.
[58] Weiland T., Kundu S., Trent J.r., Hoy J., Hargrove M., Bis-histidyl hexacoordination in hemoglobins facilitates heme reduction kinetics., J Am Chem Soc 126 (2004) 11930-11935.
[59] Russwurm M., Koesling D., NO activation of guanylyl cyclase., EMBO J 23 (2004) 4443-4450.
[60] Ignarro L., Haem-dependent activation of guanylate cyclase and cyclic GMP formation by endogenous nitric oxide: a unique transduction mechanism for transcellular signaling., Pharmacol Toxicol 67 (1990) 1-7.
[61] Eich R., Li T., Lemon D., Doherty D., Curry S., Aitken J., Mathews A., Johnson K., Smith R., Phillips G.J., Olson J., Mechanism of NO-induced oxidation of myoglobin and hemoglobin., Biochemistry 35 (1996) 6976-6983.
[62] Brunori M., Nitric oxide, cytochrome-c oxidase and myoglobin., Trends Biochem Sci 26 (2001) 21-23.
[63] Gardner P., Nitric oxide dioxygenase function and mechanism of flavohemoglobin, hemoglobin, myoglobin and their associated reductases., J Inorg Biochem 99 (2005) 247-266.
[64] Gardner P., Gardner A., Martin L., Salzman A., Nitric oxide dioxygenase: an enzymic function for flavohemoglobin., Proc Natl Acad Sci U S A 95 (1998) 10378-10383.
[65] Gow A., Luchsinger B., Pawloski J., Singel D., Stamler J., The oxyhemoglobin reaction of nitric oxide., Proc Natl Acad Sci U S A 96 (1999) 9027-9032.
[66] Gardner P., Gardner A., Brashear W., Suzuki T., Hvitved A., Setchell K., Olson J., Hemoglobins dioxygenate nitric oxide with high fidelity., J Inorg Biochem 100 (2006) 542-550.
[67] Van Doorslaer S., Dewilde S., Kiger L., Nistor S., Goovaerts E., Marden M., Moens L., Nitric oxide binding properties of neuroglobin. A characterization by EPR and flash photolysis., J Biol Chem 278 (2003) 4919-4925.

[68] Smagghe B., Trent J.r., Hargrove M., NO dioxygenase activity in hemoglobins is ubiquitous in vitro, but limited by reduction in vivo., PLoS One 3 (2008) e2039.
[69] Ford P., Fernandez B., Lim M., Mechanisms of reductive nitrosylation in iron and copper models relevant to biological systems., Chem Rev 105 (2005) 2439-2455.
[70] Fernandez B., Lorkovic I., Ford P., Mechanisms of ferriheme reduction by nitric oxide: nitrite and general base catalysis., Inorg Chem 43 (2004) 5393-5402.
[71] Hoshino M., Masahiro M., Reiko K., Seki H., Ford Peter C., Studies on the Reaction Mechanism for Reductive Nitrosylation of Ferrihemoproteins in buffer solutions, Journal of American Chemical Society 118 (1996) 5702-5707.
[72] Brunori M., Giuffrè A., Nienhaus K., Nienhaus G., Scandurra F., Vallone B., Neuroglobin, nitric oxide, and oxygen: functional pathways and conformational changes., Proc Natl Acad Sci U S A 102 (2005) 8483-8488.
[73] Perazzolli M., Romero-Puertas M., Delledonne M., Modulation of nitric oxide bioactivity by plant haemoglobins., J Exp Bot 57 (2006) 479-488.
[74] Minning D., Gow A., Bonaventura J., Braun R., Dewhirst M., Goldberg D., Stamler J., Ascaris haemoglobin is a nitric oxide-activated 'deoxygenase'. Nature 401 (1999) 497-502.
[75] Perazzolli M., Dominici P., Romero-Puertas M., Zago E., Zeier J., Sonoda M., Lamb C., Delledonne M., Arabidopsis nonsymbiotic hemoglobin AHb1 modulates nitric oxide bioactivity., Plant Cell 16 (2004) 2785-2794.
[76] Dordas C., Hasinoff B., Rivoal J., Hill R., Class-1 hemoglobins, nitrate and NO levels in anoxic maize cell-suspension cultures., Planta 219 (2004) 66-72.
[77] Delledonne M., NO news is good news for plants., Curr Opin Plant Biol 8 (2005) 390-396.
[78] Halligan K., Jourd'heuil F., Jourd'heuil D., Cytoglobin Is Expressed in the Vasculature and Regulates Cell Respiration and Proliferation via Nitric Oxide Dioxygenation., J Biol Chem 284 (2009) 8539-8547.
[79] Igamberdiev A., Bykova N., Hill R., Nitric oxide scavenging by barley hemoglobin is facilitated by a monodehydroascorbate reductase-mediated ascorbate reduction of methemoglobin., Planta 223 (2006) 1033-1040.
[80] de Sanctis D., Dewilde S., Pesce A., Moens L., Ascenzi P., Hankeln T., Burmester T., Bolognesi M., Crystal structure of cytoglobin: the fourth globin type discovered in man displays heme hexa-coordination., J Mol Biol 336 (2004) 917-927.
[81] Vallone B., Nienhaus K., Brunori M., Nienhaus G., The structure of murine neuroglobin: Novel pathways for ligand migration and binding., Proteins 56 (2004) 85-92.
[82] Vallone B., Nienhaus K., Matthes A., Brunori M., Nienhaus G., The structure of carbonmonoxy neuroglobin reveals a heme-sliding mechanism for control of ligand affinity., Proc Natl Acad Sci U S A 101 (2004) 17351-17356.
[83] de Sanctis D., Ascenzi P., Bocedi A., Dewilde S., Burmester T., Hankeln T., Moens L., Bolognesi M., Cyanide binding and heme cavity conformational transitions in Drosophila melanogaster hexacoordinate hemoglobin., Biochemistry 45 (2006) 10054-10061.
[84] Hargrove M., Brucker E., Stec B., Sarath G., Arredondo-Peter R., Klucas R., Olson J., Phillips G.J., Crystal structure of a nonsymbiotic plant hemoglobin., Structure 8 (2000) 1005-1014.
[85] Hoy J., Robinson H., Trent J.r., Kakar S., Smagghe B., Hargrove M., Plant hemoglobins: a molecular fossil record for the evolution of oxygen transport., J Mol Biol 371 (2007) 168-179.

[86] Trent J.r., Kundu S., Hoy J., Hargrove M., Crystallographic analysis of synechocystis cyanoglobin reveals the structural changes accompanying ligand binding in a hexacoordinate hemoglobin., J Mol Biol 341 (2004) 1097-1108.
[87] Yoon J., Herzik M., Winter M., Tran R., Olea C., Marletta M., Structure and Properties of a Bis-Histidyl Ligated Globin from Caenorhabditis elegans . Biochemistry (2010).
[88] Schmidt M., Gerlach F., Avivi A., Laufs T., Wystub S., Simpson J., Nevo E., Saaler-Reinhardt S., Reuss S., Hankeln T., Burmester T., Cytoglobin is a respiratory protein in connective tissue and neurons, which is up-regulated by hypoxia., J Biol Chem 279 (2004) 8063-8069.
[89] Ostojić J., Sakaguchi D., de Lathouder Y., Hargrove M., Trent J.r., Kwon Y., Kardon R., Kuehn M., Betts D., Grozdanić S., Neuroglobin and cytoglobin: oxygen-binding proteins in retinal neurons., Invest Ophthalmol Vis Sci 47 (2006) 1016-1023.
[90] Schmidt M., Laufs T., Reuss S., Hankeln T., Burmester T., Divergent distribution of cytoglobin and neuroglobin in the murine eye., Neurosci Lett 374 (2005) 207-211.
[91] Goodman M., Hargrove M., Quaternary structure of rice nonsymbiotic hemoglobin., J Biol Chem 276 (2001) 6834-6839.
[92] Fago A., Hundahl C., Dewilde S., Gilany K., Moens L., Weber R., Allosteric regulation and temperature dependence of oxygen binding in human neuroglobin and cytoglobin. Molecular mechanisms and physiological significance., J Biol Chem 279 (2004) 44417-44426.
[93] Pesce A., Couture M., Dewilde S., Guertin M., Yamauchi K., Ascenzi P., Moens L., Bolognesi M., A novel two-over-two alpha-helical sandwich fold is characteristic of the truncated hemoglobin family., EMBO J 19 (2000) 2424-2434.
[94] Laberge M., Yonetani T., Common dynamics of globin family proteins., IUBMB Life 59 (2007) 528-534.
[95] de Sanctis D., Pesce A., Nardini M., Bolognesi M., Bocedi A., Ascenzi P., Structure-function relationships in the growing hexa-coordinate hemoglobin sub-family., IUBMB Life 56 (2004) 643-651.
[96] Van Doorslaer S., Vinck E., Trandafir F., Ioanitescu I., Dewilde S., Moens L., Tracing the structure-function relationship of neuroglobin and cytoglobin using resonance Raman and electron paramagnetic resonance spectroscopy., IUBMB Life 56 (2004) 665-670.
[97] Du W., Syvitski R., Dewilde S., Moens L., La Mar G., Solution 1h NMR characterization of equilibrium heme orientational disorder with functional consequences in mouse neuroglobin., J Am Chem Soc 125 (2003) 8080-8081.
[98] Walker F., The heme environment of mouse neuroglobin: histidine imidazole plane orientations obtained from solution NMR and EPR spectroscopy as compared with X-ray crystallography., J Biol Inorg Chem 11 (2006) 391-397.
[99] Brunori M., Vallone B., Neuroglobin, seven years after., Cell Mol Life Sci 64 (2007) 1259-1268.
[100] Vinck E., Van Doorslaer S., Dewilde S., Mitrikas G., Schweiger A., Moens L., Analyzing heme proteins using EPR techniques: the heme-pocket structure of ferric mouse neuroglobin., J Biol Inorg Chem 11 (2006) 467-475.
[101] Vinck E., Van Doorslaer S., Dewilde S., Moens L., Structural change of the heme pocket due to disulfide bridge formation is significantly larger for neuroglobin than for cytoglobin., J Am Chem Soc 126 (2004) 4516-4517.
[102] Durley R., Mathews F., Refinement and structural analysis of bovine cytochrome b5 at 1.5 A resolution., Acta Crystallogr D Biol Crystallogr 52 (1996) 65-76.

[103] Xu Z., Farid R., Design, synthesis, and characterization of a novel hemoprotein., Protein Sci 10 (2001) 236-249.
[104] Pesce A., Dewilde S., Nardini M., Moens L., Ascenzi P., Hankeln T., Burmester T., Bolognesi M., Human brain neuroglobin structure reveals a distinct mode of controlling oxygen affinity., Structure 11 (2003) 1087-1095.
[105] Hargrove M., Barry J., Brucker E., Berry M., Phillips G.J., Olson J., Arredondo-Peter R., Dean J., Klucas R., Sarath G., Characterization of recombinant soybean leghemoglobin a and apolar distal histidine mutants., J Mol Biol 266 (1997) 1032-1042.
[106] Burmester T., Hankeln T., What is the function of neuroglobin?, J Exp Biol 212 (2009) 1423-1428.
[107] Wakasugi K., Nakano T., Morishima I., Oxidized human neuroglobin acts as a heterotrimeric Galpha protein guanine nucleotide dissociation inhibitor., J Biol Chem 278 (2003) 36505-36512.
[108] Wakasugi K., Morishima I., Identification of residues in human neuroglobin crucial for Guanine nucleotide dissociation inhibitor activity., Biochemistry 44 (2005) 2943-2948.
[109] Lewerenz J., Letz J., Methner A., Activation of stimulatory heterotrimeric G proteins increases glutathione and protects neuronal cells against oxidative stress., J Neurochem 87 (2003) 522-531.
[110] Wakasugi K., Kitatsuji C., Morishima I., Possible neuroprotective mechanism of human neuroglobin., Ann N Y Acad Sci 1053 (2005) 220-230.
[111] Moens L., Dewilde S., Globins in the brain., Nature 407 (2000) 461-462.
[112] Burmester T., Hankeln T., Neuroglobin: a respiratory protein of the nervous system., News Physiol Sci 19 (2004) 110-113.
[113] Schmidt M., Giessl A., Laufs T., Hankeln T., Wolfrum U., Burmester T., How does the eye breathe? Evidence for neuroglobin-mediated oxygen supply in the mammalian retina., J Biol Chem 278 (2003) 1932-1935.
[114] Sun Y., Jin K., Mao X., Zhu Y., Greenberg D., Neuroglobin is up-regulated by and protects neurons from hypoxic-ischemic injury., Proc Natl Acad Sci U S A 98 (2001) 15306-15311.
[115] Schmidt-Kastner R., Haberkamp M., Schmitz C., Hankeln T., Burmester T., Neuroglobin mRNA expression after transient global brain ischemia and prolonged hypoxia in cell culture., Brain Res 1103 (2006) 173-180.
[116] Mammen P., Shelton J., Goetsch S., Williams S., Richardson J., Garry M., Garry D., Neuroglobin, a novel member of the globin family, is expressed in focal regions of the brain., J Histochem Cytochem 50 (2002) 1591-1598.
[117] Hundahl C., Stoltenberg M., Fago A., Weber R., Dewilde S., Fordel E., Danscher G., Effects of short-term hypoxia on neuroglobin levels and localization in mouse brain tissues., Neuropathol Appl Neurobiol 31 (2005) 610-617.
[118] Fago A., Mathews A., Brittain T., A role for neuroglobin: resetting the trigger level for apoptosis in neuronal and retinal cells., IUBMB Life 60 (2008) 398-401.
[119] Sun Y., Jin K., Peel A., Mao X., Xie L., Greenberg D., Neuroglobin protects the brain from experimental stroke in vivo., Proc Natl Acad Sci U S A 100 (2003) 3497-3500.
[120] Wang X., Liu J., Zhu H., Tejima E., Tsuji K., Murata Y., Atochin D., Huang P., Zhang C., Lo E., Effects of neuroglobin overexpression on acute brain injury and long-term outcomes after focal cerebral ischemia., Stroke 39 (2008) 1869-1874.

[121] Liu J., Yu Z., Guo S., Lee S., Xing C., Zhang C., Gao Y., Nicholls D., Lo E., Wang X., Effects of neuroglobin overexpression on mitochondrial function and oxidative stress following hypoxia/reoxygenation in cultured neurons., J Neurosci Res 87 (2009) 164-170.
[122] Khan A., Wang Y., Sun Y., Mao X., Xie L., Miles E., Graboski J., Chen S., Ellerby L., Jin K., Greenberg D., Neuroglobin-overexpressing transgenic mice are resistant to cerebral and myocardial ischemia., Proc Natl Acad Sci U S A 103 (2006) 17944-17948.
[123] Jin K., Mao Y., Mao X., Xie L., Greenberg D., Neuroglobin expression in ischemic stroke., Stroke 41 (2010) 557-559.
[124] Moschetti T., Giuffrè A., Ardiccioni C., Vallone B., Modjtahedi N., Kroemer G., Brunori M., Failure of apoptosis-inducing factor to act as neuroglobin reductase., Biochem Biophys Res Commun 390 (2009) 121-124.
[125] Trandafir F., Hoogewijs D., Altieri F., Rivetti di Val Cervo P., Ramser K., Van Doorslaer S., Vanfleteren J., Moens L., Dewilde S., Neuroglobin and cytoglobin as potential enzyme or substrate., Gene 398 (2007) 103-113.
[126] Fago A., Mathews A., Moens L., Dewilde S., Brittain T., The reaction of neuroglobin with potential redox protein partners cytochrome b5 and cytochrome c., FEBS Lett 580 (2006) 4884-4888.
[127] Raychaudhuri S., Skommer J., Henty K., Birch N., Brittain T., Neuroglobin protects nerve cells from apoptosis by inhibiting the intrinsic pathway of cell death., Apoptosis 15 (2010) 401-411.
[128] Kawada N., Kristensen D., Asahina K., Nakatani K., Minamiyama Y., Seki S., Yoshizato K., Characterization of a stellate cell activation-associated protein (STAP) with peroxidase activity found in rat hepatic stellate cells., J Biol Chem 276 (2001) 25318-25323.
[129] Springer B.A., Sliger S.G., Olson J.S., Phillips G.N.J., Mechanisms of ligand recognition in myoglobin, Chemical Reviews 94 (1994) 699-714.
[130] Fordel E., Geuens E., Dewilde S., Rottiers P., Carmeliet P., Grooten J., Moens L., Cytoglobin expression is upregulated in all tissues upon hypoxia: an in vitro and in vivo study by quantitative real-time PCR., Biochem Biophys Res Commun 319 (2004) 342-348.
[131] Xi Y., Obara M., Ishida Y., Ikeda S., Yoshizato K., Gene expression and tissue distribution of cytoglobin and myoglobin in the Amphibia and Reptilia: possible compensation of myoglobin with cytoglobin in skeletal muscle cells of anurans that lack the myoglobin gene., Gene 398 (2007) 94-102.
[132] Hodges N., Innocent N., Dhanda S., Graham M., Cellular protection from oxidative DNA damage by over-expression of the novel globin cytoglobin in vitro., Mutagenesis 23 (2008) 293-298.
[133] Shivapurkar N., Stastny V., Okumura N., Girard L., Xie Y., Prinsen C., Thunnissen F., Wistuba I., Czerniak B., Frenkel E., Roth J., Liloglou T., Xinarianos G., Field J., Minna J., Gazdar A., Cytoglobin, the newest member of the globin family, functions as a tumor suppressor gene., Cancer Res 68 (2008) 7448-7456.
[134] Burmester T., Hankeln T., A globin gene of Drosophila melanogaster., Mol Biol Evol 16 (1999) 1809-1811.
[135] Gleixner E., Abriss D., Adryan B., Kraemer M., Gerlach F., Schuh R., Burmester T., Hankeln T., Oxygen-induced changes in hemoglobin expression in Drosophila., FEBS J 275 (2008) 5108-5116.
[136] Weber R., Vinogradov S., Nonvertebrate hemoglobins: functions and molecular adaptations., Physiol Rev 81 (2001) 569-628.

[137] Kraus D., Colacino J., Extended Oxygen Delivery from the Nerve Hemoglobin of Tellina alternata (Bivalvia). Science 232 (1986) 90-92.
[138] Choi D., Zea C., Do Y., Semrau J., Antholine W., Hargrove M., Pohl N., Boyd E., Geesey G., Hartsel S., Shafe P., McEllistrem M., Kisting C., Campbell D., Rao V., de la Mora A., Dispirito A., Spectral, kinetic, and thermodynamic properties of Cu(I) and Cu(II) binding by methanobactin from Methylosinus trichosporium OB3b., Biochemistry 45 (2006) 1442-1453.
[139] Robinson V., Smith B., Arnone A., A pH-dependent aquomet-to-hemichrome transition in crystalline horse methemoglobin., Biochemistry 42 (2003) 10113-10125.
[140] Sowa A., Duff S., Guy P., Hill R., Altering hemoglobin levels changes energy status in maize cells under hypoxia., Proc Natl Acad Sci U S A 95 (1998) 10317-10321.
[141] Nie X., Hill R., Mitochondrial Respiration and Hemoglobin Gene Expression in Barley Aleurone Tissue., Plant Physiol 114 (1997) 835-840.
[142] Dordas C., Hasinoff B., Igamberdiev A., Manac'h N., Rivoal J., Hill R., Expression of a stress-induced hemoglobin affects NO levels produced by alfalfa root cultures under hypoxic stress., Plant J 35 (2003) 763-770.
[143] Igamberdiev A., Seregélyes C., Manac'h N., Hill R., NADH-dependent metabolism of nitric oxide in alfalfa root cultures expressing barley hemoglobin., Planta 219 (2004) 95-102.
[144] Bruno S., Faggiano S., Spyrakis F., Mozzarelli A., Cacciatori E., Dominici P., Grandi E., Abbruzzetti S., Viappiani C., Different roles of protein dynamics and ligand migration in non-symbiotic hemoglobins AHb1 and AHb2 from Arabidopsis thaliana., Gene 398 (2007) 224-233.
[145] Vieweg M., Hohnjec N., Küster H., Two genes encoding different truncated hemoglobins are regulated during root nodule and arbuscular mycorrhiza symbioses of Medicago truncatula., Planta 220 (2005) 757-766.
[146] Sturms R., Kakar S., Trent J., Hargrove M., Trema and Parasponia hemoglobins reveal convergent evolution of oxygen transport in plants., Biochemistry (2010).
[147] Olson J., Mathews A., Rohlfs R., Springer B., Egeberg K., Sligar S., Tame J., Renaud J., Nagai K., The role of the distal histidine in myoglobin and haemoglobin., Nature 336 (1988) 265-266.
[148] Kiger L., Uzan J., Dewilde S., Burmester T., Hankeln T., Moens L., Hamdane D., Baudin-Creuza V., Marden M., Neuroglobin ligand binding kinetics., IUBMB Life 56 (2004) 709-719.
[149] Hundahl C., Fago A., Dewilde S., Moens L., Hankeln T., Burmester T., Weber R., Oxygen binding properties of non-mammalian nerve globins., FEBS J 273 (2006) 1323-1329.
[150] Watts R., Characterization of Nonsymbiotic Hemoglobins from Dicotyledonous Plants., Division of Biochemistry and Molecular Biology, vol. Ph.D., Australian National University, 1999.

CHAPTER 2. *TREMA* AND *PARASPONIA* HEMOGLOBINS REVEAL CONVERGENT EVOLUTION OF OXYGEN TRANSPORT IN PLANTS

A paper published in the journal *Biochemistry*

Ryan Sturms[1], Smita Kakar[1], James Trent, III, and Mark S. Hargrove[1,2]

Abstract:

All plants contain hemoglobins that fall into distinct phylogenetic classes. The subset of plants that carry out symbiotic nitrogen fixation express hemoglobins that scavenge and transport oxygen to bacterial symbiotes within root nodules. These "symbiotic" oxygen transport hemoglobins are distinct in structure and function from the non-oxygen transport ("nonsymbiotic") Hbs found in all plants. Hemoglobins found in two closely related plants present a paradox concerning hemoglobin structure and function. *Parasponia andersonii* is a nitrogen fixing plant that expresses a symbiotic hemoglobin (ParaHb) characteristic of oxygen transport hemoglobins in having a pentacoordinate ferrous heme iron, moderate oxygen affinity, and a relatively rapid oxygen dissociation rate constant. A close relative that does not fix nitrogen, *Trema tomentosa*, expresses hemoglobin (TremaHb) sharing 93% amino acid identity to ParaHb, but its phylogeny predicts a typical nonsymbiotic hemoglobin with a hexacoordinate

---

[1]Department of Biochemistry, Biophysics, and Molecular Biology; Iowa State University, Ames, IA 50011

[3]To whom correspondence should be addressed

heme iron, high oxygen affinity, and slow oxygen dissociation rate constant. Here we characterize heme coordination and oxygen binding in TremaHb and ParaHb to investigate whether or not two hemoglobins with such high sequence similarity are actually so different in functional behavior. Our results indicate that the two proteins resemble nonsymbiotic hemoglobins in the ferric oxidation state, and symbiotic hemoglobins in the ferrous oxidation state. They differ from each other only in oxygen affinity and oxygen dissociation rate constants, two factors key to their different functions. These results demonstrate distinct mechanisms for convergent evolution of oxygen transport in different phylogenetic classes of plant hemoglobins.

Introduction

The history of hemoglobins (Hbs) predates the photosynthetic oxygenation of earth [1-3]. The "oxygen catastrophe" that occurred approximately two billion years ago greatly increased atmospheric oxygen, forcing organisms to avoid, tolerate, or exploit this change in their physiochemical environments. Thus, early Hbs probably protected cells from oxygen toxicity [4, 5]. As aerobic organisms grew larger and evolved more specialized tissues, their surface-to-volume ratios decreased, and passive oxygen diffusion became limiting. In response to this pressure, oxygen transport mechanisms evolved nearly 500 million years ago enabling organisms to grow to unprecedented size, complexity, and diversity [2]. The modern day forms of these proteins are the hemocyanins in mollusks and arthropods, hemerythrins in marine worms, and oxygen transport Hbs in animals and plants. However, oxygen transport is certainly not the primordial, or even the most common function of Hbs [6, 7]. Bacterial and yeast Hbs destroy toxic molecules like nitric oxide encountered in their environments [8], and animals contain

specialized Hbs in neural and other tissues that are suggested to do the same [9-11]. Although a few plant species contain oxygen transport Hbs, all plants contain Hbs unrelated to oxygen transport [12]. The fact that the majority of Hbs do not function in oxygen transport suggests that the capacity for oxygen transport is a fairly recent development in the Hb evolutionary timeline.

A comparison of oxygen transport Hbs in plants and animals to the other Hbs present in the same organisms reveal distinct differences in structure and behavior [13]. Oxygen transport Hbs are present in high millimolar concentrations, and their rate constants for oxygen release are relatively rapid (greater than 1 s^{-1}). Moreover, their association equilibrium constants are moderate, enabling them to bind oxygen when it is present, yet release it when needed. The heme groups in known oxygen transporters are "pentacoordinate" with an open binding site to the iron, characterized by a single histidine coordinating the "proximal" side of the heme, leaving the "distal" site open for reversible oxygen binding (Figure 2-1). The distal site often houses another histidine (called the "distal" histidine) that does not coordinate the heme iron, but is in close proximity to and interacts with bound oxygen.

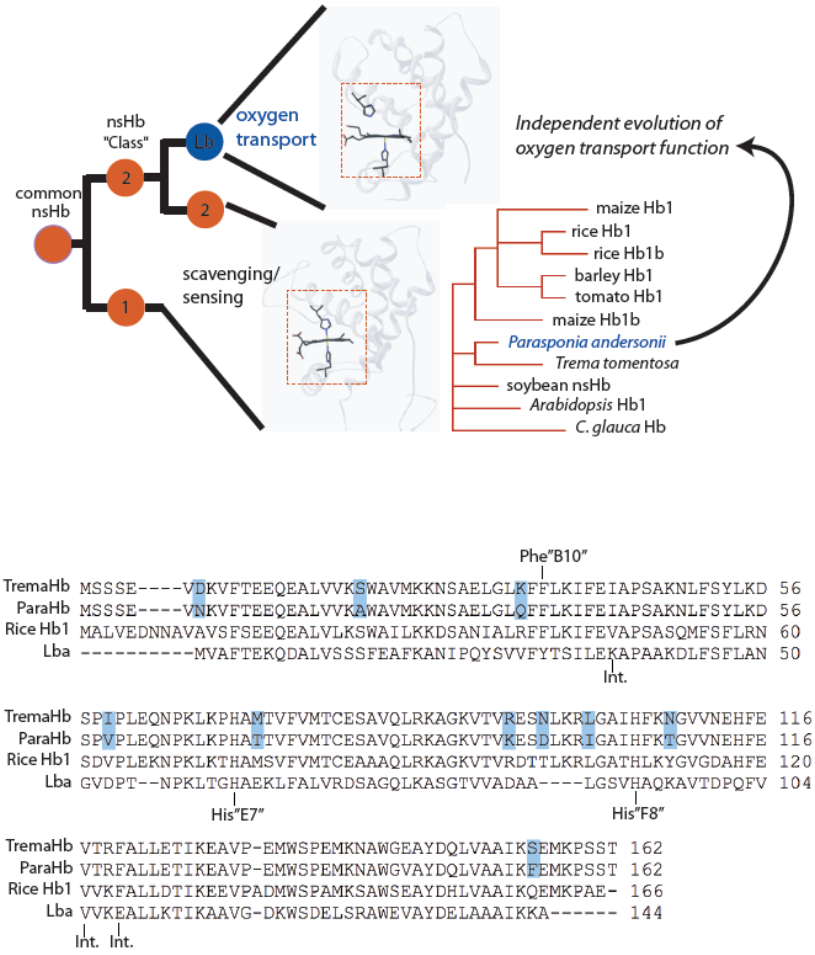

Figure 2-1. The phylogeny of oxygen transport hemoglobins in plants. Oxygen transport Hbs have evolved from two phylogenetic Classes of nonsymbiotic Hbs (nsHbs). In each case, the oxygen transport proteins are pentacoordinate in the ferrous state (top inset structure), while the precursor nsHbs are hexacoordinate (bottom inset structure). The oxygen transport leghemoglobins (Lbs) evolved from "Class 2" nonsymbiotic Hb (nsHbs), while *Parasponia andersonii* is a Class 1-derived oxygen transport Hb (ParaHb) that is 93% identical to the nsHb from *Trema tomentosa*. The amino acid sequences for ParaHb, TremaHb, rice nsHb, and soybean Lba are shown at the bottom, with the 11 differences between ParaHb and TremaHb highlighted in blue. Also indicated on the sequences are the distal (E7) and proximal (F8) histidines, phenylalanine at position B10, and the positions of conserved dimer interface amino acids (Int.).

Hbs not involved in oxygen transport, including the "nonsymbiotic" (nsHbs) found in all plants, as well as neuroglobin [14-16] and cytoglobin [17, 18] found in animals, have a second histidine reversibly coordinating the ligand binding site (Figure 2-1). While these proteins share

globin folds, their heme active sites resemble that of cytochrome *b5*. These Hbs are known as "hexacoordinate" Hbs (hxHbs), and their structures and chemistries are subjects of increasing attention due to potential roles in sensing and detoxifying nitric oxide and other environmental challenges.

It has been hypothesized that oxygen transport Hbs evolved from hxHbs independently in both plants and animals [14, 19, 20]. In both cases, the chemical challenge was to express hemoglobin with stable pentacoordinate heme coordination. This is a difficult task to achieve because the change in spin state of the iron d-shell electrons upon histidine coordination is energetically very favorable [21-23], and holding a histidine near the heme iron without allowing it to bind presents a formidable thermodynamic challenge. Thus, an oxygen transport Hb must provide a protein scaffold that can offset this coordination energy in order to stabilize a pentacoordinate heme center.

The evolution of oxygen transport function in plant Hbs occurred more recently (around 200 million years ago [20, 24-26]) than in animal Hbs, making them a useful system for investigating protein structural elements that are instrumental in this change of function. The phylogeny of plant Hbs can be divided into three general classes, two of which are known predecessors of oxygen transport globins [12]. The familiar oxygen transport "leghemoglobins" (Lbs) common to the legume family evolved from "Class 2" nsHbs, and still share ~ 40% sequence identity with nsHbs (compared to less than 20% for red blood cell Hb and non-oxygen transport Hbs in animals) [13]. Plant oxygen transport Hbs have also evolved independently and much more recently from "Class 1" nsHbs [19, 24, 25] (Figure 2-1). This more recent event has left pairs of proteins that have different functions, but share very similar primary structures. An extreme example is found in *Parasponia andersonii* [27] (a non-legume which fixes N_2 in root

nodules) and *Trema tomentosa* [28] (which does not fix N_2). Their Hbs are 93% identical (differing in only 11 positions with no primary sequence gaps), yet *Parasponia andersonii* Hb (ParaHb) is a pentacoordinate oxygen transporter and *Trema tomentosa* (TremaHb) is predicted to be a typical hexacoordinate nsHb (Figure 2-1).

ParaHb has been shown to be pentacoordinate in the ferrous oxidation state, and to have rate and affinity constants for oxygen that are appropriate for transport [29, 30]. However, little is known about TremaHb or ferric ParaHb. The comparative experiments presented here were designed to test whether these proteins are truly as divergent in structure and chemistry as their physiological expression would suggest, or whether their behavior mirrors the similarity of their sequence identity. The former result would reveal a surprising difference in physical behavior for two proteins sharing such high sequence identity, and the latter would suggest that pentacoordinate oxygen transporters could play the role of nsHbs, and that hexacoordination *per se* is not an important structural feature for their physiological function.

Experimental Procedures:

***Production of Proteins*-** Recombinant rice nsHb1 and soybean Lba were produced as described previously [31, 32]. Codon-optimized cDNA for *Parasponia andersonii* (genebank number u27194) and *Trema tomentosa* hemoglobins (genebank number 1402313a) were synthesized by Epoch Biolabs using assembly PCR. These cDNAs were inserted in to a pET 28a plasmid for expression in the BL21 Star DE3 *E. coli* strain. A second sequence for *Trema tomentosa* hemoglobin (genebank number y00296) was deposited more recently that differs from the former by lacking the conserved Val^{117} amino acid. Both Trema cDNAs were expressed in E. coli, but only the former (which included Val^{117}) produced soluble hemoglobin.

The BL21 Star DE3 host strain was grown in 2-liter Erlenmeyer flasks that were inoculated using a 100 milliliter starter culture grown overnight to saturation. The expression media used was 1 liter of Terrific Broth supplemented with 1 milliliter of 50 milligram/milliliter Kanamycin per flask. The flasks were cultured at 37° C while being shaken for 18-20 hours at 250 rpm without induction before being harvested by centrifugation (9,000 rpm for 10 minutes). The collected cells were lyzed by homogenization before being purified in a three-step process: (1) ammonium sulfate fractionation (60 and 90 percent), (2) immobilized metal affinity chromatography (BD TALON), and (3) Size exclusion chromatography (HiPrep 26/60 Sephacryl S-100 High Resolution). Collected fractions were dialyzed into 10 millimolar TRIS buffer and concentrated using Amicon Millipore concentrators. Purification efficiency was measured by spectroscopic analysis of Soret/280 ratios. All absorbance spectra were measured using either a Cary-50 Bio or an Ocean Optics USB4000 Spectrophotometer. Ferric protein was made by oxidizing each Hb with potassium ferricyanide followed by desalting over a G-25 column. Ferrous hemoglobins were generated by reducing ferric samples with sodium dithionite.

Kinetic Experiments- Flash Photolysis and stopped-flow reactions were used to measure CO binding for all proteins as described previously [33, 34]. Oxygen association and dissociation rate constants were measured by flash photolysis and rapid mixing with CO, respectively [35]. All kinetic traces were fit to exponential decays using Igor Pro. Calculation of rate constants for hexacoordination and CO binding used the method described by Smagghe et al. [34]. Affinity constants for azide were measured using previously described methods [36].

Electrochemical and quaternary structure analysis- Midpoint reduction potentials were measured by potentiometric titration using an apparatus described in detail previously [37]. The biphasic reduction curve exhibited by ParaHb was evident under a range of conditions. This prompted our analysis of the oligomeric state of the ferric proteins by equilibrium analytical ultracentrifugation. This procedure followed one published earlier [38] with the exception that a newer model Beckman Coulter ProteomeLab XLA ultracentrifuge was used. Molecular mass was calculated from the linear portions of the plots in Figure 2-4 using Equation 1 where M is molecular mass, r is the radial position of the sample, v is partial specific volume (fixed at 0.72 ml/g), ρ is solvent density (fixed at 0.9982 g/ml), the angular velocity ω = 3,099 radians/s (29,600 rpm), R = 8.31441 x 10^7 (g cm^2)/(s^2 k mole), and T was 293 ° K

$$\ln(Abs) = \frac{M(1-v\rho)\omega^2}{2RT} r^2 \qquad \text{Equation 1.}$$

Results:

The experiments presented here are designed to measure three characteristics that distinguish the structure and reactivity of oxygen transport proteins from those of nsHbs. These characteristics are endogenous histidine coordination in the ferric oxidation state, endogenous histidine coordination in the ferrous oxidation state, and the kinetics of oxygen binding. NsHbs are hexacoordinate in both oxidation states, as described by the following reaction [33].

$$Hb_{Hex} \underset{k_H}{\overset{k_{-H}}{\leftrightarrow}} Hb_{Pent} + L \underset{k_L}{\overset{k'_L}{\leftrightarrow}} Hb_L \qquad \text{Equation 2.}$$

In this equation, Hb_{Hex} and Hb_{Pent} are the hexacoordinate and pentacoordinate forms of the Hb, and the rate constants for distal histidine coordination (H) and exogenous ligand (L) binding are written at the top (for association) and bottom (for dissociation) of each step. The influence of distal histidine coordination on equilibrium binding affinity can be evaluated by the following equation.

$$K_{eff} = \frac{K_{L,pent}}{1 + K_H} \qquad \text{Equation 3.}$$

Here $K_{L,pent}$ is k'_L/k_L (the affinity constant in the absence of the influence of histidine coordination), and K_H (k_H/k_{-H}) is the affinity constant for endogenous histidine coordination. Equation 3 predicts a decrease in affinity for exogenous ligand binding when histidine coordination is tight.

The rates of exogenous ligand binding can be influenced by histidine coordination as described by Equation 4, which allows measurement of k_H and k_{-H} using appropriate ligands in the ferric and ferrous oxidation states [33].

$$k_{obs} = \frac{k_{-H} k'_L [L]}{k_H + k_{-H} + k'_L [L]} \qquad \text{Equation 4.}$$

Equation 4 predicts a limited rate of exogenous ligand binding when coordinated histidine dissociation is slow.

Coordination and ligand binding in the ferric oxidation state- A principal distinction between oxygen transport Hbs and nsHbs is hexacoordination in the latter, which is generally

much stronger in the ferric than the ferrous oxidation state [21, 37]. Coordination state is evident from the visible-region absorbance spectra in both oxidations states [39, 40] as exemplified for hxHbs by rice nsHb, and for pentacoordinate Hbs by soybean Lba (Figure 2-2). The prominent band at 529 nm and shoulder at 560 nm of rice nsHb is characteristic of a ferric, low-spin hemichrome heme center. In contrast, the larger degree of absorbance at 484 nm, and the peak at 620 nm in the spectrum of Lba are characteristic charge-transfer bands found in high-spin, pentacoordinate ferric heme proteins. The absorbance spectra of recombinant ParaHb is (as shown by Appleby et al. [19] for the native protein) largely low-spin (hexacoordinate), but with a measurable fraction of high-spin character evident from a minor 620 nm absorbance band. However, TremaHb is entirely low-spin and functionally indistinguishable from rice nsHb.

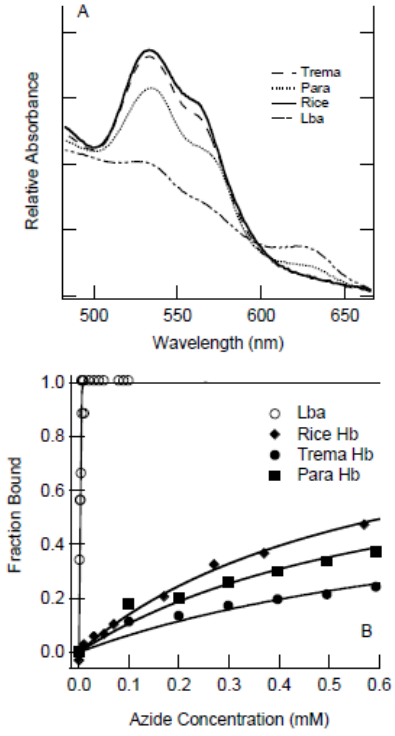

Figure 2-2. Coordination and ligand binding in the ferric oxidation state. A) Absorbance spectra of oxidized TremaHb and rice nsHb are typical of hexacoordinate, low spin ferric hemoglobins. That of soybean Lba is characteristic of a high spin, pentacoordinate complex. The ParaHb spectrum represents a mixture of high and low spin heme. B) Azide binding to each

protein shows that TremaHb, ParaHb, and rice nsHb bind with much lower affinity than soybean Lba, indicating competition from histidine coordination in the former three Hbs.

To measure the impact of hexacoordination in ParaHb and TremaHb, equilibrium affinities for the ferric ligand, azide, were measured along with soybean Lba and rice nsHb as pentacoordinate and hexacoordinate controls, respectively. The binding curves for each are shown in Figure 2-2B. In these experiments, Lba binds azide stoichiometrically with an affinity constant precluding measurement at this protein concentration (5 μM). The other three proteins however, bind azide with much lower affinities (each constant is on the order of 3 mM), as would be expected from Equation 3 for hxHbs with higher values of K_H. The data in Figure 2-2 reveal that TremaHb and ParaHb are predominately hexacoordinate in the ferric oxidation states. Thus, they share similarity to nsHbs rather than Lbs for this property.

Coordination and ligand binding in the ferrous oxidation state- Heme coordination in the ferrous oxidation state is evident from splitting of the visible bands seen in low-spin complexes. *Bis*-histidyl ferrous heme coordination results in prominent peaks at 528 and 556 nm that resemble the visible spectrum of cytochrome *b5*. Figure 2-3A shows the absorbance spectra of rice nsHb, ParaHb, and TremaHb in this region. To provide a reference for the degree of histidine coordination in these proteins, absorbance spectra for human neuroglobin (Ngb) (fraction of coordination ~ 1) and Lba (fraction of coordination ~ 0) are included. The ratio of absorbance at 555nm to that at 540nm has been shown to reflect the fraction of hexacoordination [34] (Figure 2-3B). The line in Figure 2-3B was established empirically for this relationship [34]. These data estimate that both TremaHb and ParaHb are fractionally coordinated at a ratio less than 0.2.

The low degree of ferrous hexacoordination in TremaHb and ParaHb is supported by the kinetics of CO binding. Figure 2-3C demonstrates the effect of histidine coordination in rice nsHb, showing CO binding time courses for [CO] ranging from 12 to 500 μM. In each case (Figures 2-3C-E), the y-axes are normalized to absorbance change expected for the reaction. The time courses for rice nsHb are relatively slow, show appreciable loss of amplitude only at the highest [CO], and coalesce to a concentration-independent rate constant as [CO] is raised (Figure 2-3F). These phenomena are characteristic of hexacoordination as exhibited by rice nsHb, described by Equation 4 when K_H is appreciable, and k_H and k_{-H} are on the order of k'_{CO} [34]. In contrast, CO binding to ParaHb (Figure 2-3D) and TremaHb (Figure 2-3E) is much faster, and the majority of the absorbance change is lost in the dead time of the reaction at even moderate [CO] (the maximum [CO] in Figures 2-3D and E is 125 μM). Furthermore, there is a linear relationship between the observed rate constants and [CO]. Lba is not included in Figure 2-3 because its rate of CO binding is too fast for analysis by rapid mixing. These characteristics are common to bimolecular CO binding in the absence of appreciable K_H, and demonstrate that ParaHb and TremaHb resemble Lba and other pentacoordinate Hbs in the ferrous oxidation state.

Values of k_{-H2} can be estimated from the data in Figure 2-3 by examination of the rate constant for binding to the slower fraction (~15%) at the highest [CO] [34]. These values are reported in Table 2-1 along with the bimolecular rate constants for CO association. Knowing k_{-H2} and K_H allows an estimation of the rate constant for histidine binding (k_{H2}), which is also reported in Table 2-1.

Table 2-1

Ferrous Ligand Binding and Hexacoordination Values	$k'_{CO,pent}$ ($\mu M^{-1}s^{-1}$)	k_{H2} (s^{-1})	k_{-H2} (s^{-1})	K_{H2}
Lba	13			~ 0
Rice Hb	6.8	75	40	1.9
Para Hb	10	~ 7[3]	~ 70[2]	~ 0.1[1]
Trema Hb	43	~ 5[3]	~ 50[2]	~ 0.1[1]

[1] is estimated from the ferrous absorption spectrum and the amplitude of CO binding at high [CO]
[2] is k_{obs} at high [CO]
[3] is estimated from K_H and k_{-H}

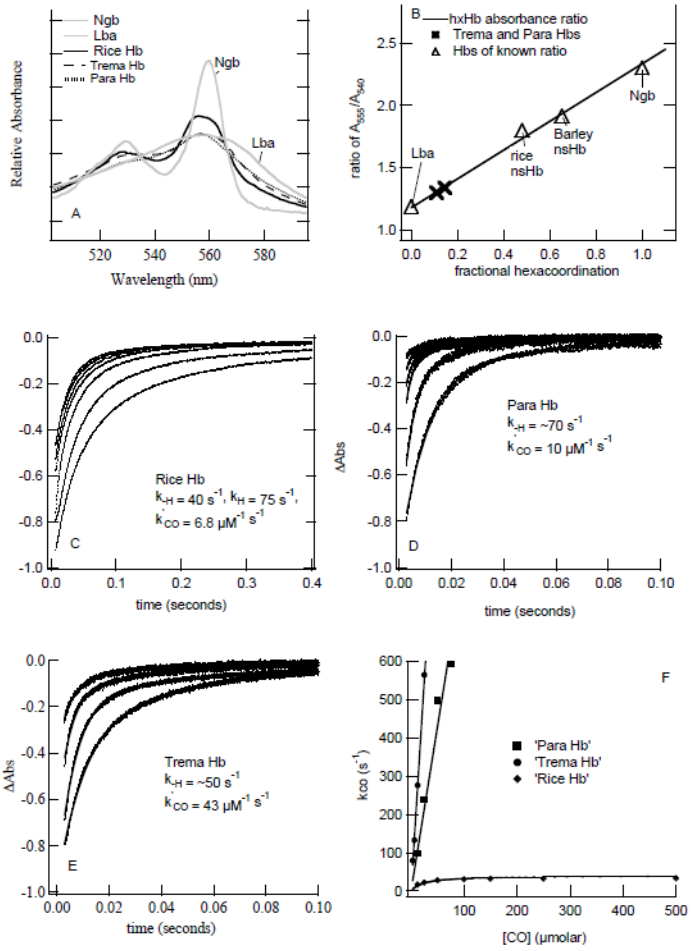

Figure 2-3. Coordination and ligand binding in the ferrous oxidation state. A) Absorbance spectra of each Hb in the ferrous oxidation state is compared to human neuroglobin (Ngb) which is completely hexacoordinate in ferrous oxidation state. B) Empirical quantification of the ratio of absorbance at 555nm/540nm indicates that ParaHb and TremaHb have a fraction of histidine coordination of < 0.2. C-E) Time courses for CO binding to each Hb at varying [CO] reveal the fraction of hexacoordinate Hb and the rate constants for histidine binding and dissociation. F) The concentration dependence of the observed rate constant for the fast phase of CO binding to each Hb shows that ParaHb and TremaHb are predominately pentacoordinate, and rice nsHb has an appreciable fraction of hexacoordinate heme.

Electrochemical analysis- Binding of the distal histidine to form a *bis*-histidyl heme complex is generally favored more in the ferric oxidation state than the ferrous [21]. The data above suggest that hexacoordination is significant in ferric TremaHb and ParaHb, but not in the ferrous forms of each protein. As is the case for other hexacoordinate heme proteins, this should result in midpoint reduction potentials that are more negative than for Hbs that are strictly pentacoordinate [37]. To test this hypothesis, potentiometric titration was used to measure the midpoint reduction potentials for Para and Trema Hbs compared to Lba and rice nsHb. As demonstrated previously [37], the midpoint reduction potential for rice nsHb is -132 mv (versus SHE), and that of Lba is +13 mv. As expected for histidine coordination preferentially in the ferric oxidation state, the midpoint reduction potential for TremaHb is -138 mv. Surprisingly, the ParaHb redox titration is biphasic, with 50% of the population having a midpoint reduction potential of 0 mv, and 50% at -150 mv.

There are many ways in which heme coordination by histidine can influence midpoint reduction potentials in hxHbs. For example, differential coordination strength in the ferric and ferrous oxidation states leads to lower reduction potentials in all hxHbs due to tighter binding in the ferric oxidation state [37]. However, none of the known reactions can account for biphasic equilibrium redox titration curves, as they are all at rapid-exchange on the time scale of a potentiometric titration and would result in an observed average behavior. A mechanistic

explanation for biphasic redox titration requires the assumption of dissimilar heme sites that are not inter-converting. Alternatively, but less likely, the same result would be expected from a change in coordination state slower than the time scale (hours) of the experiment.

Two dissimilar heme sites is difficult to rationalize with a monomeric Hb (like Lba). Likewise, rice nsHb has a dissociation equilibrium constant for dimerization of 86 μM [38], leaving it mostly monomeric in our experiments (5 μM in Hb concentration). However, the original purification of native ParaHb reported it as a "readily dissociable dimer" [19]. Our potentiometric titration results would be easier to explain if in fact ParaHb had a much lower K_D for dimerization. This possibility was measured using equilibrium analytical ultracentrifugation to analyze the quaternary structure of ferric ParaHb and TremaHb (Figure 2-4B). In this experiment, rice nsHb, TremaHb, and ParaHb were analyzed at a concentration of 5 μM (in heme). At this concentration, rice nsHb is mainly monomeric and has an apparent molecular mass of 17.3 kD. However, at the same concentration, TremaHb and ParaHb have molecular masses of 32.8 and 31 kD respectively, indicating that they are largely dimeric even at this low concentration. From these data and Equation 1, it can be estimated that K_D values for dimerization for these proteins are no greater than 1 μM. These results show that ParaHb is in fact dimeric in our potentiometric titration experiments, and make asymmetric heme sites a plausible cause of the biphasic redox titration curve observed for this protein.

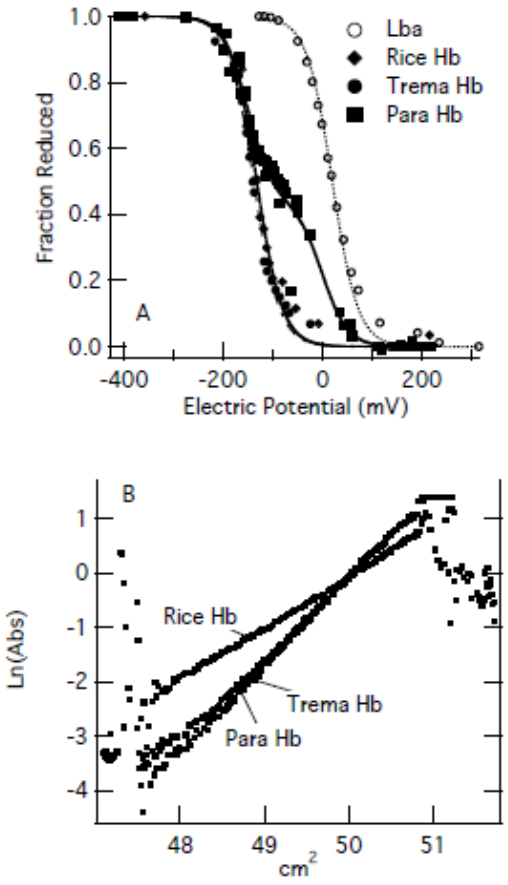

Figure 2-4. Potentiometric titrations and equilibrium analytical ultracentrifugation analysis. A) Nernst plots of potentiometric titrations were used to measure the ferrous/ferric redox potential for each Hb. B) Each ferric Hb was analyzed at 5 µM by equilibrium analytical ultracentrifugation monitored at 410 nm. The slopes of the plots for ParaHb and TremaHb indicate a tighter dimer than that observed for rice nsHb.

Oxygen binding- Our results so far suggest that in the ferric oxidation state, TremaHb and ParaHb resemble nsHbs; but in the ferrous state, they both share more similarity with pentacoordinate oxygen transporters like Lba. Our final test to distinguish between oxygen transport Hbs and typical hexacoordinate Hbs is a measurement of oxygen affinity and kinetics.

ParaHb has kinetic and affinity constants for oxygen similar to Lbs [12, 19]. To compare these results with those of TremaHb, Figure 2-5A shows oxygen binding (following flash photolysis), and Figure 2-5B time courses for oxygen dissociation for both proteins (again with Lba and rice nsHb as controls). The association rate constants for TremaHb and ParaHb are similar (210 and 170 $\mu M^{-1}s^{-1}$, respectively). However, the oxygen dissociation rate constants are quite distinct at 0.38 and 12 s^{-1}, respectively. This 30-fold difference in respective oxygen dissociation rate constants is a clear functional distinction between ParaHb and TremaHb. The oxygen dissociation rate constant for TremaHb (0.38 s^{-1}) groups it with the nsHbs, and the rate constant for Para Hb (12 s^{-1}) is consistent with the oxygen transport function of the Lbs (Table 2-2).

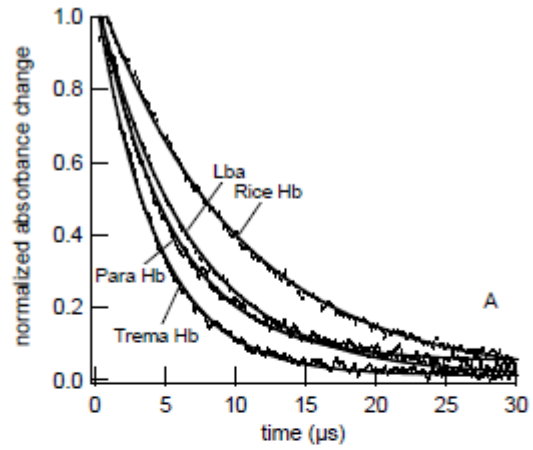

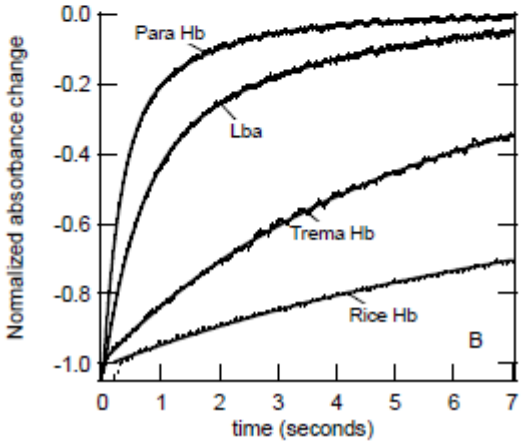

Figure 2-5. The kinetics of oxygen binding to ParaHb and TremaHb A) Time courses for oxygen association and B) dissociation for ParaHb, TremaHb, rice nsHb, and soybean Lba in air. The dissociation curves in B were measured against displacement by 1 mM CO.

Table 2-2

Protein	$k'_{O2,pent}$ ($\mu M^{-1}s^{-1}$)	k_{O2} (s^{-1})	$K_{O2,pent}$ (μM^{-1})	K_{O2} (μM^{-1})
Rice Hb1	60	0.038	1600	540
Soybean Lba	130	5.6	23	23
T. tomentosa	210	0.38	550	500
P. andersonii (native)	165	15	11	11
P. andersonii (recombinant)	170	12	14	13

Discussion

The rationale for this investigation was the high level of sequence similarity between ParaHb, a typical plant oxygen transport protein, and TremaHb, which is predicted to be distinct from known oxygen transporters in heme coordination and oxygen binding kinetics. There were two possible outcomes anticipated. The first was that TremaHb could have been identical to ParaHb in its behavior implying that the physical differences between nsHbs and oxygen transport Hbs are not necessary for nsHb function, which would mean that oxygen transporters could possibly function as nsHbs. The second possible outcome was a difference between the two proteins, demonstrating that a surprisingly small number of amino acid changes are responsible for a large shift in structure and function. With respect to oxygen binding, our results support the latter conclusion. The oxygen affinity and binding kinetics of TremaHb are not suitable for oxygen transport, and completely in line with Class 1 nsHbs. However, with respect to hexacoordination, the conclusions are mixed; both Hbs are predominately

hexacoordinate in the ferric oxidation state, and mostly pentacoordinate in the ferrous oxidation state. They are distinct from other nsHbs in having ~ 20 (Class 1) or ~ 800 (Class 2) fold lower affinities for ferrous distal histidine coordination. Furthermore, in contrast to both Lbs and Class 1 nsHbs, ParaHb and TremaHb are tightly associated dimers. The implications of these results to the evolution of oxygen transport Hbs is discussed below.

Independent evolution of oxygen transport Hbs in plants: Class 1 versus Class 2 oxygen transport hemoglobins- The two phylogenetic Classes of nsHbs that have given rise to oxygen transport globins have distinct physical attributes, including the degree of hexacoordination found in each, and their affinity constants for oxygen (Table 2-3) [12]. In contrast, ParaHb and Lbs (which evolved from Class 1 and Class 2 nsHbs, respectively) are similar in their affinities for oxygen, and both lack significant histidine coordination in the ferrous oxidation state. The convergence of similar oxygen transport globins from dissimilar starting points required different molecular changes in each Class of nsHb. In an effort to compare the molecular mechanisms that lead to the development of plant oxygen transport globins, average values for the rate and affinity constants for ferrous hexacoordination and oxygen binding for each nsHb Class are provided in Table 2-3 along with rate and affinity constants for oxygen binding to the plant oxygen transport Hbs (taken from Smagghe *et al.* [12]).

Table 2-3

Protein	k_{H2} (s^{-1})	k_{-H2} (s^{-1})	K_{H2}	$k'_{O2,pent}$ ($\mu M^{-1}s^{-1}$)	k_{O2} (s^{-1})	$K_{O2,pent}$ (μM^{-1})	K_{O2} (μM^{-1})
Class 1 nsHbs	130	75	1.7	67	0.14	1200	410
Rice Hb E7L				620	51	12	12
Class 2 nsHbs	1500	25	84	76	1.1	260	2.9
Plant Oxygen Transporters				230	13	20	20
Lba E7V				400	24	17	17

If we choose to define the requirements of an oxygen transport Hb based solely on affinity and kinetics of oxygen binding, Class 2 nsHbs are not far off the mark. With equilibrium constants averaging 3 μM^{-1}, and dissociation rate constants averaging 1.1 s^{-1}, they would require only slight modification to attain the values shared by the Lbs. On the other hand, Class 1 nsHbs would have to significantly lower their affinity for oxygen (by ~ 20-fold) and increase their oxygen dissociation rate constants (~10-fold). In addition to these changes, is the apparent requirement of a pentacoordinate ferrous heme, based on the knowledge that all observed oxygen transporter Hbs are pentacoordinate in this oxidation state.

One possibility for overcoming the challenges of designing affinity, kinetics, and coordination is to change the distal histidine to an amino acid that cannot coordinate the heme iron. In fact, the mutant protein E7L of rice nsHb (in which the distal histidine is replaced by leucine) meets all of these requirements for oxygen transport [41] (Table 2-3). Likewise, histidine substitution mutations in soybean Lba are well-suited for oxygen transport based on these criteria [35] (Table 2-3). However, all oxygen transport Hbs in plants (and in nearly all other organisms) are not only pentacoordinate, but also contain histidine at position E7 near the ligand binding site. When considering the constraints of pentacoordinate ferrous heme and a

nearby distal histidine, the act of converting both classes of nsHbs to oxygen transporters involves reducing the oxygen affinity values presented in Table 2-3 for Class 1 and Class 2 nsHbs ($K_{O2,pent}$) to ~ 20 μM^{-1}. The oxygen affinities can be lowered by increasing the oxygen dissociation rate constant by ~ 90 and ~ 12-fold for Class 1 and 2 nsHbs, respectively.

The molecular details resulting in the changes in oxygen dissociation rate constants are still unclear, though some hints are provided from biophysical studies of Lbs and nsHbs. Oxygen release can be controlled by hydrogen bonding with the distal histidine [42], by the nature of the proximal histidine-heme bond [43-45], and by control of geminate rebinding through cavities and tunnels in the protein matrix surrounding the heme [46, 47]. Previous research indicates that the distal histidine in Class 2 nsHbs hydrogen bonds with bound oxygen [12], but the distal histidine present in soybean Lba does not form this same hydrogen bond [31, 35]. This suggests that the evolution of oxygen transport in Class 2 Hbs resulted, at least in part, from the loss of oxygen stabilization by the distal histidine. However, until other Class 2 nsHbs and Lbs are examined, this conclusion is tentative because of potentially different mechanisms for regulating oxygen affinity in other Lbs [30, 48].

It is also known that Class 1 nsHbs use a hydrogen bond to stabilize bound oxygen [49, 50]. Whether loss of this hydrogen bond causes the decrease in oxygen affinity in ParaHb has not been addressed, but could be tested by analysis of ParaHb and TremaHb distal His mutant proteins. If the loss of this hydrogen bond were key to modulating oxygen affinity, it would be expected that distal His mutation in TremaHb would increase the oxygen dissociation rate constant, but that in ParaHb would not. However, a comparison of the amino acid sequences of these proteins reveals no obvious suspects that might influence oxygen dissociation rate constants between the two, or that would suggest a mechanism for regulating oxygen affinity

(Figure 2-1). Both have Phe at position B10 [36], an apolar side chain at position F7 [45, 51], and there are no substitutions predicted to be closer than ~10 Å to the distal heme pocket. Thus, a molecular explanation for the nearly 50-fold difference in oxygen affinity between ParaHb and TremaHb will require a detailed study of the structures of these Hbs and the behavior of key mutant proteins derived from each.

Why are oxygen transport Hbs pentacoordinate, and why do they retain a distal histidine? It has been proposed that oxygen transport Hbs evolved from hexacoordinate hemoglobins (hxHbs) in both plants and animals [19, 20, 52]. In both cases, the functions of the precursor hxHbs are not yet clear, and the necessity of hexacoordination is accordingly unknown [12, 53]. The oxygen transport Hbs that evolved from them share similar features of pentacoordinate ferrous heme, relatively rapid oxygen dissociation, and in nearly all cases a distal histidine. The few exceptions among known oxygen transporters have substitutions of glutamine, which is capable of electrostatic interactions with ligands similar to, but somewhat weaker than histidine [54-56]. The requirement of a pentacoordinate ferrous heme is probably due to the effect of hexacoordination on heme oxidation, as it has been shown that both plant and animal hxHbs oxidize significantly faster than oxygen transport Hbs [15, 36]. For example, a *bis*-histidyl myoglobin mutant protein oxidizes much more rapidly than the wild type protein [57]. The reason for this could be due to the ability of the *bis*-histidyl heme center to more rapidly transfer electrons [58], or to the more negative reduction potentials that accompany disproportionately strong ferric distal histidine coordination [15, 37].

The requirement for a distal histidine arises from the need for stabilization of bound oxygen (in some Hbs), ligand discrimination, and slowing of heme oxidation and subsequent hemin dissociation [59, 60]. The examples given above of the HisE7L mutant proteins of rice nsHb and soybean Lba have appropriate kinetic and equilibrium constants for oxygen transport, but they are much poorer than their respective wild-type proteins in discriminating for oxygen against other potential ligands like carbon monoxide [41]. Likewise, replacement of the distal histidine in most Hbs increases heme oxidation due to lower oxygen affinity and increased solvent access to the heme pocket [42, 61]. Thus, oxygen transport Hbs require that histidine be located precariously near the ligand binding site, but not so near as to coordinate the ferrous heme iron. This requirement of the cognate globin reveals that the architecture of oxygen transport proteins is a delicate balance of structure and coordination that is highlighted in comparison to their hxHb evolutionary precursors.

References

[1] R.C. Hardison, PNAS, vol. 93, 1996, pp. 5675-5679.
[2] R.C. Hardison, American Scientist, vol. 87, 1999, pp. 126-133.
[3] R.C. Hardison, J. Exp. Bot., vol. 201, 1998, pp. 1099-1117.
[4] J. Raymond, D. Segre, Science, vol. 311, 2006, pp. 1764-1767.
[5] P. Falkowski, Science, vol. 311, 2006, pp. 1724-1725.
[6] T. Hankeln, B. Ebner, C. Fuchs, F. Gerlach, M. Haberkamp, T.L. Laufs, A. Roesner, M. Schmidt, B. Weich, S. Wystub, S. Saaler-Reinhardt, S. Reuss, M. Bolognesi, D. De Sanctis, M.C. Marden, L. Kiger, L. Moens, S. Dewilde, E. Nevo, A. Avivi, R.E. Weber, A. Fago, T. Burmester, J Inorg Biochem, vol. 99, 2005, pp. 110-119.
[7] J.B. Wittenberg, B.A. Wittenberg, M. Guertin, J. Biol. Chem., vol. 277, 2002, pp. 871-874.
[8] P.R. Gardner, A.M. Gardner, L.A. Martin, A.L. Salzman, Proc. Natl. Acad. Sci. USA, vol. 95, 1998, pp. 10378-10383.
[9] Y. Sun, K. Jin, X. Mao, Y. Zhu, D.A. Greenberg, Proc. Natl. Acad. Sci. U.S.A., vol. 98, 2001, pp. 15306-15311.
[10] Y. Sun, K. Jin, A. Peel, X.O. Mao, L. Xie, D.A. Greenberg, PNAS, vol. 100, 2003, pp. 3497-3500.
[11] A.A. Khan, Y. Wang, Y. Sun, X.O. Mao, L. Xie, E. Miles, J. Graboski, S. Chen, L.M. Ellerby, K. Jin, D.A. Greenberg, Proc Natl Acad Sci U S A, vol. 103, 2006, pp. 17944-17948.

[12] B.J. Smagghe, J.A. Hoy, R. Percifield, S. Kundu, M.S. Hargrove, G. Sarath, J.L. Hilbert, R.A. Watts, E.S. Dennis, W.J. Peacock, S. Dewilde, L. Moens, G.C. Blouin, J.S. Olson, C.A. Appleby, Biopolymers, vol. 91, 2009, pp. 1083-1096.
[13] S. Kundu, Trent, J.T., III, and Hargrove, M.S., Trends in Plant Sc., vol. 8, 2003, pp. 387-393.
[14] T. Burmester, B. Welch, S. Reinhardt, T. Hankeln, Nature, vol. 407, 2000, pp. 520-523.
[15] S. Dewilde, L. Kiger, T. Burmester, T. Hankeln, V. Baudin-Creuza, T. Aerts, M. Marden, R. Caubergs, L. Moens, J. Biol. Chem., vol. 276, 2001, pp. 38949-38955.
[16] J.T. Trent, III., R.A. Watts, M.S. Hargrove, J. Biol. Chem., vol. 276, 2001, pp. 30106-30110.
[17] T. Burmester, B. Ebner, B. Weich, T. Hankeln, Mol Biol Evol, vol. 19, 2002, pp. 416-421.
[18] J.T. Trent, III., M.S. Hargrove, J. Biol. Chem., vol. 277, 2002, pp. 19538-19545.
[19] C.A. Appleby, J.D. Tjepkema, M.J. Trinick, Science, vol. 220, 1983, pp. 951-953.
[20] B. Trevaskis, R.A. Watts, C.R. Andersson, D.J. Llewellyn, M.S. Hargrove, J.S. Olson, E.S. Dennis, W.J. Peacock, Proc Natl Acad Sci U S A, vol. 94, 1997, pp. 12230-12234.
[21] A.B. Cowley, M.L. Kennedy, S. Silchenko, G.S. Lukat-Rodgers, K.R. Rodgers, D.R. Benson, Inorg Chem, vol. 45, 2006, pp. 9985-10001.
[22] M. Nesset, N. Shokhirev, P. Enemark, S. Jacobson, F. Walker, Inorg. Chem., vol. 35, 1996, pp. 5188-5200.
[23] M. Safo, M. Nesset, F. Walker, P. Debrunner, W. Robert Scheidt, J. Am. Chem. Soc., vol. 119, 1997, pp. 9438-9448.
[24] E. Guldner, E. Desmariais, N. Galtier, B. Godelle, J. Evol. Biol., 2004, pp. 48-54.
[25] E. Guldner, B. Godelle, N. Galteir, J. Mol. Evol., vol. 59, 2004, pp. 416-425.
[26] P.W. Hunt, R.A. Watts, B. Trevaskis, D.J. Llewellyn, J. Burnell, E.S. Dennis, W.J. Peacock, Plant Mol. Bio., vol. 47, 2001, pp. 677-692.
[27] A. Kortt, M. Trinick, C. Appleby, Eur. J. Biochem, vol. 175, 1988, pp. 141-149.
[28] D. Bogusz, C.A. Appleby, J. Landsmann, E.S. Dennis, M.J. Trinick, W.J. Peacock, Nature, vol. 331, 1988, pp. 178-180.
[29] J.B. Wittenberg, B.A. Wittenberg, Q.H. Gibson, M.J. Trinick, C.A. Appleby, J. Biol. Chem., vol. 261, 1986, pp. 13624–13631.
[30] Q.H. Gibson, J.B. Wittenberg, B.A. Wittenberg, D. Bogusz, C.A. Appleby, J. Biol. Chem., vol. 264, 1989, pp. 100–107.
[31] M.S. Hargrove, J.K. Barry, E.A. Brucker, M.B. Berry, G.N. Phillips, Jr., J.S. Olson, R. Arredondo-Peter, J.M. Dean, R.V. Klucas, G. Sarath, J. Mol. Biol., vol. 266, 1997, pp. 1032-1042.
[32] M. Hargrove, E. Brucker, B. Stec, G. Sarath, R. Arredondo-Peter, R. Klucas, J. Olson, G. Phillips, Structure Fold. Des., vol. 8, 2000, pp. 1005-1014.
[33] B.J. Smagghe, P. Halder, M.S. Hargrove, Methods Enzymol, vol. 436, 2008, pp. 359-378.
[34] B.J. Smagghe, G. Sarath, E. Ross, J.L. Hilbert, M.S. Hargrove, Biochemistry, vol. 45, 2006, pp. 561-570.
[35] S. Kundu, M.S. Hargrove, Proteins, vol. 50, 2003, pp. 239-248.
[36] B.J. Smagghe, S. Kundu, J.A. Hoy, P. Halder, T.R. Weiland, A. Savage, A. Venugopal, M. Goodman, S. Premer, M.S. Hargrove, Biochemistry, vol. 45, 2006, pp. 9735-9745.
[37] P. Halder, J.T. Trent, III., M.S. Hargrove, PROTEINS: Structure, Function, and Bioinformatics, vol. 66, 2007, pp. 172-182.
[38] M.D. Goodman, M.S. Hargrove, J. Biol. Chem., vol. 276, 2001, pp. 6834-6839.

[39] C.A. Appleby, Biochim Biophys Acta, vol. 189, 1969, pp. 267-279.
[40] T. Yonetani, T. Iizuka, M.R. Waterman, J Biol Chem, vol. 246, 1971, pp. 7683-7689.
[41] R. Arredondo-Peter, M.S. Hargrove, G. Sarath, J.F. Moran, J. Lohrman, J.S. Olson, R.V. Klucas, Plant Physiol., vol. 115, 1997, pp. 1259-1266.
[42] B.A. Springer, K.D. Egeberg, S.G. Sligar, R.J. Rohlfs, A.J. Mathews, J.S. Olson, J. Biol. Chem., vol. 264, 1989, pp. 3057-3060.
[43] M.F. Perutz, Nature, vol. 228, 1970, pp. 726–739.
[44] S.J. Smerdon, S. Krzywda, A.J. Wilkinson, R.E. Brantley, Jr., T.E. Carver, M.S. Hargrove, J.S. Olson, Biochemistry, vol. 32, 1993, pp. 5132-5138.
[45] S. Kundu, B. Snyder, K. Das, P. Chowdhury, J. Park, J.W. Petrich, M.S. Hargrove, Proteins, vol. 46, 2002, pp. 268-277.
[46] E.E. Scott, Q.H. Gibson, J.S. Olson, J Biol Chem, vol. 276, 2001, pp. 5177-5188.
[47] M.D. Salter, K. Nienhaus, G.U. Nienhaus, S. Dewilde, L. Moens, A. Pesce, M. Nardini, M. Bolognesi, J.S. Olson, J Biol Chem, vol. 283, 2008, pp. 35689-35702.
[48] S. Kundu, G. Blouin, S. Premer, G. Sarath, J. Olson, M. Hargrove, Biochemistry, vol. 43, 2004, pp. 6241-6252.
[49] R. Arredondo-Peter, J.F. Moran, G. Sarath, P. Luan, R.V. Klucas, Plant Physiol., vol. 114, 1997, pp. 493-500.
[50] R. Watts, Division of Biochemistry and Molecular Biology, vol. Australian National University, 1999, pp. PhD thesis.
[51] S.J. Smerdon, G.G. Dodson, A.J. Wilkinson, Q.H. Gibson, R.S. Blackmore, T.E. Carver, J.S. Olson, Biochemistry, vol. 30, 1991, pp. 6252–6260.
[52] T. Burmester, B. Weich, S. Reinhardt, T. Hankeln, Nature, vol. 407, 2000, pp. 520-523.
[53] T. Hankeln, B. Ebner, C. Fuchs, F. Gerlach, M. Haberkamp, T. Laufs, A. Roesner, M. Schmidt, B. Weich, S. Wystub, S. Saaler-Reinhardt, S. Reuss, M. Bolognesi, D. De Sanctis, M. Marden, L. Kiger, L. Moens, S. Dewilde, E. Nevo, A. Avivi, R. Weber, A. Fago, T. Burmester, J. Inorg. Biochem., vol. 99, 2005, pp. 110-119.
[54] R.J. Rohlfs, A.J. Mathews, T.E. Carver, J.S. Olson, B.A. Springer, K.D. Egeberg, S.G. Sligar, J. Biol. Chem., vol. 265, 1990, pp. 3168-3176.
[55] J.S. Olson, G.N. Phillips, Jr., J. Biol. Inorg. Chem., vol. 2, 1997, pp. 544-552.
[56] K.L. Dikshit, Y. Orii, N. Navani, S. Patel, H.Y. Huang, B.C. Stark, D.A. Webster, Arch. Biochem. Biophys., vol. 349, 1998, pp. 161-166.
[57] Y. Dou, S.J. Admiraal, M. Ikeda-Saito, S. Krzywda, A.J. Wilkinson, T. Li, J.S. Olson, R.C. Prince, I.J. Pickering, G.N. George, J. Biol. Chem., vol. 270, 1995, pp. 15993-16001.
[58] T. Weiland, S. Kundu, J. Trent, J. Hoy, M. Hargrove, J. Am. Chem. Soc., vol. 126, 2004, pp. 11930-11935.
[59] M.S. Hargrove, J.S. Olson, Biochemistry, vol. 35, 1996, pp. 11310-11318.
[60] R.t. Aranda, H. Cai, C.E. Worley, E.J. Levin, R. Li, J.S. Olson, G.N. Phillips, Jr., M.P. Richards, Proteins, vol. 75, 2009, pp. 217-230.
[61] R.E. Brantley, Jr., S.J. Smerdon, A.J. Wilkinson, E.W. Singleton, J.S. Olson, J. Biol. Chem., vol. 268, 1993, pp. 6995-7010.

CHAPTER 3. THE CRYSTAL STRUCTURE OF *PARASPONIA* HEMOGLOBIN REVEALS QUATERNARY STRUCTURE-LINKED HEME COORDINATION

A paper to be submitted to *Biochemistry*

Smita Kakar[1], Ryan Sturms[1], Andrea Savage, Alan Dispirito[1], Jay Nix[2] and Mark S. Hargrove[1,3]

Abstract:

All plants contain hemoglobins that are scavengers and/or signaling molecules, while a small number of plant species contain oxygen transport hemoglobins. In fact, the evolution of oxygen transport function in plants is fairly recent, and has left protein pairs with very similar primary structures but variable functions. One such example is that of hemoglobins from *Parasponia andersonii* and *Trema tomentosa*. Although these proteins differ in only 11 residues, Parasponia is a pentacoordinate oxygen transporter and Trema is believed to be hexacoordinate non-symbiotic hemoglobin.

[1]Department of Biochemistry, Biophysics, and Molecular Biology; Iowa State University, Ames, IA 50011
[2]Advanced Light Source, Lawrence Berkeley National Laboratory, Berkeley, CA 94720, USA
[3]To whom correspondence should be addressed

It has been shown that the oxygen dissociation rate constants of the two proteins are 30-fold different and is evident of a functional distinction between ParaHb and TremaHb. Furthermore, ParaHb shows evidence of functionally distinct subunits within its dimeric quaternary structure. In order to investigate the differences between these proteins, we have used X-ray crystallography to solve their structures in the ferric oxidation state. Trema Hb is a dimer of equivalent subunits similar in its overall structure to other plant Hbs. However, even though ParaHb is nearly identical to TremaHb, it possesses asymmetric heme sites that are distinct in their biochemistry. A monomeric mutant of ParaHb has been used to test the linkage between quaternary structure, heme coordination, and redox chemistry, demonstrating a clear relationship between these properties.

Introduction:

Hemoglobins are defined by an alpha-globin fold and a heme. The heme consists of a protoporphyrin ring containing an iron that exists mostly in the ferrous (Fe^{2+}) or ferric (Fe^{3+}) oxidation state. Based on the coordination state of iron, Hbs can be classified as pentacoordinate, where five of the six iron coordination sites are occupied by four pyrrole nitrogen atoms and the 'proximal histidine' side chain, or hexacoordinate, in which the sixth coordination site of the heme iron is reversibly coordinated by an endogenous ligand, mostly a 'distal' histidine side chain.

Most well-known Hbs such as Hb and its monomeric partner, myoglobin, are pentacoordinate and function as oxygen transporters. The first Hb found in plants,

leghemoglobin (Lb) is also pentacoordinate and carries oxygen to respiring bacteroids that occur in root nodules of legumes as a symbiote. However, the evolutionary predecessors of Lbs are 'hexacoordinate' and do not occur in a symbiotic relationship, hence they are called 'Non-symbiotic plant Hbs" (nsHbs). Characterization of Hb from Barley expanded the occurrence of hxHb from dicots to monocots [1], supporting the hypothesis that Hbs are present in roots or other tissues in all plants. These nsHbs probably serve to function as scavengers and/or signaling molecules [2].

The plant oxygen transport Hbs have evolved from their hexacoordinate counterparts on two independent occasions [3]. Based on oxygen affinities and functions, plant Hbs can be classified as Lbs, Class 1 nsHbs or Class2 nsHbs [4]. The most familiar oxygen transporters, Lbs have evolved from Class2 nsHbs [5]. An independent evolution of plant oxygen transporters has occurred more recently from Class1 nsHbs [6-8], which has left pairs of proteins with high sequence similarity but different functions. One such example is Hbs from *Parasponia andersonii* [9] and Trema tomentosa [10]. *Parasponia* Hb is a pentacoordinate oxygen transporter that evolved from hxHb similar to *Trema* Hb.

Kinetic studies have shown that the oxygen dissociation rate constants for the two proteins are 30-fold different [11, 12], evident of a functional distinction between *Parasponia* Hb and *Trema* Hb. Electrochemistry data for *Parasponia* Hb shows a biphasic titration curve pointing towards a mixed spin-state heme population [13]. Quaternary structure studies reveal that *Parasponia* Hb is a dimer thereby supporting a mixed-spin heme hypothesis [13].

To test this assumption and in order to study the evolutionary path resulting in pentacoordinate oxygen transport hemoglobins and structural events involved in alteration in protein function, we have used X-ray crystallography to solve the structures of these hemoglobins in their ferric oxidation states. These structures suggest that the mixture of spin states observed for *Parasponia* Hb results from asymmetric heme sites in a dimeric molecule. These structures are presented along with investigations of linkage between heme coordination and quaternary structure.

Materials and Methods:

Protein preparation- Codon optimized cDNA for *P.andersonii* (Genbank number u27194) and *T.tomentosa* Hbs (GenBank number 1402313a) were synthesized and cloned as described previously [13]. Para mutant I43N was made using Quickchange mutagenesis kit from Agilent Technologies. Para Hb and Trema Hb proteins were expressed, and purification was achieved using a three-step process as described earlier [13]. The mutant was expressed in host strain BL21 Star DE3 cells as described for the wild-type Para Hb. Purification included ammonium sulfate fractionation, DEAE-cellulose and CM-Sephadex column chromatography. The purification efficiency for the proteins used for crystallization as measured by the ratio of absorbance at the Soret peak and that at 280 nm was 3.2 and 2.9 for Trema Hb and Para Hb respectively. The proteins were oxidized by addition of a slight molar excess of potassium ferricyanide that is removed by passage of the protein sample through a G-25 size exclusion resin equilibrated with 10 mM HEPES buffer, pH 7.0. Ferrous hemoglobins were generated by

reducing ferric samples with sodium dithionite. Absorbance spectra were measured using a Cary-50 Bio Spectrophotometer.

Crystallization and data collection- Crystals were grown using the hanging drop vapor diffusion method at 25ºC. Trema Hb crystals grew in well buffer conditions consisting of 1.6M Ammonium sulfate and 0.1M Hepes buffer, pH7.0 after 3 days. The crystallization conditions for Para Hb crystals were 1.6M Ammonium sulfate, 10% Dioxane, 0.1M MES pH 7.0 with 0.1M phenol as an additive. Drops consisting of 1 ul of 3mM ferric protein and 1 ul well buffer produced crystals overnight. Native diffraction datasets for Trema and Para Hb crystals were collected at 100K on a Rigaku/MSC home source generator. Single wavelength anomalous dispersion dataset for Trema Hb was collected at the Advanced Light Source (beamline 4.2.2), using anomalous scattering from the heme iron.

Structure determination and refinement- Diffraction data were integrated and processed using d*TREK**.** Atomic positions for the two iron atoms were located by HKL2MAP (SHELXD) [14] and the phases were calculated with SOLVE [15]. Model building was performed using RESOLVE [16]. Manual model rebuilding was done using the software O [17] and SPDBV [18] and the atomic model was refined using REFMAC5 [19] from the CCP4 suite [20]. The resolution for Trema Hb structure was extended to 1.8 Å using the native data set and further refinement was carried out using REFMAC5. The Para Hb structure was solved and refined using the Trema Hb structure phases for molecular replacement. The molecular replacement solution was obtained using MOLREP [21] and final refinement was done using

REFMAC5. The buried surface area was calculated using CNS [22]. All structure figures were generated in PYMOL [23].

Quaternary structure and electrochemical analysis of ParaI43N mutant- The oligomeric state of ferric Para I43N mutant protein was determined by equilibrium analytical ultracentrifugation using the procedure published for quaternary structure measurements for wild type Para and Trema Hb [13]. The procedure used to collect data was same as described before [24], except that a newer model Beckman Coulter ProteomeLab XLA ultracentrifuge was used. Molecular mass was calculated from the linear portions of the plots in Figure 3-5A using Equation 1, where M is molecular mass, r is the radial position of the sample, v is partial specific volume (fixed at 0.72 mL/g), F is solvent density (fixed at 0.9982 g/mL), the angular velocity ω = 3099 rads/s (29600 rpm), R = 8.31441 _107 (g cm2)/(s2 K mol), and T was 293 K.

$$\ln(Abs) = \frac{M(1-v\rho)\omega^2}{2RT} r^2 \quad \text{Equation 1}$$

Potentiometric titration was used to measure midpoint reduction potentials using an apparatus described previously [25]. Midpoint potentials were obtained by fitting absorbance data to the following equation:

$$F_{reduced} = \frac{e^{-\left(\frac{nF(E_{obs}-E_{mid})}{RT}\right)}}{1+e^{-\left(\frac{nF(E_{obs}-E_{mid})}{RT}\right)}} \quad \text{Equation 2}$$

Results:

The structure of Trema and Para Hemoglobins- The structures of ferric Trema and Parasponia hemoglobin were solved to 1.8 Å and 2.1 Å, respectively. Figure 3-1A shows a backbone overlay of the two structures. Data collection and refinement statistics are given in Table 3-1. The electron density is well-defined for all amino acids except for the first 8 at the N-terminus and the last at the C-terminus, and these are not included in the final model. The asymmetric unit contains 2 molecules arranged as a dimer. The two structures are very similar, with a main-chain r.m.s.d. of 0.5 Å, and both are also generally similar to the structure of rice nsHb 1 (r.m.s.d. of 1.359 Å). Figure 3-1B shows an overlay of Para Hb with Rice Hb1. To test for the presence of non crystallographic symmetry between the subunits in the asymmetric units, both structures were refined with and without non crystallographic symmetry (NCS) constraints.

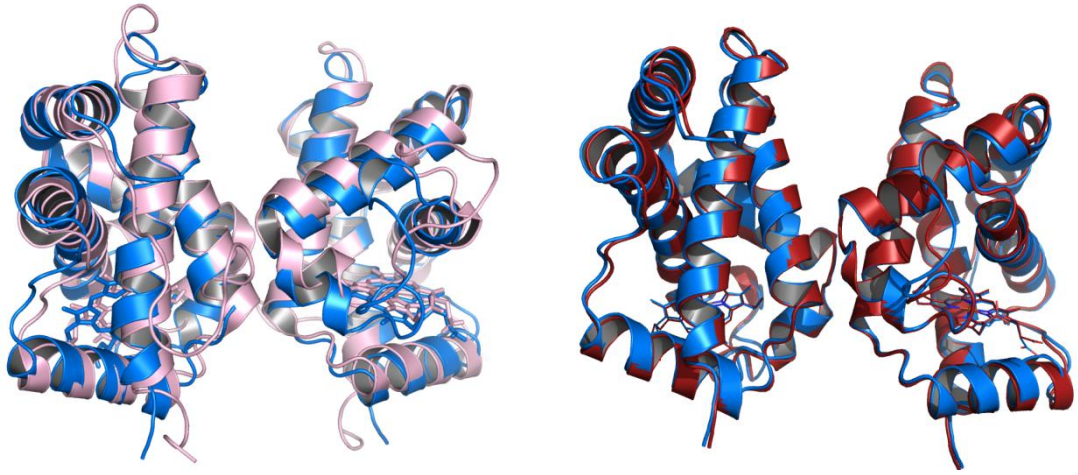

Figure 3-1. Crystal structures of *Parasponia* and *Trema* hemoglobins. A) Structural overlay of *Parasponia* and *Trema* Hb, B) Structural overlay of *Parasponia* and Rice Hb.

While the Trema Hb structure did not benefit much from the removal of NCS constraints, that of Para was greatly improved by allowing the subunits to adopt distinct structures (Table 3-1). The R_{free} and R_{crys} for Para Hb are 40 and 31 when refined with NCS restraints, and 28 and 20 when refined without them. A comparison of heme pockets in the two subunits reveals that the proximal histidine of one of the chains of Parasponia Hb is different from the other, with the imidazole side chain adopting distinct conformations in each chain. The proximal His N□-heme iron distance in Para Hb Chain A is 1.9 Å, while that of Chain B is tilted and rotated with a His N□-heme iron distance 2.7 Å. On the other hand, the two subunits in the Trema Hb asymmetric unit are equivalent, with N□-heme iron distances of 2.0 Å each.

Table 3-1. Data collection and refinement statistics

Data Collection Statistics	Native Trema Hb	SAD Trema Hb	Para Hb
Wavelength (nm)	1.54	1.72	1.54
Resolution (Å)	70.74-1.84 (1.9-1.84)[a]	50-2.01 (2.08-2.01)	37.65-2.1 (2.18-2.10)
R-merge (%)	0.064 (0.297)	0.056(0.273)	0.099(0.68)
Completeness (%)	75.7 (14.9)	87.8 (52.4)	99.1 (90.8)
Unique, Total Reflections	23868, 150655	89616, 619984	20933, 131304
Redundancy	6.31 (2.1)	7.0 (3.8)	6.27 (3.69)

Refinement/Quality Statistics		
Space Group	P212121	P212121
Unit Cell Bond lengths Bond angles	 a = 55.87,b = 70.74,c = 89.59 α = 90,β = 90, γ = 90	 a = 55.04,b = 72.04,c = 88.32 α = 90, β = 90, γ = 90
Molecules in Asymmetric Unit	2	2
Refined residues, Waters	310, 350	310, 200
R_{cryst} (%)- no NCS restraints	18.83	20.506
R_{cryst} (%)- with NCS restraints	22.585	31.928
R_{free} (%)[b]- no NCS restraints	25.378	28.875
R_{free} (%)- with NCS restraints	27.708	40.458
Average B factor (Å^2)	30.531	42.5
Ramachandran Plot		
Most favored (%)	98.3	95.9
Additionally allowed (%)	1.7	2.7
Generously allowed (%)	0	1.4
Rmsd		
Bond lengths (Å)	0.022	0.026
Bond angles (deg)	1.922	2.286

[a] Outer shell statistics are shown in parentheses.
[b] Calculated using 5% of reflections.

To demonstrate the necessity of fitting electron density differently in the two structures, the electron density for the hemes along with the distal and proximal histidines for each structure

is shown in Figure 3-2. Figure 3-2A shows the Chain A heme pocket fit into Chain A electron density. Figure 3-2B shows an attempt to fit Chain B proximal His coordinates into Chain A electron density. Figure 3-2C is the result of trying to fit Chain A proximal His parameters into Chain B density. Figure 3-2D shows that the Chain B proximal His is best fit in Chain B electron density maps. Attempts were made to fit different rotamers of His side- chain into the density. However, the conformation shown in Figure 3-2D was the best fit to the data. A comparison of the two subunits in Para Hb to those of Trema Hb reveals that both subunits in Trema Hb resemble Chain A of Para Hb.

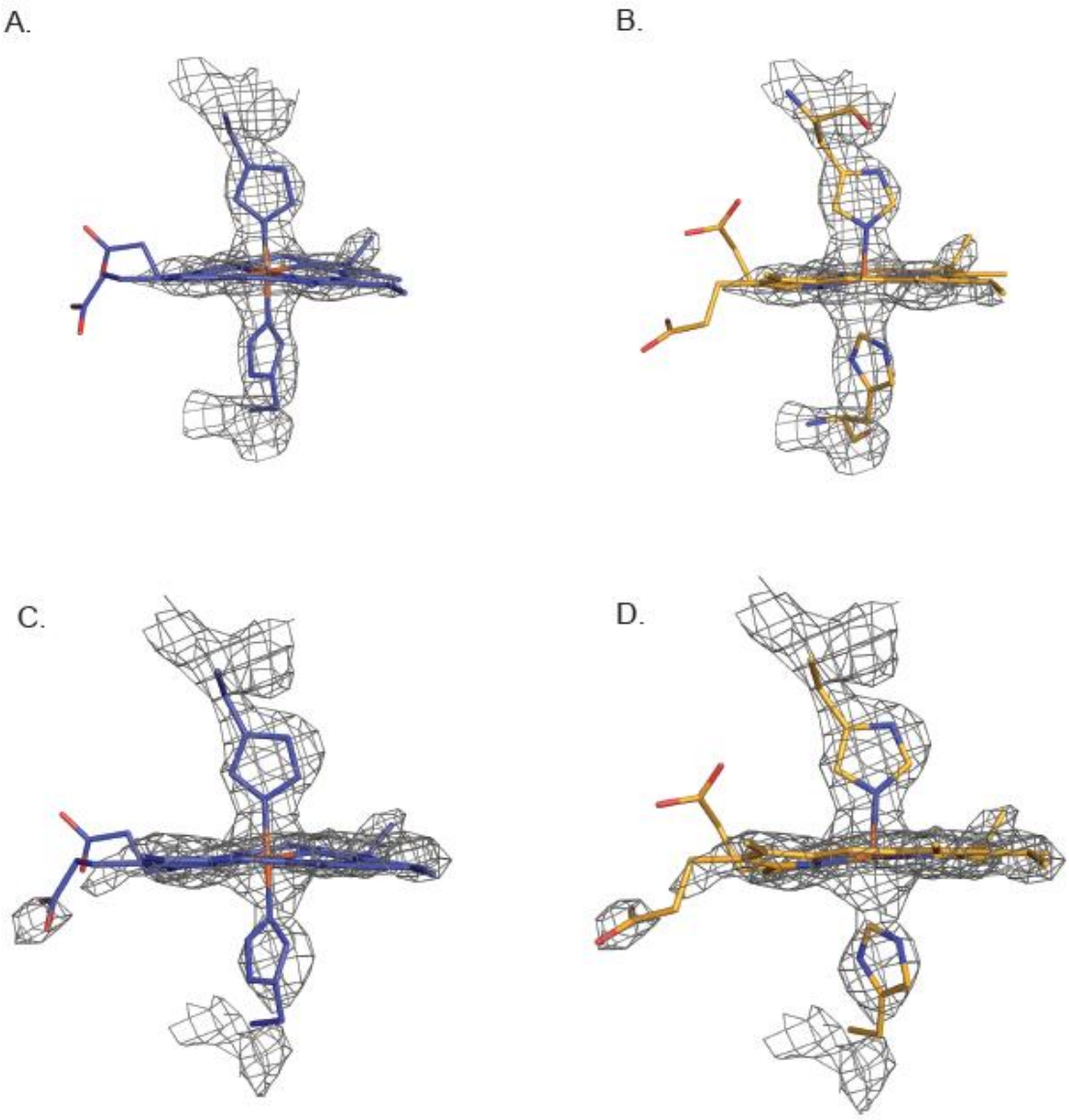

Figure 3-2: Electron density of heme pockets of Chain A and Chain B of *Parasponia* Hb. A) Chain A heme pocket structure coordinates fit into Chain A electron density, B) Chain B heme pocket fit into Chain A electron density, C) Chain A heme pocket fit into Chain B electron density, D) Chain B heme pocket fit into Chain B electron density.

Figure 3-2 A and 3-2 B are overlays of heme pockets of Chains A and B of Trema and Para Hb showing a distinct histidine rotamer in Chain B of Para Hb.

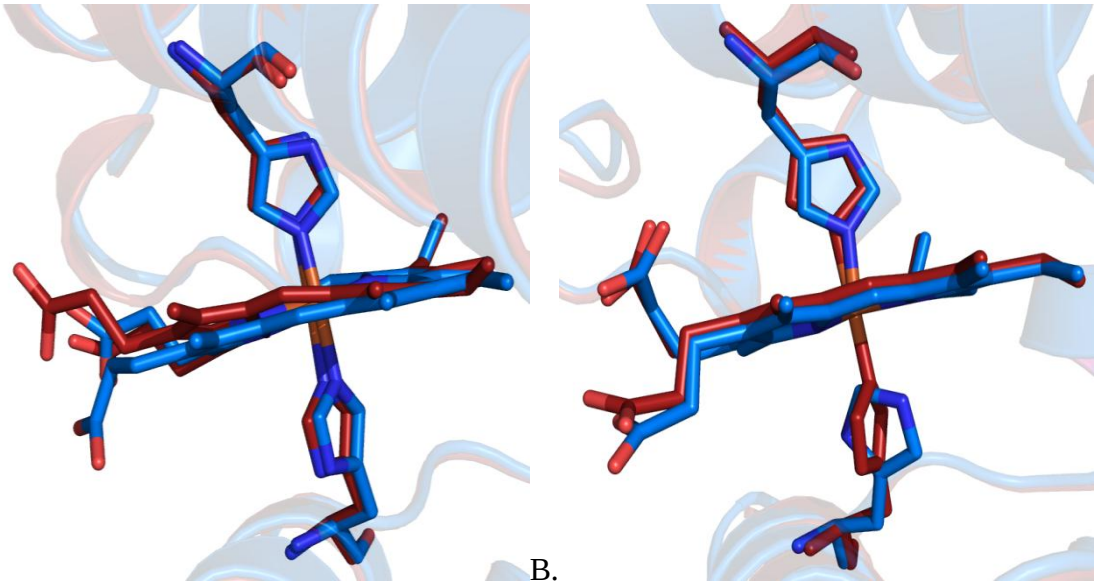

A. B.

Figure 3-3: Comparison of the Heme pockets of Parasponia (cyan) and Trema (red) heme pockets. A) Chain A and B) Chain B.

The Dimer Interface of Para Hb- The dimer contacts between two subunits of Para Hb are shown in Figure 3-4. Para Hb forms a tight dimer in which the subunits are held together by hydrogen bonds (between P45, S46, and E116) and a cluster of hydrophobic residues (I43, V117, and F120) in the BC loop and G-helix regions of both molecules. An additional hydrogen bond contact at 2.7 Å that is not seen in Rice Class 1 Hb structure is between the side chain of Glu113 of one subunit and the His 114 of the other. Rice class 1 Hb instead has an alanine at position 113. The total buried surface area as a consequence of dimerization in Trema Hb is 606.61 $Å^2$ per subunit and 594.31 $Å^2$ in case of Para Hb. The buried surface areas are larger than that of rice Hb1 (554 $Å^2$) [26], but are low when compared to values for other stable dimer [27].

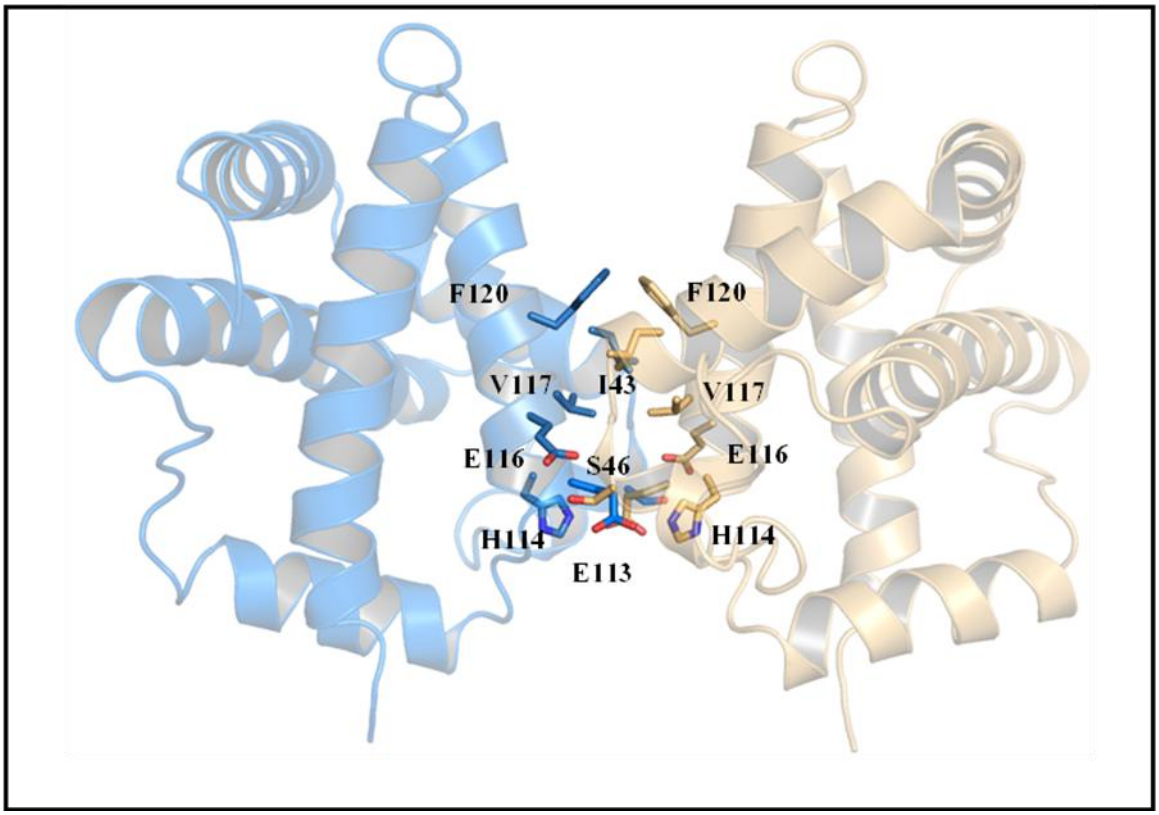

Figure 3-4: Dimer Interface of *Parasponia* Hb. Interface residues for both subunits are shown. Ser46, Glu116 and His114, Glu113 are involved in hydrogen bonding interactions, while Phe 120, V117 and I43 form a hydrophobic pocket at the interface.

Para I43N and coordination in ferric and deoxy states- In order to test whether the asymmetric hemes in the structure of Para Hb are the root of the biphasic reduction potentials observed for the wild-type protein, a point mutation from Ile 43 to Asn 43 was made at the dimer interface to break the bridging hydrophobhic contacts with the goal of producing monomeric Para Hb. The molecular mass of the I43N mutant protein was measured by equilibrium analytical ultracentrifugation (Figure 3-5A). The experiment was conducted with 5µM wild-type and Para I43N Hb, and molecular masses were calculated using equation 1. The data show that the Para I43N mutant protein has a molecular mass of 14.3 KDa and is thus monomeric at this

concentration. In comparison (and as a control experiment), wild type Para Hb is has a calculated molecular mass of 32 KDa, indicating that it is dimeric as previously published [13].

Figure 3-5B shows the absorbance traces of Para wild type and I43N mutants. The ferric absorption spectra of wild-type Para Hb and the Para I43N mutant protein are similar, exhibiting the mixed-spin state previously published for the wild type protein (as compared to rice nsHb1, included in this figure as a control for a low-spin hxhb). Figure 3-5C shows the ferrous absorbance spectra of these proteins in the visible region. As has been previously published, wild type ParaHb is largely high spin, with a slight (~15%) contribution of low spin character. In contrast, the I43N mutant protein is completely high spin. Rice nsHb1 serves as the control for hxHb with a low spin spectrum. Thus, there is some linkage between quaternary structure and heme coordination evident from a comparison of wild type Para Hb and the monomeric I43N mutant protein.

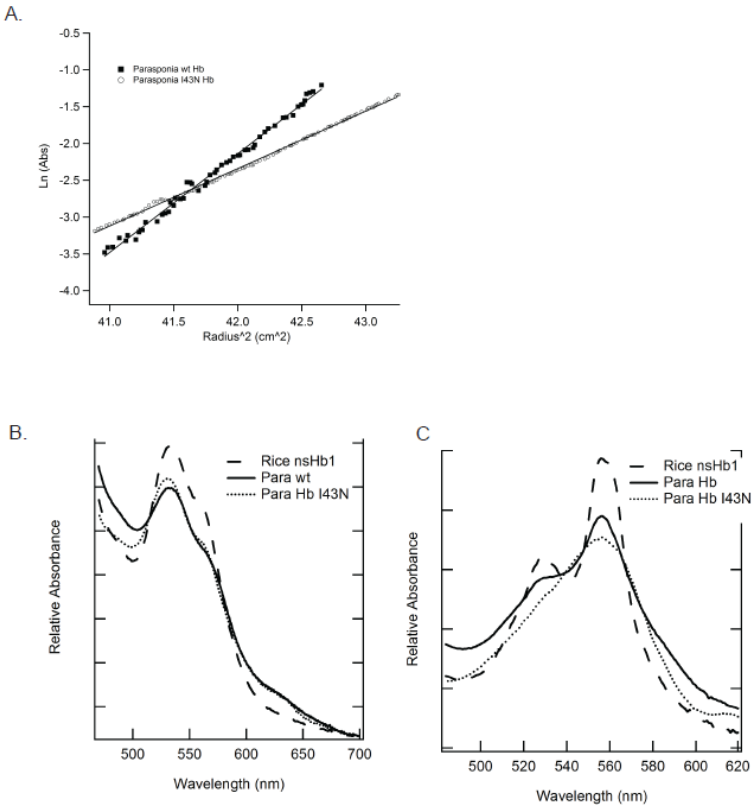

Figure 3-5. Equilibrium Analytical Ultracentrifugation and Absorbance analysis of ParaHb and Para I43N Hb. A) Each ferric Hb was analyzed by equilibrium analytical ultracentrifugation at 410 nm. B) Absorbance spectra of ferric Para Hb and ParaI43N Hb showing hexacoordination in both proteins. C) Absorbance spectra of deoxy Para and ParaI43N Hb showing partial hexacoordination in wild-type and pentacoordinate features in the mutant protein.

Electrochemistry- Previously published redox titrations for wild type Para Hb showed that there are two mid-point reduction values and a biphasic titration curve was obtained. One explanation for this is distinct, non-exchanging heme centers associated with this dimeric protein. To test this hypothesis, the mid-point reduction potential of the Para I43N was measured by potentiometric titration, and compared to wild type Para Hb (Figure 3-6). The titration curve associated with the I43N mutant protein is monophasic, with a midpoint reduction potential of +17.7, supporting the distinct heme coordination observed in the structure of wild type ParaHb as the cause of the biphasic redox titration observed for this protein [13].

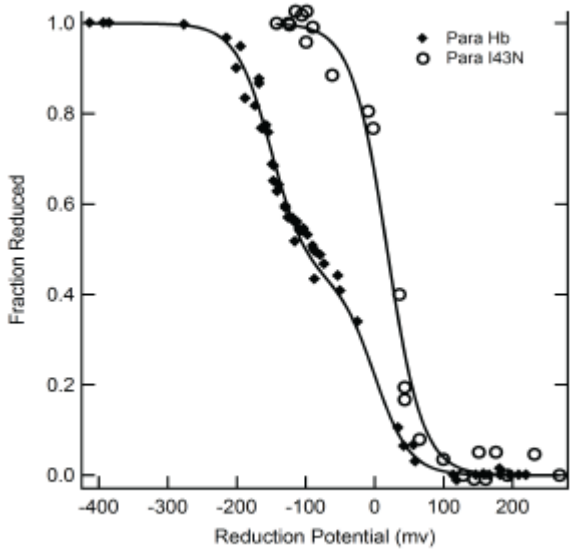

Figure 3-6: Potentiometric titrations of Para and Para I43N Hbs. Nernst plots were used to measure the redox potential for each Hb.

Discussion:

The unusual absorbance and electrochemistry results reported earlier for Para Hb, coupled with a high sequence similarity yet different functions prompted the structural investigation of Trema and Para Hb. The two structures in the ferric form are very similar except for the proximal histidine in a single chain of Para Hb that is in a conformation that has not been seen for any Hb. Previously reported structures of plant Hbs have shown displacements and structural transitions involving the distal histidine. With respect to coordination, Para Hb is a mixture of heme states, one subunit being completely hexacoordinate, and the other, pentacoordinate with distal histidine being the fifth ligand. This could possibly mean that ligand binding can occur in either of the two ways. First, ligands can bind on the proximal side of heme in Para Hb. The second scenario could involve an incoming ligand displacing the distal histidine accompanied by coordination of the proximal histidine to heme iron. However, Trema Hb is completely hexacoordinate, and the ligands displace distal histidine for subsequent binding to the heme. The difference in oxygen dissociation rates as published previously [13] might be related to this distinction in heme coordination in Trema and Para Hbs.

References:

[1] Taylor E.R., Nie X.Z., MacGregor A.W., Hill R.D., A cereal haemoglobin gene is expressed in seed and root tissues under anaerobic conditions, Plant Molecular Biology 24 (1994) 853-862.
[2] Igamberdiev A.U., Bykova N.V., Hill R.D., Nitric oxide scavenging by barley hemoglobin is facilitated by a monodehydroascorbate reductase-mediated ascorbate reduction of methemoglobin, Planta 223 (2006) 1033-1040.
[3] Kakar S., Hoffman F.G., Storz J.F., Fabian M., Hargrove M., Structure and Reactivity of Hexacoordinate Hemoglobins., Biophysical Chemistry In press, Review. (2010).
[4] Smagghe B., Hoy J., Percifield R., Kundu S., Hargrove M., Sarath G., Hilbert J., Watts R., Dennis E., Peacock W., Dewilde S., Moens L., Blouin G., Olson J., Appleby C., Review: correlations between oxygen affinity and sequence classifications of plant hemoglobins., Biopolymers 91 (2009) 1083-1096.
[5] Kundu S., Trent, J. T., 3rd, Hargrove, M. S., Plants, humans and hemoglobins, Trends in Plant Science 8 (2003) 387-393.
[6] Appleby C.A., Tjepkema J.D., Trinick M.J., Hemoglobin in a Nonleguminous Plant, Parasponia: Possible Genetic Origin and Function in Nitrogen Fixation, Science 220 (1983) 951-953.
[7] Guldner E., Godelle B., Galtier N., Molecular adaptation in plant hemoglobin, a duplicated gene involved in plant-bacteria symbiosis, Journal of Evolutionary Biology 59 (2004) 416-425.
[8] Guldner E., Desmarais E., Galtier N., Godelle B., Molecular evolution of plant haemoglobin: two haemoglobin genes in Nymphaeaceae Euryale ferox, Journal of Evolutionary Biology 17 (2004) 48-54.
[9] Kortt A.A., Trinick M.J., Appleby C.A., Amino acid sequences of hemoglobins I and II from root nodules of the non-leguminous Parasponia rigida-rhizobium symbiosis, and a correction of the sequence of hemoglobin I from Parasponia andersonii, Eur J Biochem 175 (1988) 141-149.
[10] Bogusz D., Appleby C.A., Landsmann J., Dennis E.S., Trinick M.J., Peacock W.J., Functioning haemoglobin genes in non-nodulating plants, Nature 331 (1988) 178-180.
[11] Wittenberg J.B., Appleby C.A., Wittenberg B.A., The Kinetics of the Reactions of Leghemoglobin with Oxygen and Carbon Monoxide, J. Biol. Chem. 247 (1972) 527-531.
[12] Gibson Q., Wittenberg J., Wittenberg B., Bogusz D., Appleby C., The kinetics of ligand binding to plant hemoglobins. Structural implications., J Biol Chem 264 (1989) 100-107.
[13] Sturms R., Kakar S., Trent J., Hargrove M., Trema and Parasponia hemoglobins reveal convergent evolution of oxygen transport in plants., Biochemistry (2010).
[14] Pape T., Schneider, T. R., HKL2MAP: a graphical user interface for macromolecular phasing with SHELX programs, Journal of Applied Crystallography 37 (2004) 843-844.
[15] Terwilliger T.C., Berendzen J., Automated MAD and MIR structure solution, Acta Crystallographica. Section D, Biological Crystallography 55 (1999) 849-861.
[16] Terwilliger T.C., Maximum likelihood density modification, Acta Crystallographica. Section D, Biological Crystallography D56 (2000) 965-972.
[17] Jones T.A., Zou J.Y., Cowan S.W., Kjeldgaard, Improved methods for building protein models in electron density maps and the location of errors in these models, Acta Crystallographica. Section D, Biological Crystallography 47 (Pt 2) (1991) 110-119.

[18] Schwede T., Kopp J., Guex N., Peitsch M., SWISS-MODEL: An automated protein homology-modeling server., Nucleic Acids Res 31 (2003) 3381-3385.
[19] Murshudov G.N., Vagin A.A., Dodson E.J., Refinement of macromolecular structures by the maximum-likelihood method, Acta Crystallographica. Section D, Biological Crystallography 53 (1997) 240-255.
[20] CCP4, The CCP4 suite: programs for protein crystallography, Acta Crystallographica. Section D, Biological Crystallography 50 (1994) 760-763.
[21] Teplyakov A., Vagin, A., MOLREP: an Automated Program for Molecular Replacement, J. Appl. Cryst. 30 (1997) 1022-1025.
[22] Brunger A.T., Adams P.D., Clore G.M., DeLano W.L., Gros P., Grosse-Kunstleve R.W., Jiang J.S., Kuszewski J., Nilges M., Pannu N.S., Read R.J., Rice L.M., Simonson T., Warren G.L., Crystallography & NMR system: A new software suite for macromolecular structure determination, Acta Crystallogr D Biol Crystallogr 54 (1998) 905-921.
[23] DeLano W.L., The PyMOL Molecular Graphics System, DeLano Scientific, http://www.pymol.org, San Carlos, CA, USA, 2002.
[24] Goodman M.D., Hargrove M.S., Quaternary structure of rice nonsymbiotic hemoglobin, Journal of Biological Chemistry 276 (2001) 6834-6839.
[25] Halder P., Trent J.r., Hargrove M., Influence of the protein matrix on intramolecular histidine ligation in ferric and ferrous hexacoordinate hemoglobins., Proteins 66 (2007) 172-182.
[26] Hargrove M.S., Brucker, E. A., Stec, B., Sarath, G., Arredondo-Peter, R., Klucas, R. V., Olson, J. S., Phillips, G. N., Jr., Crystal structure of a nonsymbiotic plant hemoglobin, Structure Folding and Design 8 (2000) 1005-1014.
[27] Janin J., Miller S., Chothia C., Surface, Subunit Interfaces and Interior of Oligomeric Proteins, J. Mol. Biol. 204 (1988) 155-164.

CHAPTER 4. HEXACOORDINATION IN *PHYSCOMITRELLA* (MOSS) HEMOGLOBIN IS REGULATED BY TYR^{CD1}

A paper to be submitted to *Protein Science*

Smita Kakar[1], Benoit Smagghe[2], James Trent, III, Raul Arredondo-Peter, Gautam Sarath, and Mark S. Hargrove[1,3]

Abstract:

Plant hemoglobin chemistry and structures have been extensively studied since years. Non- symbiotic hemoglobins are widespread and have been identified in bryophytes, gymnosperms and angiosperms. These are non-oxygen transporters with low oxygen dissociation rates. Most of the studies have been focused on angiosperm non symbiotic hemoglobins. Very little research has been conducted on 'ancient' bryophyte hemoglobins that include mosses, liverworts and hornworts. An interesting feature of a moss species, *Physcomitrella patens* is a tyrosine at "CD1" position instead of a highly conserved phenylalanine in other non symbiotic plant hemoglobins. The initial biophysical studies suggest a role of Tyr^{CD1} in influencing the heme coordination state.

[1]Department of Biochemistry, Biophysics, and Molecular Biology; Iowa State University, Ames, IA 50011
[2] Immune Disease Institute, Boston, MA 02115, USA
[3]To whom correspondence should be addressed

Introduction:

Once considered to be limited to oxygen transport in animals, hemoglobins (Hbs) with a wide variety of functions are now known to exist in most living organisms [1-3]. In fact, many plants and animals contain multiple globin genes whose functions have yet to be identified [4, 5]. It is presumed that most globins are "Hbs", meaning that they exploit the heme prosthetic group for their modes of action. Heme, which houses an iron atom coordinated by four porphyrin pyrrole nitrogens, provides the propensity for the binding of small electronegative molecules like oxygen, carbon monoxide, nitric oxide, cyanide, or larger basic molecules like acetate, imidazole, and phenol [6]. Both the oxidation state of the iron and the chemical environment and coordination state in the globin have dramatic influences on the functional behavior of Hbs [7].

The vast majority of knowledge about the structure and function of Hbs stems from research directed at how oxygen transporters reversibly bind oxygen. A structural feature common among oxygen transporter Hbs is pentacoordinate heme, resulting from one coordinate covalent bond between a conserved "proximal" histidine in the globin and an axial site on the heme iron. The second axial site is left open for reversible oxygen binding. Oxygen transport Hbs often also contain a second conserved histidine, the "distal" His^{E7} (where "E7" designates a position within the common globin fold), which lies near the oxygen binding site, but does not coordinate the heme iron, and helps to regulate oxygen affinity (Figure 4-1). Another conserved side chain near the heme is Phe^{CD1}, which lies just above the heme plane and is thought to stabilize bound heme, and regulate the hydrophobic and electrostatic environment of the heme pocket [8]. Another class of hemoglobins, defined by their coordination state, is hexacoordinate hemoglobins (hxHbs). HxHbs are common in higher plants and animals, and

display hexacoordination with reversible binding of the His^{E7} to the second axial site of the heme iron. In the presence of exogenous ligands like oxygen and carbon monoxide, the distal histidine is displaced and these (and other) ligands will form stable complexes [9, 10]. However, the affinity and reactivity with exogenous ligands are affected by hexacoordination, and it is possible that structural changes conferred by this reversible change in coordination state are linked to the physiological activity of hxHbs [11].

Research with hxHbs and heme model compounds demonstrates that the hexacoordinate heme iron is much more stable than the pentacoordinate counterpart, particularly in the ferric oxidation state, due to smaller low-spin heme iron [12] . In fact, the design of pentacoordinate heme proteins and model compounds is difficult due to the propensity for hexacoordination by a nearby histidine [13, 14]. Thus, evolution of a pentacoordinate oxygen transporter with a distal histidine would require specific events to prevent hexacoordination. It has therefore been proposed that hxHbs were likely the evolutionary progenitors of oxygen transport Hbs in both plants and animals [15-17] .

While this may not be true in animals [18], it appears so in plants, where the pentacoordinate "leghemoglobins" evolved from its hexacoordinate predecessors the, "nonsymbiotic Hbs" (nsHbs). Recent investigations of nsHbs have revealed functionally significant variation in quaternary structure, coordination state, and redox potential associated with the evolution of oxygen transport function [16]. However, previous studies of plant Hbs have been limited to relatively recently evolved angiosperms, and little is known about the

coordination state of the evolutionarily more ancient plant hemoglobins found in bryophytes, including moss (*Physcomitrella*) and liverworts (*Marchantia*).

Figure 4-1 shows the classification of plant globins into three clades based on sequence alignments.

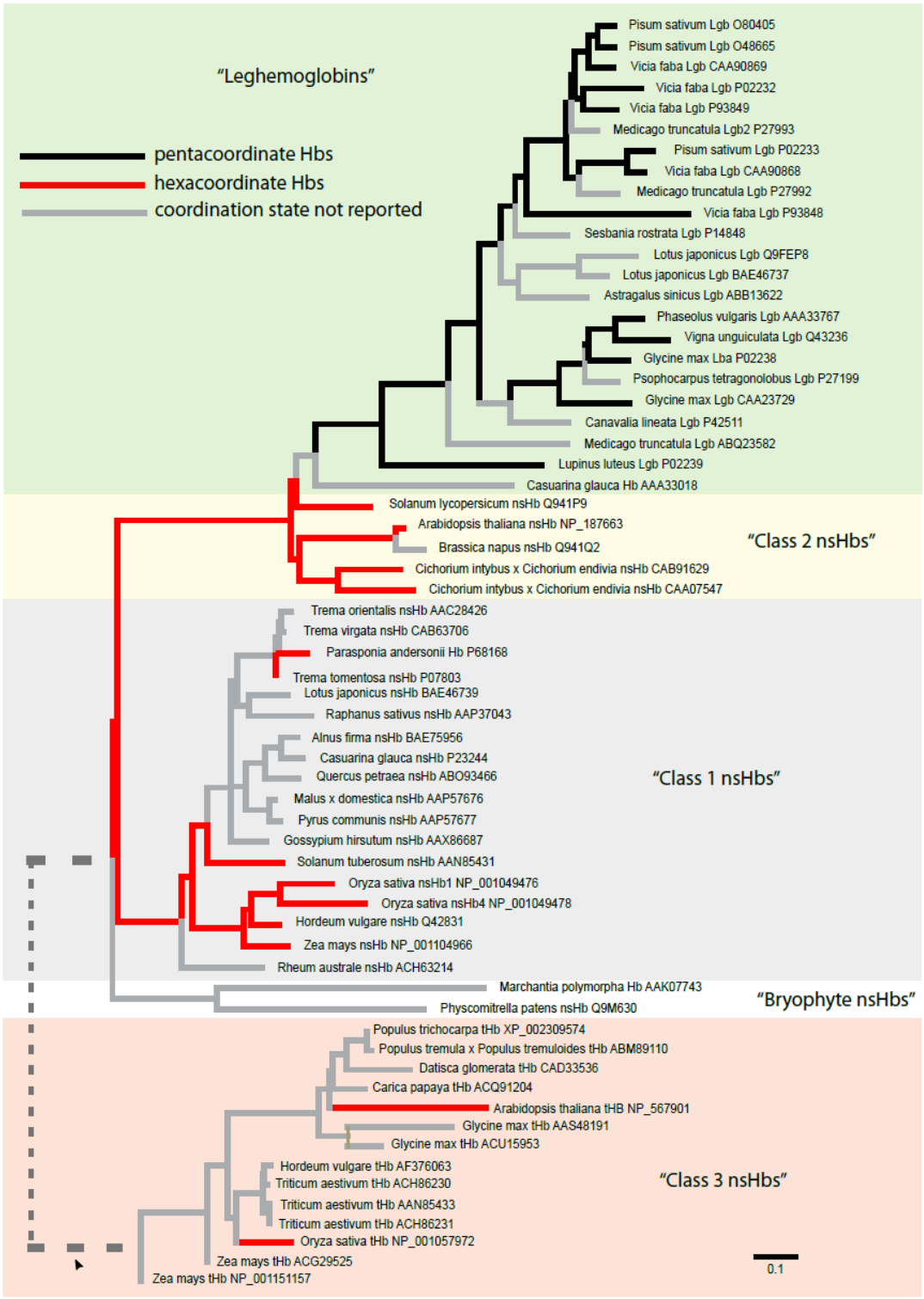

Figure 4-1. Maximum likelihood phylogram of select plant globin sequences. Plant globins can classified into three "classes", each containing hexacoordinate members (red lines). The term nonsymbiotic hemoglobin" (nsHb) is in deference to the previously discovered symbiotic "leghemoglobins", which are pentacoordinate oxygen transporters.

Here we report an investigation of the coordination state, quaternary structure, and midpoint reduction potentials of the nsHb from *Physcomitrella patens* (*Phy*Hb). This protein is notable in that it represents the common ancestor to the angiosperm nsHbs and leghemoglobins, and contains a tyrosine at heme pocket position CD1. Position CD1 normally houses a highly conserved phenylalanine (Figure 4-2), and the natural substitution of tyrosine at CD1 in *Phy*Hb is one of few known examples of a variation at this position [19]. Figure 4-3 shows a sequence alignment of proteins from Class 1, Class 2, Bryophyte nsHb, leghemoglobin and myoglobin. Our results with wild type *Phy*Hb and proteins with substitutions at His^{E7} and Tyr^{CD1} demonstrate that *Phy*Hb is a monomeric hexacoordinate Hb whose coordination state is controlled by Tyr^{CD1}. Furthermore, the redox potential of *Phy*Hb is affected to an unprecedented degree by mutations at His^{E7} and Tyr^{CD1}, demonstrating the conservation of a low redox potential in nsHbs that is not just a consequence of heme hexacoordination.

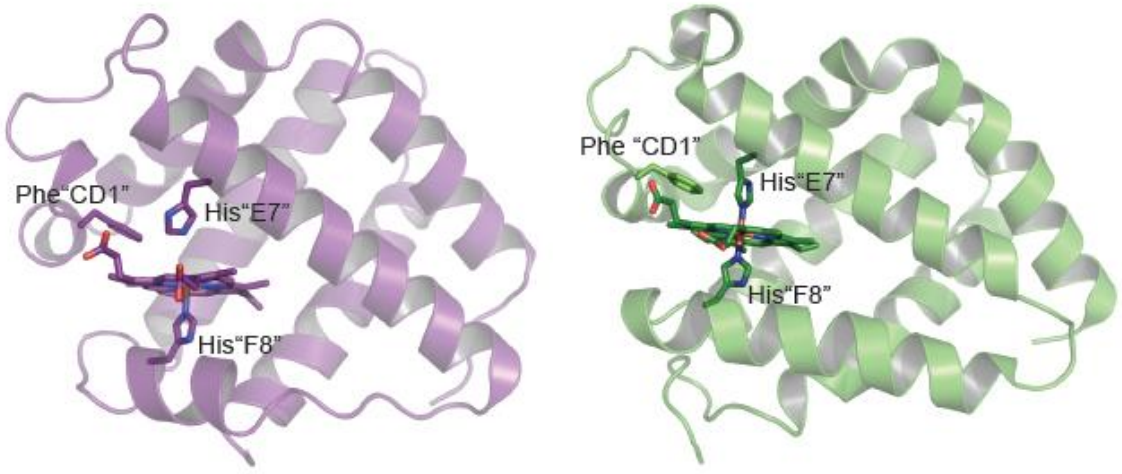

Figure 4-2. Ribbon structures of Pentacoordinate and Hexacoordinate hemoglobins. Pentacoordinate heme (left) of soybean hemoglobin (1BIN.pdb) and Hexacoordinate heme (right) of Drosophila Hb (2BK9.pdb) showing conserved Phe at "CD1" position. The figure also shows distal "E7" and proximal "F8" histidines.

```
                                                                "B10"          "CD1"
RiceHb1   1    MA--LVEDNNAVAV--------SFSEEQEALVLKSWAILKKDSANIALRFFLKIFEVAPSASQMFSFLRN--SDVPLEKN   68
Tom Hb2   1    MG----------------------FTDKQEALVRDSWEFMKQDIPQLSLRFFSLILEIAPVAKNMFSFLKD--SDELPENN   57
MossHb    1    MASAVVNQSEAAAVRAPSKPVKTYSKENEQLVKQSWEILKKDAQRNGINFFRKVFEIAPGAKAMYSFLRD--STIPFEEN   78
Mb        1    MG----------------------LSDGEWQLVLNVWGKVEADIPGHGQEVLIRLFKGHPETLEKFDKFKHLKSEDEMKAS   59
Lba       1    MG----------------------AFTEKQEALVSSSFEAFKANIPQYSVVFYTSILEKAPAAKDLFSFLSNG----VDPSN   56

                    HisE7                                  HisF8
RiceHb1   69   PKLKTHAMSVFVMTCEAAAQLRKAGKVTVRDTTLKRLGATHLKY-GVGDAHFEVVKFALLDTIKEEVPADMWSPAMKSAW   147
Tom Hb2   58   PKLRAHAVKVFKMTCESAIQLREKGEVVVGETTLKYLGSIHLQK-RVADPHFEVVKEALLRTVKEATG-NKWKDEMKEAW   135
MossHb    79   PKVKNHARYVFMMTGDAAVQLGEKGAYQVLESKLQKLAATHVNA-GVTDDQFEIVKEAILYAIEMGVP-DLWSPELKSAW   156
Mb        60   EDLKKHGATVLTALGGI---LKKKGH---HEAEIKPLAQSHATKHKIPVKYLEFISECIIQVLQSKHPGDFGADA-QGAM   132
Lba       57   PKLTGHAEKLFGLVRDSAGQLKANGTV-VADA---ALGSIHAQK-AITDPQFVVVKEALLKTIKEAVG-DKWSDELSSAW   130

RiceHb1   148  SEAYDHLVAAIKQEMKPAE-----  166
TomHb2    136  SEAYDQLASAIKAEMHAEAAA---  156
MossHb    157  GDAYDMLAEQVKAEMHAQRSAATS  180
Mb        133  NKALELFRKDMASNYKELGFQG--  154
Lba       131  EVAYDELAAAIKKAF---------  145
```

Figure 4-3. Sequence alignments of representative members from each class of plant hemoglobins and myoglobin. Rice Hb from Class 1, Tomato Hb from Class 2, Moss Hb from Bryophytes, Leghemoglobin (Lba) and Myoglobin (Mb) are aligned sequentially, showing a tyrosine at "CD1" position in Moss Hb.

Materials and Methods:

Production of Proteins:

The cDNA for *Physcomitrella patens* (GenBank number AF218049) was generously provided by Dr. Raúl Arredondo Peter. The cDNA was inserted into a pET28a plasmid for expression in *E.coli*, BL21 Star DE3 strain. Mutants were generated for *Phy*Hb by site directed mutagenesis using the Quickchange mutagenesis kit from Agilent Technologies. The distal histidine His^{E7}, H84 was mutated to a leucine. The Tyr^{CD1} was mutated to a phenylalanine. A double mutant incorporating amino acid changes at both His^{E7} and Tyr^{CD1} was also made to rule out the effects of any side chain capable of providing hexacoordination.

All proteins were expressed in BL-21 (DE3) cells with induction using 0.5 mM IPTG. Cells were grown in 2 liter Erlenmeyer flasks containing 1 liter Terrific Broth and were inoculated with a 100 ml starter culture supplemented with 1ml of 50 mg/ml kanamycin. The flasks were incubated at 37° C with shaking at 250 rpm for 18 hours. The cells were harvested by centrifugation at 6000 rpm for 5 min after which they were homogenized. Purification was achieved in three steps: 1) Ammonium sulfate fractionation (45% and 90%), 2) Immobilized metal affinity chromatography (BD Talon) and 3) gel filtration chromatography (Sephacryl S-200 resin). The efficiency of purification was measured by the ratio of Soret and peak at 280 nm.

UV-Visible Spectroscopy:

All absorbance spectra were measured using a Cary-50 Bio spectrophotometer. Ferric protein was prepared by oxidizing the protein with potassium ferricyanide followed by desalting over a G-25 column. Ferrous hemoglobins were generated by reducing ferric samples with sodium dithionite.

In order to calibrate spectral changes accompanying fractional hexacoordination, an imidazole titration of soybean leghemoglobin was conducted since it binds imidazole in the ferrous form thus mimicking hxHbs. Imidazole was added to sodium dithionite reduced protein in 100 mM potassium phosphate, pH 7.0 to achieve final concentrations ranging from 0.02 to 1.6 mM. The curve in Figure 4-4C is fitted to the following equation to extract *K*D:

$$F_H = \frac{[\text{Imidazole}]}{K_D + [\text{Imidazole}]} \quad \text{Equation 1}$$

Quaternary Structure Analysis:

Quaternary structure of *Phy*Hb was measured using equilibrium analytical ultracentrifugation following a procedure described previously (Chapter 2) [20]. The concentration of proteins used was 5μM. Molecular mass was calculated from the linear portions of the plots in Figure 4-5 using Equation 2, where M is molecular mass, r is the radial position of the sample, v is partial specific volume (fixed at 0.72 mL/g), F is solvent density (fixed at 0.9982 g/mL), the angular velocity = 3099 rads/s (29600 rpm), R = 8.31441 _107 (g cm2)/(s2 K mol), and T was 293 K.

$$\ln(Abs) = \frac{M(1-v\rho)\omega^2}{2RT} r^2 \quad \text{Equation 2}$$

Electrochemistry:

Potentiometric titrations were conducted using the method described previously except that titrations were performed in an anaerobic chamber eliminating the need to degas and purge all reagents with argon [7]. Absorbance spectra were collected by monitoring the Soret peak. Midpoint potentials were derived by fitting data to the following equation:

$$F_{reduced} = \frac{e^{-\left(\frac{nF(E_{obs}-E_{mid})}{RT}\right)}}{1+e^{-\left(\frac{nF(E_{obs}-E_{mid})}{RT}\right)}} \quad \text{Equation 3}$$

Homology Modeling:

The Swiss-Model server [21] was used for automated comparative modeling of the three-dimensional structure of *Phy*Hb. The steps in modeling included template superposition, target-template alignment, model building and energy minimization [21-23].

Results:

Coordination in the ferric oxidation state: The visible spectrum of *Phy*Hb in the ferric form is characteristic of a typical hexacoordinate, low spin nsHb (Figure 4-4A). However, the Y65F mutant spectrum is completely hexacoordinate with a prominent band at 529nm and a shoulder at 560nm, supporting a role of Tyr^{CD1} (65) in providing competition to bis-histidyl hexacoordination. Surprisingly, the HisE7L mutant absorbance trace is indicative of a low-spin hemichrome heme center, possible because Tyr^{CD1}provides some degree of hexacoordination in the ferric oxidation state in the absence of His E7. However, replacements of the side chains of both E7 and Tyr^{CD1}results in a high-spin, pentacoordinate complex as seen in Lba absorbance spectra with peaks at 484nm and 620nm that are characteristic of a ligand to metal charge transfer.

Coordination in the ferrous oxidation state: Figure 4-4B shows the deoxy absorbance spectra of *Phy*Hb, *Phy*Hb E7L, *Phy*Hb Y65F and *Phy*Hb E7L, Y65F double mutant. Both *Phy*Hb and Y65F mutant are hexacoordinate in the deoxy state evident from splitting of the visible bands and characteristic peaks at 530 and 556 nm. The E7L mutant however, is high spin in the ferrous state with single peak at 540 nm. The double mutant spectrum has a single peak at 540 nm depicting pentacoordination in deoxy state too. Figure 4-4C shows the absorbance traces upon addition of a series of imidazole concentrations to Lba. This experiment was conducted in order to provide a reference for the degree of histidine coordination in these Hbs. The ratio of

absorbance at 537nm to 591nm was plotted against the fraction of hexacoordination (F_D) (Figure

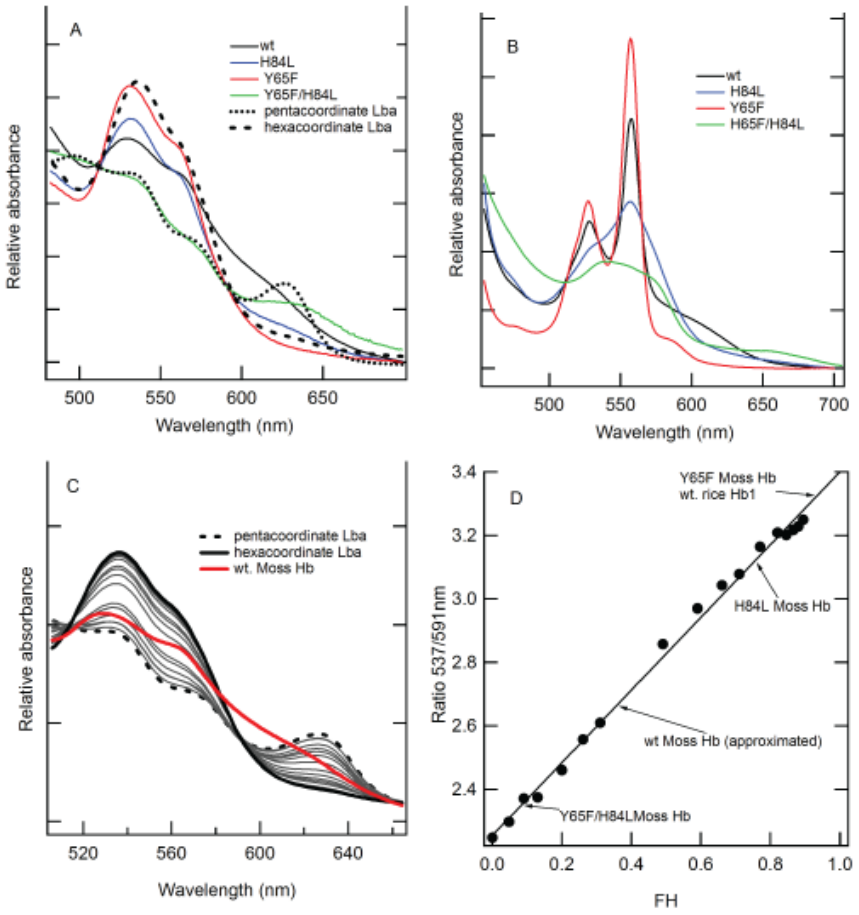

4-4D).

Figure 4-4. Spectral data for *Phy*Hb and its mutants. A) Absorbance traces of ferric forms of proteins in the visible spectral region, B) Absorbance spectra of deoxy forms of proteins, C) Imidazole titration plot of Leghemoglobin, and D) Plot showing approximate fractions of hexacoordination in *Phy*Hb and its mutants.

Quaternary structure and Electrochemistry: The molecular mass of PhyHb from equilibrium analytical studies was calculated to be 25 kDa that is close to that of a monomer (20 kDa). Figure 4-5 shows the equilibrium data for *Phy*Hb along with Rice nsHb1 which is a

monomer at the concentrations of proteins used in the experiment [20] and Para Hb that is a dimer [16].

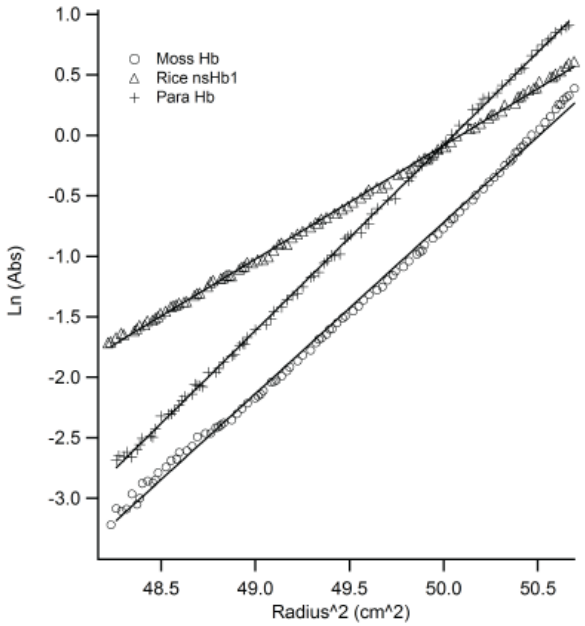

Figure 4-5. Equilibrium Analytical Ultracentrifugation Analysis of *Phy*Hb. The plots for Rice nsHb1 (monomer) and *Parasponi*a Hb (dimer) are also shown.

The midpoint reduction potential of *Phy*Hb is -180mv that is characteristic of a typical hexacoordinate protein and is even lower than rice nsHb that is -132mv. *Phy*Y65F has a reduction potential of +30 mv, while the midpoint reduction potentials of E7L mutant and double mutant E7L, Y65F was calculated to be +173 mv and +120 mv, respectively.

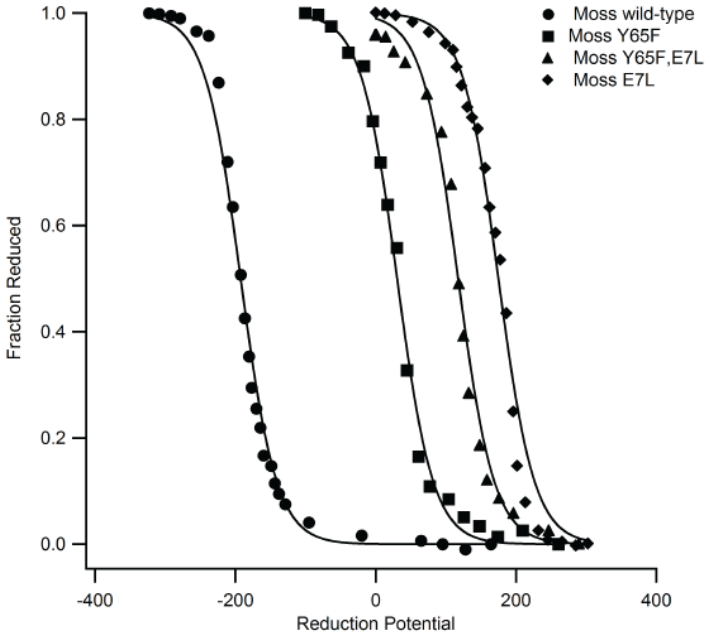

Figure 4-6: Redox potentials of *Phy*Hb and its mutants. *Phy*Hb is shown as circles and has a low midpoint potential. All mutants have highly positive redox potentials with respect to the wild type.

Modeled structure of PhyHb: Homology modeling method has been used to thread the sequence of *Phy*Hb onto the structure of RiceHb (1D8U.pdb) as a template. The percentage sequence similarity among the two sequences is 48.4. An overlay of the published Rice nsHb1 and modeled *Phy*Hb is shown in Figure 4-7A. A close look at the heme pocket shows that the side chain of Tyr^{CD1} in *Phy*Hb lies perpendicular to the Phe CD1 side chain in Rice Hb (Figure 4-7B). The two structures overlay very well with differences at two residues in the heme vicinity. First, Tyr^{CD1} in *Phy*Hb is replaced by Phe^{CD1} in Rice nsHb1 and secondly, there is a tyrosine at position E10 in *Phy*Hb that is a serine in the rice Hb1 sequence.

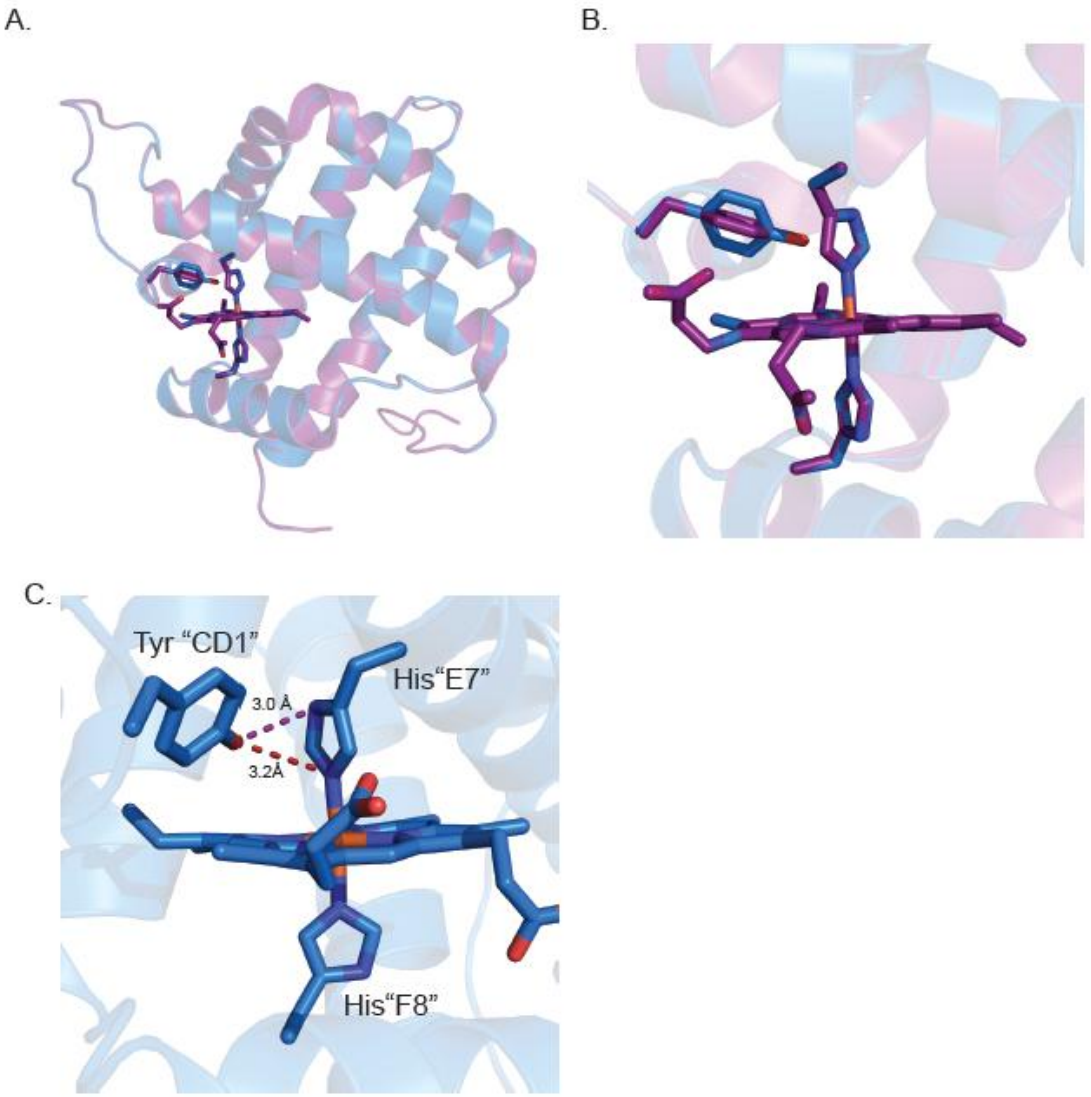

Figure 4-7. Modeled structure of *Phy*Hb. A) Ribbon structure overlay of RiceHb1 (purple) and *Phy*Hb (blue). B) Heme pockets of RiceHb1 (purple) and *Phy*Hb (blue) showing a Tyr ^{CD1} in the *Phy*Hb. C) Possible interactions of CD1 and E7 residues in *Phy*Hb, tyr ^{CD1} lies in close proximity to both nitrogen atoms in histidine side chain.

Discussion:

There is a tyrosine at the "CD1" position in *Phy*Hb that is a phenylalanine in most Hbs and is a highly conserved residue. The only other example of Tyr^{CD1} is seen in a class of truncated hemoglobins from Gram-positive bacteria. These include *Mycobacterium tuberculosis, M. leprae, M. avium, S.coelicolor* and *Clostridium diphtherae* [19]. The presence of Tyr instead of Phe could possibly be an ancient functional adaptation of these Hbs. This tyrosine seems to have a role in heme coordination evident from high spin spectra in Fe3+ and Fe2+ states of the double mutant *Phy*E7L, Y65F. Moreover, the redox potential of *Phy*Hb is typical of hexacoordinate Hbs. Mutation at His^{E7} and Tyr^{CD1} are vastly different from *Phy*Hb that cannot be accounted for based solely on heme coordination.

References

[1] T. Hankeln, B. Ebner, C. Fuchs, F. Gerlach, M. Haberkamp, T. Laufs, A. Roesner, M. Schmidt, B. Weich, S. Wystub, S. Saaler-Reinhardt, S. Reuss, M. Bolognesi, D. De Sanctis, M. Marden, L. Kiger, L. Moens, S. Dewilde, E. Nevo, A. Avivi, R. Weber, A. Fago, T. Burmester, J Inorg Biochem, vol. 99, 2005, pp. 110-119.
[2] J. Wittenberg, M. Bolognesi, B. Wittenberg, M. Guertin, J Biol Chem, vol. 277, 2002, pp. 871-874.
[3] B. Smagghe, J. Hoy, R. Percifield, S. Kundu, M. Hargrove, G. Sarath, J. Hilbert, R. Watts, E. Dennis, W. Peacock, S. Dewilde, L. Moens, G. Blouin, J. Olson, C. Appleby, Biopolymers, vol. 91, 2009, pp. 1083-1096.
[4] R. Watts, P. Hunt, A. Hvitved, M. Hargrove, W. Peacock, E. Dennis, Proc Natl Acad Sci U S A, vol. 98, 2001, pp. 10119-10124.
[5] T. Burmester, T. Hankeln, J Exp Biol, vol. 212, 2009, pp. 1423-1428.
[6] A. Cowley, D. Benson, Inorg Chem, vol. 46, 2007, pp. 48-59.
[7] P. Halder, J.r. Trent, M. Hargrove, Proteins, vol. 66, 2007, pp. 172-182.
[8] M. Hargrove, A. Wilkinson, J. Olson, Biochemistry, vol. 35, 1996, pp. 11300-11309.
[9] R. Arredondo-Peter, M. Hargrove, G. Sarath, J. Moran, J. Lohrman, J. Olson, R. Klucas, Plant Physiol, vol. 115, 1997, pp. 1259-1266.
[10] M. Hargrove, Biophys J, vol. 79, 2000, pp. 2733-2738.
[11] J. Hoy, H. Robinson, J.r. Trent, S. Kakar, B. Smagghe, M. Hargrove, J Mol Biol, vol. 371, 2007, pp. 168-179.
[12] A. Cowley, M. Kennedy, S. Silchenko, G. Lukat-Rodgers, K. Rodgers, D. Benson, Inorg Chem, vol. 45, 2006, pp. 9985-10001.

[13] M.K. Safo, Nesset, M.J.M., Walker, F.A., Debrunner, P.G., and Scheidt, W.R., Journal of American Chemical Society, vol. 119, 1997, pp. 9438-9448.
[14] S.N. Nesset MJM, Enemark PD, Jacobson SE, Waliker FA, Inorganic Chemistry, vol. 35, 1996, pp. 5188-5200.
[15] S. Dewilde, L. Kiger, T. Burmester, T. Hankeln, V. Baudin-Creuza, T. Aerts, M. Marden, R. Caubergs, L. Moens, J Biol Chem, vol. 276, 2001, pp. 38949-38955.
[16] R. Sturms, S. Kakar, J. Trent, M. Hargrove, Biochemistry, 2010.
[17] T. Burmester, B. Weich, S. Reinhardt, T. Hankeln, Nature, vol. 407, 2000, pp. 520-523.
[18] S. Kakar, F.G. Hoffman, J.F. Storz, M. Fabian, M. Hargrove, Biophysical Chemistry, vol. In press, Review., 2010.
[19] M. Mukai, P. Savard, H. Ouellet, M. Guertin, S. Yeh, Biochemistry, vol. 41, 2002, pp. 3897-3905.
[20] M. Goodman, M. Hargrove, J Biol Chem, vol. 276, 2001, pp. 6834-6839.
[21] T. Schwede, J. Kopp, N. Guex, M. Peitsch, Nucleic Acids Res, vol. 31, 2003, pp. 3381-3385.
[22] K. Arnold, L. Bordoli, J. Kopp, T. Schwede, Bioinformatics, vol. 22, 2006, pp. 195-201.
[23] N. Guex, M. Peitsch, Electrophoresis, vol. 18, 1997, pp. 2714-2723.

CHAPTER 5. IDENTIFICATION OF REDUCTASES TO SUSTAIN NITRIC OXIDE SCAVENGING IN HEXACOORDINATE HEMOGLOBINS

Introduction:

Functions of hexacoordinate hemoglobins are still in question. Their low intracellular concentrations coupled with numerous biophysical studies support the concept that most do not play a role in oxygen transport. One of the many non-oxygen transport functions of Hbs is detoxification of nitric oxide (NO).

In animals, NO is synthesized from the amino acid, L-arginine by members of a family of proteins called NO synthases (NOS). NO is involved in numerous cellular functions such as neurotransmission, neuroprotection, blood pressure regulation and in the immune response [1], and can be toxic if produced in excess. In pro-oxidative cells, NO can undergo oxidative-reductive reactions to form toxic products such as ‘reactive nitrogen species’ (RNS) [1, 2]. RNS are implicated in pathogenesis of neurodegenerative disorders [1, 3, 4].

A number of physiologically significant reactions have been observed for NO and hemoglobins. 1) Bacterial and yeast flavohemoglobins (flavoHbs) scavenge NO resulting from oxidative bursts, increasing resistance to immune response during infection [5]. It was this reaction that defined the term "NO dioxygenase". 2) NO scavenging by cell free Hb-based blood substitutes results in severe hypertension [6]. 3) NO is scavenged by myoglobin in cardiac tissue [7]. 4) Hb from the parasitic worm *Ascaris* is reported to be an NO-activated dioxygenase [8]. 5)

The Hb from *Mycobacterium tuberculosis* is reported to be a NO scavenger [9]. 6) NO bound to human Hb thiols has been implicated in vascular control [10, 11].

Hemoglobins have been shown to scavenge Nitric Oxide in smooth muscle and around the endothelium [7, 12]. No such observation has been made for other actively respiring tissues such as brain and retina. It may be possible that during hypoxia, Ngb that is present in the brain and retina scavenges NO in these tissues [13]. Elucidating such a mechanism for hxhbs could impact a number of medical conditions related to neurodegeneration, stroke and eye diseases.

The most well-known of these reactions is the "NO dioxygenase" (NOD) reaction by flavoHb in bacteria and yeast. In this reaction, the ferrous oxy-Hb rapidly binds NO to form ferric Hb and nitrate. If the resulting ferric Hb is reduced to the ferrous form, the reaction becomes catalytic. In case of flavohemoglobin (flavoHb), rapid reduction is accomplished by a flavin-containing reductase domain [14]. Myoglobin, found in skeletal muscle has recently been found to inhibit damage induced by NO indicating that it may act as a potential NO-scavenger [7].

All hexacoordinate Hbs can scavenge Nitric Oxide if a reductase is present to convert the ferric Hb to the ferrous form. The limitation to the ability of a Hb to act as an NO scavenger is the rate of re-reduction of the ferric heme iron. Any ferrous Hb can bind oxygen or nitric oxide. The resulting complexes, O_2-Hb and NO-Hb, will rapidly react with NO and O_2, respectively, yielding ferric Hb and nitrate. The reaction becomes catalytic if the resulting ferric Hb is reduced (Figure 5-1). In fact, any reaction requiring ferrous Hb needs this reductase, so finding a

reductase would be a breakthrough in hemoglobin research. However, no cognate reductase has been identified to continue the reaction.

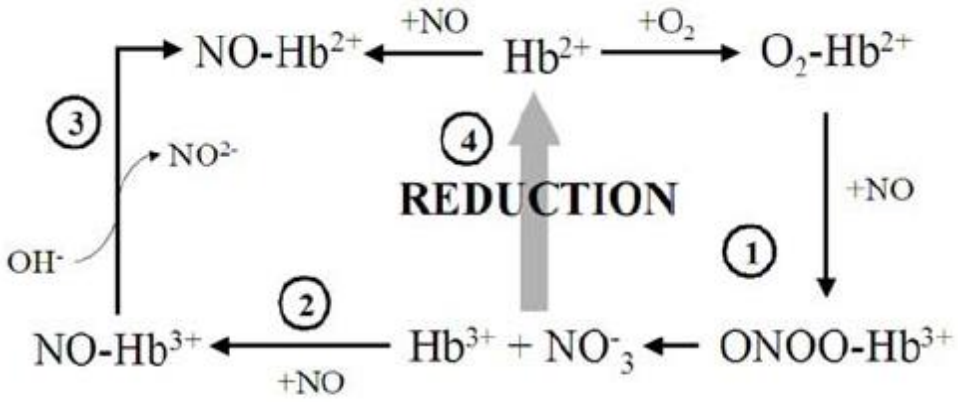

Figure 5-1: NO reactions with hemoglobins. The following reactions have been investigated: 1. NO dioxygenation reaction, 2. NO binds to ferric Hb, 3. NO-induced reduction and 4. Reduction of ferric Hb.

Previous work [15] has led to the idea of a selection-based screen for Hb reductase activity in *E. coli*. Neither Ngb nor Cgb alone provides *E. coli* protection against NO. The presence of a reductase, either naturally or after expression from a second plasmid, would confer protection and the cells would survive. One such case is SynHb, in which an endogenous *E. coli* reductase was induced to confer survival in NO toxic environment.

In this project, Ngb was coexpressed with a library of cDNAs from human liver to screen for reductases with activity against Ngb. Figure 5-2 describes the reductase screening system.

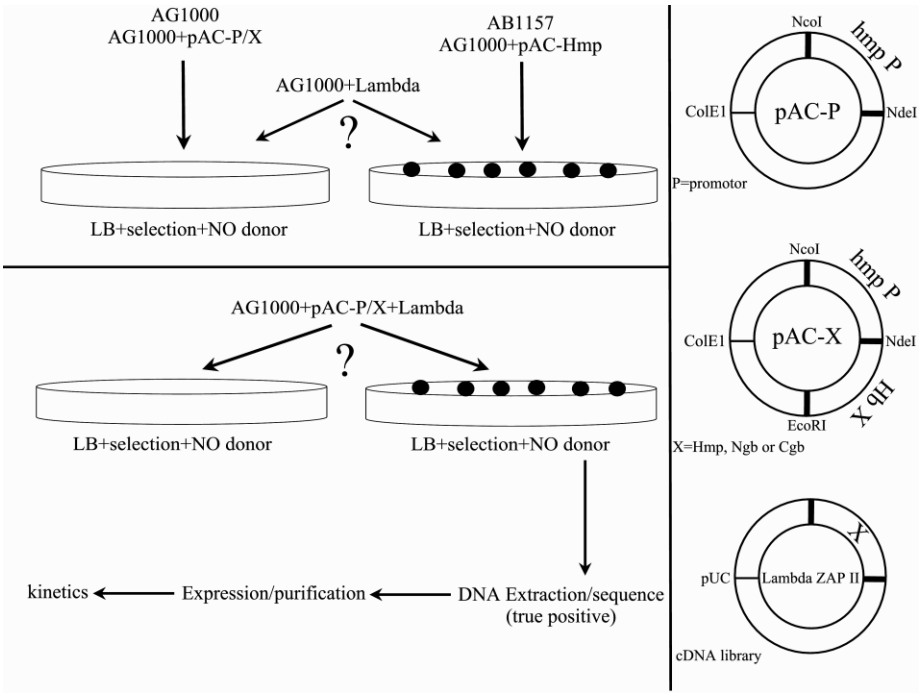

Figure 5-2: Diagrammatic representation of the dual expression screen of a human cDNA library for reductase activity against Ngb. The plasmids involved are shown to the right, the positive controls at the top, and the screen below them. (AB1157 and AG1000 (AB1157Φ (*hmp-lacZ*)262; Cm^r) are the two E.coli strains).

Methods:

Essential controls were established to carry out these experiments on solid media, because previous work was done in liquid cultures. Appropriate concentrations of the NO donor suitable for re-establishing controls for media plates were determined. The NO donor used was GSNO (S-Nitrosoglutatione). GSNO did not provide the desired effect initially because the NO produced escaped from the plate. To fix this problem, two methods were implemented: 1) a filter paper disk was used which acts as a reservoir of GSNO on the plate. 2) Parafilm was placed

around the plate before incubation, in order to prevent escape of NO. Both methods worked with the same efficiency. Figure 5-3 shows the two methods used.

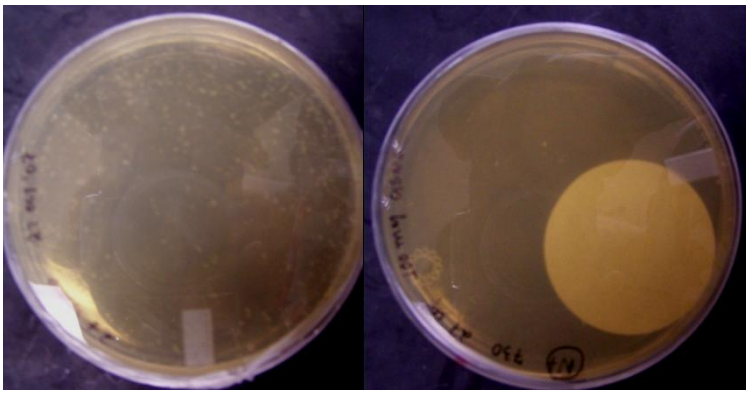

Figure 5-3: Plates showing the parafilm and filter paper disc method.

No selection was used for wild type strain (AB1157). For the AG1000 strain, 35 µg/ml chloramphenicol was added and for AG1000 expressing Ngb, 12 µg/ml tetracycline was also added to the media plates. The wild type strain (AB1157) and the *hmp* mutant strain (AG1000) expressing flavoHb on the pACYC plasmid are able to grow in the presence of GSNO, but the AG1000 strain alone and those expressing Ngb gene are impaired. The concentration of GSNO used in these experiments is the minimum amount required to observe clear hmp- phenotype (no colonies).

Screening of a cDNA library was carried out using the electroporation method in AG1000 cells expressing the Ngb gene in pACYC plasmid**.** For media plates used for co-expression, 100µg/ml ampicillin was also added (along with chloramphenicol and tetracycline). The plates were incubated for a period of 16 hours. The gene conferring NO resistance to Ngb

was isolated from colonies obtained in these dual screens. Two such genes were seen to confer NO protection to Ngb. Single plasmid experiments were performed to rule out false positives. Plasmid extracted from cDNA library was transformed in AG1000 strain.

Results:

This work resulted in the identification of two genes that conferred *in vivo* protection in the presence of NO. These genes were isolated, sequenced and a blast run resulted in sequence alignments with haptoglobin and the other corresponded to a fragment of hexosaminidase. Haptoglobin was cloned into pET28 vector and tested for activity *in vitro.* An NO electrode was used to measure NO consumption with time. A combination of glucose -6-phosphate, glucose-6-phosphate dehydrogenase, 60 µM NADP and 1 µM ferredoxin reductase was used as an artificial reduction system and a positive control in the experiments to observe NO consumption. However, haptoglobin did not consume NO at a rate expected for an efficient NO scavenger (Figure 5-4). Hexosaminidase needs to be tested for activity *in vitro*.

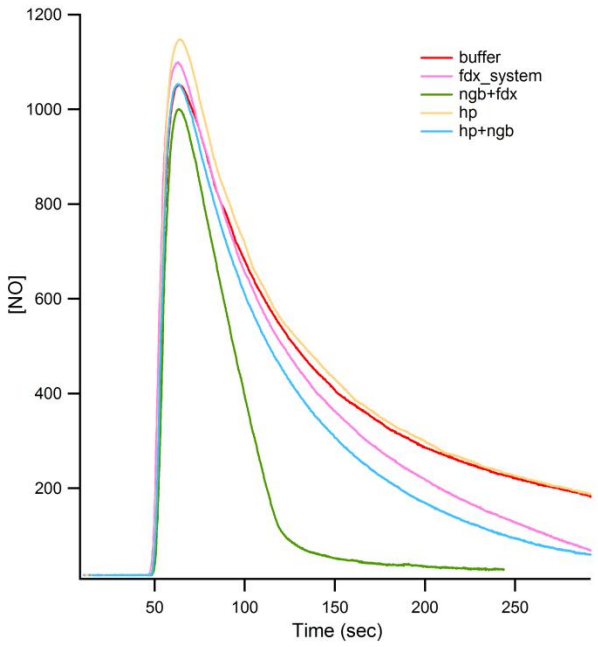

Figure 5-4: **NO consumption test for Haptoglobin**. Fdx- reduction system alone, hp- haptoglobin, Ngb+fdx- Ngb along with the reduction system, Ngb+hp- Ngb in the presence of haptoglobin.

Conclusions:

There is very little evidence for the proposed cytoprotective role of hexacoordinate hemoglobins that are now known to be ubiquitous among biological organisms. The essential goal of this project is to understand the functions of hxhbs by investigating their catalytic activity. The work done has tested the efficacy of various methods to screen a library of cDNAs. The methods described above have been established using necessary controls and candidate genes. However, this was the only method used to screen for candidate genes from a cDNA pool.

The results obtained are not truly negative since the library used could be unsuitable for such a screen or the system employed may not be a true mimic of *in vivo* conditions.

Identifying additional candidates and testing them empirically for *in vitro* activity using biochemical techniques would be helpful in justifying NO scavenging activity of this newly discovered family of hemoglobins.

References:

[1] F. Guix, I. Uribesalgo, M. Coma, F. Muñoz, Prog Neurobiol, vol. 76, 2005, pp. 126-152.
[2] P. Pacher, J. Beckman, L. Liaudet, Physiol Rev, vol. 87, 2007, pp. 315-424.
[3] R. Sultana, H. Poon, J. Cai, W. Pierce, M. Merchant, J. Klein, W. Markesbery, D. Butterfield, Neurobiol Dis, vol. 22, 2006, pp. 76-87.
[4] A. Castegna, V. Thongboonkerd, J. Klein, B. Lynn, W. Markesbery, D. Butterfield, J Neurochem, vol. 85, 2003, pp. 1394-1401.
[5] P. Gardner, A. Gardner, L. Martin, A. Salzman, Proc Natl Acad Sci U S A, vol. 95, 1998, pp. 10378-10383.
[6] D. Doherty, M. Doyle, S. Curry, R. Vali, T. Fattor, J. Olson, D. Lemon, Nat Biotechnol, vol. 16, 1998, pp. 672-676.
[7] U. Flögel, M. Merx, A. Godecke, U. Decking, J. Schrader, Proc Natl Acad Sci U S A, vol. 98, 2001, pp. 735-740.
[8] D. Minning, A. Gow, J. Bonaventura, R. Braun, M. Dewhirst, D. Goldberg, J. Stamler, Nature, vol. 401, 1999, pp. 497-502.
[9] M. Couture, T. Das, H. Lee, J. Peisach, D. Rousseau, B. Wittenberg, J. Wittenberg, M. Guertin, J Biol Chem, vol. 274, 1999, pp. 6898-6910.
[10] L. Jia, C. Bonaventura, J. Bonaventura, J. Stamler, Nature, vol. 380, 1996, pp. 221-226.
[11] A. Lipton, M. Johnson, T. Macdonald, M. Lieberman, D. Gozal, B. Gaston, Nature, vol. 413, 2001, pp. 171-174.
[12] M. Brunori, Trends Biochem Sci, vol. 26, 2001, pp. 21-23.
[13] T. Hankeln, B. Ebner, C. Fuchs, F. Gerlach, M. Haberkamp, T. Laufs, A. Roesner, M. Schmidt, B. Weich, S. Wystub, S. Saaler-Reinhardt, S. Reuss, M. Bolognesi, D. De Sanctis, M. Marden, L. Kiger, L. Moens, S. Dewilde, E. Nevo, A. Avivi, R. Weber, A. Fago, T. Burmester, J Inorg Biochem, vol. 99, 2005, pp. 110-119.
[14] A. Ilari, A. Bonamore, A. Farina, K. Johnson, A. Boffi, J Biol Chem, vol. 277, 2002, pp. 23725-23732.
[15] B. Smagghe, J.r. Trent, M. Hargrove, PLoS One, vol. 3, 2008, pp. e2039.

CHAPTER 6. CONCLUSIONS

The discovery of reversible histidine coordination and exogenous ligand binding in Hbs was surprising in light of the relative inertness of cytochrome *b5*. The structures of hxHbs in the hexacoordinate and ligand-bound states have revealed different mechanisms for achieving histidine dissociation from the ligand binding site, ranging from the large conformational changes observed in SynHb to modest repositioning of the heme in Ngb. The conformational changes accompanying ligand binding in SynHb and rice nsHb are relatively large, indicating a degree of flexibility in the globin fold that was not anticipated from previous globin structures. These conformational changes could be a component of the mechanism of action of hxHbs, or a structural necessity for reversible ligand binding; an answer to this question must await identification of physiological function(s).

It was first thought that, in general, pentacoordinate Hbs evolved from hxHbs. This makes sense from a structural perspective; a distal histidine nearby but not coordinating the heme iron would be difficult to stabilize in a flexible globin. It was logical to consider that pentacoordinate Hbs evolved from hxHbs by stabilizing the pentacoordinate conformation of the hxHb, and reducing the flexibility of the globin to lock it into only this conformation. However, the animal Hb phylogeny does not support this conclusion, showing instead that pentacoordinate Hbs predate hxHbs in animals. This is an important consideration as it suggests selection for a hexacoordinate heme center and the accompanying chemistry and potential conformational variability. It is thus likely that these properties will be linked to function, and should be carefully considered as these physiological activities are identified.

Based on the current description of hxHbs, it seems likely that their function(s) involve 1) exogenous ligand binding, 2) a change in heme iron oxidation state, and 3) a role in signaling. These conclusions are based on the following observations, respectively. 1) Hexacoordination and affinity for exogenous ligands is conserved across each group of hxHbs, and even across the classes of plant nsHbs. 2) Hexacoordination facilitates electron transfer. If the goal were simply to bind and release ligands, a pentacoordinate heme would be preferred (as in oxygen transport Hbs). 3) HxHbs are present in very low concentrations, and ligand binding could trigger conformational and redox changes that regulate interactions with other signaling molecules.

Identification of the function of proteins is the next frontier of biochemistry, and is certainly the rate-limiting step in our understanding of hxHbs. The magnitude of this problem is realized by considering the difficulty that would face researchers trying to discover the function of the red blood cell Hb subunits using only recombinant proteins in the laboratory. The behavior of these isolated chains reflects that of native Hb in some ways, but could also lead down many false paths. This is the situation with hxHbs, where the results from *in vitro* experiments are certainly telling us something about physiological function, but are also providing much more information than can be assimilated into clear hypothesis in the background of a much smaller number of physiological studies. A confident interpretation of biochemistry will only come from its ability to explain a clear physiological function.

ACKNOWLEDGEMENTS

I would like to take this opportunity to express my gratitude to my advisor, Dr. Mark Hargrove, for his guidance and support throughout the course of my Ph.D. I could not have asked for a better mentor than him. I would also like to thank my POS committee members, past and current lab mates, my BBMB department colleagues and the University for all the ways in which they have supported and helped me. I really appreciate all the help and the invaluable time provided by Dr. Alan Dispirito in my research projects. I would also like to thank my parents Dr. Ashok Kakar and Mrs. Rupam Kakar and my grandparents because of whose influence I pursued a doctoral degree, and Vijay's parents for their continued support and guidance throughout this time. I would like to thank Harvinder, Mamta, Hemank and my brother, Prateek Kakar, who always encouraged me in tough times. A special note of thanks to Divya Sinha, Yashdeep Phanse and Kuldeep Wadhwa who have been my friends throughout, for their constant support and for innumerable fun moments we have had together. My sincere and special thanks go to my husband, Dr. Vijay Walia, for his constant inspiration, encouragement and helpful discussions. I could not have done this without him.